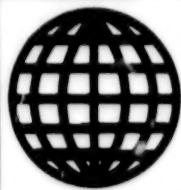


JPRS-UEQ-92-007
8 JUNE 1992



**FOREIGN
BROADCAST
INFORMATION
SERVICE**

JPRS Report

Science & Technology

***Central Eurasia:
Engineering & Equipment***

Science & Technology

Central Eurasia: Engineering & Equipment

JPRS-UEQ-92-007

CONTENTS

8 June 1992

Aviation and Space Technology

An Experimental and Theoretical Investigation of the Stability of the Skin of Trilayer Structures [S.A. Askerov; <i>IZVESTIYA VYSSHIKH UCHEBNYKH ZAVEDENIY: AVIATIONNAYA TEKHNIKA</i> , No 2, Apr-Jun 91]	1
The Load-Bearing Capacity of Laminar Composite Shells and Plates at an Elevated Temperature [E.S. Sibgatullin; <i>IZVESTIYA VYSSHIKH UCHEBNYKH ZAVEDENIY: AVIATIONNAYA TEKHNIKA</i> , No 2, Apr-Jun 91]	1
Discontinuous Control of Manipulator With Inertial Drives. Part I [A.S. Meshchanov; <i>IZVESTIYA VYSSHIKH UCHEBNYKH ZAVEDENIY: AVIATIONNAYA TEKHNIKA</i> , No 3, Jul-Sep 91]	1
An Experimental Investigation of Heat Transfer in Model Nozzles [V.G. Zubkov; <i>IZVESTIYA VYSSHIKH UCHEBNYKH ZAVEDENIY: AVIATIONNAYA TEKHNIKA</i> , No 2, Apr-Jun 91]	2
An Analog Model of the Three-Dimensional Circulation of a Maneuvering Helicopter [L.N. Makarov, I.N. Rodionov, et al.; <i>IZVESTIYA VYSSHIKH UCHEBNYKH ZAVEDENIY: AVIATIONNAYA TEKHNIKA</i> , No 2, Apr-Jun 91]	2
The Execution of a Method for Calculating a Rotor's Characteristics With Consideration for Vibrations of the Shaft [A.Yu. Liss; <i>IZVESTIYA VYSSHIKH UCHEBNYKH ZAVEDENIY: AVIATIONNAYA TEKHNIKA</i> , No 2, Apr-Jun 91]	2
The Nonlinear Deformation of Discretely Stiffened Thin Shells [B.A. Antufyev; <i>IZVESTIYA VYSSHIKH UCHEBNYKH ZAVEDENIY: AVIATIONNAYA TEKHNIKA</i> , No 2, Apr-Jun 91]	3
Determining the End Losses in Turbine Cascades With Consideration for the Effect of Inlet Boundary Layer [Ye.N. Bogomolov; <i>IZVESTIYA VYSSHIKH UCHEBNYKH ZAVEDENIY: AVIATIONNAYA TEKHNIKA</i> , No 2, Apr-Jun 91]	3
The Axial Turbine Stage With the Greatest Peripheral Work [A.A. Sergiyenko; <i>IZVESTIYA VYSSHIKH UCHEBNYKH ZAVEDENIY: AVIATIONNAYA TEKHNIKA</i> , No 2, Apr-Jun 91]	3
The Synthesis of Nonlinear Controllers To Stabilize Objects Damaged by Parametric and External Effects [B.V. Ulanov; <i>IZVESTIYA VYSSHIKH UCHEBNYKH ZAVEDENIY: AVIATIONNAYA TEKHNIKA</i> , No 2, Apr-Jun 91]	4
Effect of the Scale of the Inhomogeneity of an Oncoming Flow on the Characteristics of Combustion in the Afterburner of a Bypass Engine [V.N. Gruzdev, I.Ye. Kuznetsov; <i>IZVESTIYA VYSSHIKH UCHEBNYKH ZAVEDENIY: AVIATIONNAYA TEKHNIKA</i> , No 3, Jul-Sep 91]	4
Problems in Designing Pyrolytic Drives [A.B. Kondratyev, V.A. Chashchin, et al.; <i>IZVESTIYA VYSSHIKH UCHEBNYKH ZAVEDENIY: AVIATIONNAYA TEKHNIKA</i> , No 3, Jul-Sep 91]	5
The Problem of Diagnosing the Operating Mode of Aircraft Engine's Air Intake [S.V. Puzach, Yu.A. Polyakov, et al.; <i>IZVESTIYA VYSSHIKH UCHEBNYKH ZAVEDENIY: AVIATIONNAYA TEKHNIKA</i> , No 3, Jul-Sep 91]	5
Optimizing the Startup of Mobile Power Plants [L.S. Vernovskiy, V.N. Kashin, et al.; <i>IZVESTIYA VYSSHIKH UCHEBNYKH ZAVEDENIY: AVIATIONNAYA TEKHNIKA</i> , No 2, Apr-Jun 91]	6
An Analysis of the Trajectories of an Energy Model of an Aircraft's Motion [K.A. Pavlov, A.A. Gorelov; <i>IZVESTIYA VYSSHIKH UCHEBNYKH ZAVEDENIY: AVIATIONNAYA TEKHNIKA</i> , No 3, Jul-Sep 91]	6
Calculating Heat Transfer in Model Nozzles [V.G. Zubkov; <i>IZVESTIYA VYSSHIKH UCHEBNYKH ZAVEDENIY: AVIATIONNAYA TEKHNIKA</i> , No 3, Jul-Sep 91]	6
A Second Type of Steady Motions of Two Gravitating Bodies: Axisymmetric and Spherical-Symmetric [S.N. Kirpichnikov; <i>VESTNIK LENINGRADSKOGO UNIVERSITETA: MATEMATIKA, MEKHANIKA, ASTRONOMIYA</i> , No 3, Jul 91]	7

Optics, High Energy Devices

The Reflectivity and Refractivity of ZnS-Based Mono- and Polycrystalline Materials [N.A. Nazarova; OPTIKO-MEKHANICHESKAYA PROMYSHLENNOST, Jul 91]	8
Using a Rough Surface To Improve the Characteristics of Neutral Light Filters [M.A. Validov, G.S. Belous, et al.; OPTIKO-MEKHANICHESKAYA PROMYSHLENNOST, Jul 91]	8
The New Titanium Flint TF14: Its Composition, Properties, Advantages [V.Ye. Galant, V.N. Polukhin, et al.; OPTIKO-MEKHANICHESKAYA PROMYSHLENNOST, Jul 91]	8
An Analysis of the Illumination Engineering Characteristics of the Viewfinder of a Reflex Still Camera [A.V. Gutin; OPTIKO-MEKHANICHESKAYA PROMYSHLENNOST, Jul 91]	9
The Scattering of Surface Electromagnetic Waves on the Rough Surface of a Metal Grating [S.P. Surov, V.A. Sychugov; OPTIKO-MEKHANICHESKAYA PROMYSHLENNOST, Jul 91]	9
Optimization of a Channel Amplifier Based on Noise Factor [V.N. Yevdokimov, A.M. Tyutikov, et al.; OPTIKO-MEKHANICHESKAYA PROMYSHLENNOST, Jul 91]	9
Low-Noise Avalanche Photodiodes To Record Laser Signals in the Spectral Range From 1.5 to 2.5 μm [I.A. Andreyev, A.N. Baranov, et al.; OPTIKO-MEKHANICHESKAYA PROMYSHLENNOST, Jul 91]	10
Induced Absorption in Interference Filters [V.A. Proshin; OPTIKO-MEKHANICHESKAYA PROMYSHLENNOST, Jul 91]	10
The Aperture Characteristics of Corner Cat's Eyes [S.V. Protosko, A.D. Titov; OPTIKO-MEKHANICHESKAYA PROMYSHLENNOST, Jul 91]	11
The Effect of Changes in Laser Recorders' Operating Mode Parameters on Image Quality [A.A. Brazhnik; OPTIKO-MEKHANICHESKAYA PROMYSHLENNOST, Jul 91]	11
Calculating the Aberrations of Laser Beam Area Converters [S.I. Klimentyev, V.I. Kuprenyuk, et al.; OPTIKO-MEKHANICHESKAYA PROMYSHLENNOST, Jul 91]	11
Liquid Optical Media With a Unique Dispersing Action [V.M. Volynkin, M.V. Petrova, et al.; OPTIKO-MEKHANICHESKAYA PROMYSHLENNOST, Jul 91]	12
The Effect of Glasses' Luminescence on the Results of Measuring Fiber-Optic Wafers' Light Transmission [G.Ya. Konayeva, K.P. Pecherskaya, et al.; OPTIKO-MEKHANICHESKAYA PROMYSHLENNOST, Jul 91]	12
The Effect of Machining Regimens on the Structural Changes in the Material of a Reflector's Surface Layer [I.V. Ruban, P.D. Dudko, et al.; OPTIKO-MEKHANICHESKAYA PROMYSHLENNOST, Jul 91]	13
The Impact of Thermal and Mechanical Effects on the Properties of a Sapphire Hollow Waveguide of IR Waveguide Lasers [Ye.R. Dobrovinskaya, L.A. Litvinov, et al.; OPTIKO-MEKHANICHESKAYA PROMYSHLENNOST, Jul 91]	13
Technology and Equipment for Precision Machining of Glass Wafers for Liquid Crystal Screens [V.S. Kondratenko, V.P. Strelkov, et al.; OPTIKO-MEKHANICHESKAYA PROMYSHLENNOST, Jul 91]	14
Using Geometric Optics Methods To Calculate the Function of Energy Concentration in the Image of an Axial Point [V.I. Peysakhson, T.A. Cherevko; OPTIKO-MEKHANICHESKAYA PROMYSHLENNOST, Jul 91]	14
Superisocon With a Sensitivity in the Near-UV Range of the Spectrum and Its Use in Photometric Research in Astrophysics [A.N. Abramenko, L.G. Bogacheva, et al.; OPTIKO-MEKHANICHESKAYA PROMYSHLENNOST, Jul 91]	15
New KM145 Magnetic Ship Compass With Latitude Compensator [L.A. Kardashinskiy-Braude, V.F. Ulanov; SUDOSTROYENIYE, Sep 91]	15
An Investigation of the Structures of Mirrors Made of Silicon Carbide [V.A. Alekseyev, V.V. Bokov, et al.; OPTIKO-MEKHANICHESKAYA PROMYSHLENNOST, Jul 91]	17
Acoustooptic Optical Beam Coordinate Meter [V.A. Komotskiy, M.V. Kotyukov; AVTOMETRIYA, No 5, Sep-Oct 91]	18
Precision Laser Thermographic Image Generator [S.G. Bayev, V.P. Bessmeltsev, et al.; AVTOMETRIYA, No 5, Sep-Oct 91]	18
Mirrors for High-Power UV-Range Argon Lasers [N.D. Goldina; AVTOMETRIYA, No 5, Sep-Oct 91]	19
A Geodesic Information-Measuring System Based on Acoustooptic Sensors [M.A. Bokov, A.N. Maksimov, et al.; AVTOMETRIYA, No 5, Sep-Oct 91]	19
The Principles of Creating Integrated-Optics Multichannel Associative Correlators for Computer Systems and Circuit Engineering Problems in Designing Them [A.A. Verbovetskiy; AVTOMETRIYA, No 5, Sep-Oct 91]	20

The Kristall-2 Goniometer Unit With an Automated Control System [V.N. Berezka, V.B. Ganenko, et al.; <i>PRIBORY I TEKHNIKA EKSPERIMENTA</i> , No 3, May-Jun 91]	20
A Space Conditions Simulation To Study the Properties of Materials [M.N. Mikhaylov, Yu.A. Rylkin; <i>PRIBORY I TEKHNIKA EKSPERIMENTA</i> , No 3, May-Jun 91]	20
Two-Coordinate Electrooptical Deflector Based on a Cooled DKDP Crystal [A.B. Vankov, V.M. Volynkin, et al.; <i>PRIBORY I TEKHNIKA EKSPERIMENTA</i> , No 3, May-Jun 91]	21
New Photocathodes for Radiation With a Wavelength of About 100 Angstroms [A.L. Andrushchenko, A.M. Pavlov, et al.; <i>PRIBORY I TEKHNIKA EKSPERIMENTA</i> , No 3, May-Jun 91]	21
A High-Power Electron and Ion Beam Source With Periodic-Pulse Action [A.G. Berkovskiy, V.G. Guselnikov, et al.; <i>PRIBORY I TEKHNIKA EKSPERIMENTA</i> , No 3, May-Jun 91]	21
Electron Beam Sources at Energy Up to 1 keV [A.A. Borovik; <i>PRIBORY I TEKHNIKA EKSPERIMENTA</i> , No 3, May-Jun 91]	22
A Pulsating Device To Discharge a Quasi-Continuous Electron Beam Into Dense Gas [V.S. Zhivopistsev, A.O. Ikonnikov, et al.; <i>PRIBORY I TEKHNIKA EKSPERIMENTA</i> , No 3, May-Jun 91]	22
Impairment of the Adhesion of Protective Mirror Coatings [G.M. Kudinov, V.M. Kostin; <i>POVERHNOST: FIZIKA, KHIMIYA, MEKHANIKA</i> , No 11, Oct 91]	23
Double-Crystal X-Ray Diagnosis of Impaired Near-Surface Layers of Silicon Subjected to a Laser Effect [A.P. Petrakov, V.I. Punegov, et al.; <i>POVERHNOST: FIZIKA, KHIMIYA, MEKHANIKA</i> , No 11, Oct 91]	23
Nuclear Energy	
Country of the Nuclear Bumpkin [S. Brusin; <i>ROSSIYA</i> , No 12 (71), 18 to 24 Mar 92]	24
A Period of Half-Decay: Subjective Comments About the Rostov AES [L. Mazyrin; <i>PATRIOT</i> , No 9, Mar 92]	26
Without the Peaceful Atom There Is Nowhere To Go [PATRIOT, No 10, Mar 92]	27
Do You Wish To View Some Uranium? [Yu. Gruzlov; <i>SLOVO KYKGYZSTANA</i> , 8 Feb 92]	27
Control and Protection Systems of VVER Nuclear Power Reactors [V.K. Kalashnikov, Yu.N. Olshevskiy, et al.; <i>ELEKTROTEKHNIKA</i> , Sep 91]	29
The Technical and Economic Feasibility of Using Asynchronous Turbogenerators in an Asynchronous Mode at Electric Power Plants [A.S. Minyaylo, N.P. Shmatyuk, et al.; <i>IZVESTIYA VYSSHIKH UCHEBNYKH ZAVEDENIY: ENERGETIKA</i> , Nov 91]	29
Improving the Operating Efficiency of Steam Turbine Units at AES by Using Multistage Moisture Separation [V.M. Borovkov, A.G. Kutakhov, et al.; <i>IZVESTIYA VYSSHIKH UCHEBNYKH ZAVEDENIY: ENERGETIKA</i> , Nov 91]	30
70-MW Floating Electric Power Plant for the North [V.K. Kovalenko, V.K. Tarasov; <i>SUDOSTROYENIYE</i> , Sep 91]	31
Non-Nuclear Energy	
Underground-Type GAES: Problems and Solutions [G.L. Sarukhanov, Ya.Z. Zaslavskiy, et al.; <i>PROYEKTIROVANIYE I INZHENERNYYE IZYSKANIYA</i> , No 5, Oct 91]	32
Mechanics of Gases, Liquids, Solids	
The Heat Transfer and Drag of a Cylinder Coated With a Layer of Magnetic Fluid and Surrounded by a Transversal Flow [V.G. Bashtovoy, Nguyen Kuyet Tkhang, et al.; <i>MAGNITNAYA GIDRODINAMIKA</i> , No 3, Jul-Sep 91]	35
Dynamics of the Operation of a Pneumatic Shock Absorber With Magnetic Fluid [V.A. Boguslavskiy; <i>MAGNITNAYA GIDRODINAMIKA</i> , No 3, Jul-Sep 91]	35
The Solution of Plane Problems of the Nonstationary Filtration of a Heavy Fluid Into Unsaturated Porous Soil Within the Framework of a Model of Instantaneous Saturation [A.N. Krayko, Sh. Salomov; <i>IZVESTIYA ROSSIYSKOY AKADEMII NAUK: MEKHANIKA ZHIDKOSTI I GAZA</i> , No 1, Jan-Feb 92]	35
The Development of Instability in the Wake Behind a Plate Located Parallel to the Flow [P.A. Kuybin, V.Ya. Rudyak; <i>IZVESTIYA ROSSIYSKOY AKADEMII NAUK: MEKHANIKA ZHIDKOSTI I GAZA</i> , No 1, Jan-Feb 92]	36
A Three-Parameter Model of Turbulence: A Numerical Study of the Boundary Layer in a Nozzle With Blanket Cooling [V.I. Kovalev, V.G. Lushchik, et al.; <i>IZVESTIYA ROSSIYSKOY AKADEMII NAUK: MEKHANIKA ZHIDKOSTI I GAZA</i> , No 1, Jan-Feb 92]	36

The Motion of a Disperse Impurity in a Laminar Boundary Layer on a Plane Plate [Ye.S. Asmolov; IZVESTIYA ROSSIYSKOY AKADEMII NAUK: MEKHANIKA ZHIDKOSTI I GAZA, No 1, Jan-Feb 92]	37
The Structure and Dynamics of Finite-Amplitude Pressure Disturbances in a Fluid-Saturated Porous Medium With Gas Bubbles [V.Ye. Dontsov; IZVESTIYA ROSSIYSKOY AKADEMII NAUK: MEKHANIKA ZHIDKOSTI I GAZA, No 1, Jan-Feb 92]	37
A Model of the Precipitation of Particles From a Turbulent Gas-Dispersion Flow With Absorbing Walls [I.N. Gusev, Ye.I. Guseva, et al.; IZVESTIYA ROSSIYSKOY AKADEMII NAUK: MEKHANIKA ZHIDKOSTI I GAZA, No 1, Jan-Feb 92]	38
The Susceptibility of Supersonic Boundary Layer to Acoustic Disturbances [A.V. Fedorov, A.P. Khokhlov; IZVESTIYA ROSSIYSKOY AKADEMII NAUK: MEKHANIKA ZHIDKOSTI I GAZA, No 1, Jan-Feb 92]	38
The Convective Stability of a Horizontal Rotating Layer of Fluid With Spiral Turbulence [B.L. Smorodin; IZVESTIYA ROSSIYSKOY AKADEMII NAUK: MEKHANIKA ZHIDKOSTI I GAZA, No 1, Jan-Feb 92]	39
Selected Nonlinear Wave Effects in a Fluid-Saturated Porous Medium [R.F. Ganiyev, S.A. Petrov, et al.; IZVESTIYA ROSSIYSKOY AKADEMII NAUK: MEKHANIKA ZHIDKOSTI I GAZA, No 1, Jan-Feb 92]	39
The Circulation of a Cylinder by Rarefied Gas at a Gliding Angle [K.V. Nikolayev; IZVESTIYA ROSSIYSKOY AKADEMII NAUK: MEKHANIKA ZHIDKOSTI I GAZA, No 1, Jan-Feb 92]	39
A Theory of Stability of Periodic Flows of Viscous Gas [M.A. Brutyan, P.L. Krapivskiy; IZVESTIYA ROSSIYSKOY AKADEMII NAUK: MEKHANIKA ZHIDKOSTI I GAZA, No 1, Jan-Feb 92]	40
Characteristic Features of a Circulating Flow of Rarefied Gas in a Short Rotating Cylinder With a Fixed Face [V.D. Borisevich, S.Yu. Krylov, et al.; IZVESTIYA ROSSIYSKOY AKADEMII NAUK: MEKHANIKA ZHIDKOSTI I GAZA, No 1, Jan-Feb 92]	40
Exact Solutions of a Model Bhatnagar-Gross-Kruk Boltzmann Equation in Problems of Temperature Jump and Weak Evaporation [Ye.B. Dolgosheina, A.V. Latyshev, et al.; IZVESTIYA ROSSIYSKOY AKADEMII NAUK: MEKHANIKA ZHIDKOSTI I GAZA, No 1, Jan-Feb 92]	41
Problems of the Circulation and Correction of Shape of Thin Profiles in an Incompressible Flow [V.E. Saren; IZVESTIYA ROSSIYSKOY AKADEMII NAUK: MEKHANIKA ZHIDKOSTI I GAZA, No 1, Jan-Feb 92]	41
The Buoyancy of Bodies in Disperse Media [A.V. Ostroumov; IZVESTIYA ROSSIYSKOY AKADEMII NAUK: MEKHANIKA ZHIDKOSTI I GAZA, No 1, Jan-Feb 92]	41
The Aerodynamic Drag of a Cylinder in a Two-Phase Flow [V.A. Lashkov; IZVESTIYA ROSSIYSKOY AKADEMII NAUK: MEKHANIKA ZHIDKOSTI I GAZA, No 1, Jan-Feb 92]	42
Three-Wave Resonance and Averaged Equations of the Interaction of Two Waves in Media Described by a Cubic Schrodinger Equation [I.B. Bakholdin; IZVESTIYA ROSSIYSKOY AKADEMII NAUK: MEKHANIKA ZHIDKOSTI I GAZA, No 1, Jan-Feb 92]	42
Plane Capillary Friction of Viscous Fluid With a Multiply Connected Boundary in a Stokes Approximation [S.A. Chivilikhin; IZVESTIYA ROSSIYSKOY AKADEMII NAUK: MEKHANIKA ZHIDKOSTI I GAZA, No 1, Jan-Feb 92]	42
Radiation and Radiation Cooling of Xenon Plasma Behind a Strong Shock Wave Front [S.V. Makarychev, G.D. Smekhov, et al.; IZVESTIYA ROSSIYSKOY AKADEMII NAUK: MEKHANIKA ZHIDKOSTI I GAZA, No 1, Jan-Feb 92]	43
A Nonstationary Viscous Shock Layer During Supersonic Motion Through an Inhomogeneity [A.A. Markov; IZVESTIYA ROSSIYSKOY AKADEMII NAUK: MEKHANIKA ZHIDKOSTI I GAZA, No 1, Jan-Feb 92]	43
Motion Equation of Ball Lightning in the Air Stream Formed by a Flying Rocket [N.I. Gaydukov; IZVESTIYA ROSSIYSKOY AKADEMII NAUK: MEKHANIKA ZHIDKOSTI I GAZA, No 1, Jan-Feb 92]	43
Jet Flow on Ribbed Curvilinear Surfaces [Yu.A. Lashkov, I.N. Sokolova, et al.; IZVESTIYA ROSSIYSKOY AKADEMII NAUK: MEKHANIKA ZHIDKOSTI I GAZA, No 1, Jan-Feb 92]	44
Thermocapillary Evacuation of Fluid Coming Through a Porous Wall [Yu.V. Sanochkin; IZVESTIYA ROSSIYSKOY AKADEMII NAUK: MEKHANIKA ZHIDKOSTI I GAZA, No 1, Jan-Feb 92]	44

Generalized Model of a Plane Geofiltration Flow [V.M. Shestakov; <i>IZVESTIYA ROSSIYSKOY AKADEMII NAUK: MEKHANIKA ZHIDKOSTI I GAZA</i> , No 1, Jan-Feb 92]	45
A Body of Minimum Resistance Moving in Media Under the Assumption of the Law of Locality [N.A. Ostapenko, G.Ye. Yakunina; <i>IZVESTIYA ROSSIYSKOY AKADEMII NAUK: MEKHANIKA ZHIDKOSTI I GAZA</i> , No 1, Jan-Feb 92]	45
Designing an Airfoil With a Flap Simulated by a Point Vortex [N.B. Ilinskiy, A.V. Potashev; <i>IZVESTIYA ROSSIYSKOY AKADEMII NAUK: MEKHANIKA ZHIDKOSTI I GAZA</i> , No 1, Jan-Feb 92]	45
Formation of a Large Radiation-Induced Fire [Yu.A. Gostintsev, G.M. Makhviladze, et al.; <i>IZVESTIYA ROSSIYSKOY AKADEMII NAUK: MEKHANIKA ZHIDKOSTI I GAZA</i> , No 1, Jan-Feb 92]	46

An Experimental and Theoretical Investigation of the Stability of the Skin of Trilayer Structures

927F0175A Kazan IZVESTIYA VYSSHIKH UCHEBNIKH ZAVEDENIY: AVIATIONNAYA TEKHNIKA in Russian No 2, Apr-Jun 91 (manuscript received 12 Dec 90) pp 3-6

[Article by S.A. Askerov; UDC 624.01/04]

[Abstract] The load bearing capacity and reliability of trilayer structures with a lightweight filler depends primarily on the local stability of the compressed skin. Analysis of the results of experimental investigations of the separation of the skin from the middle layer of trilayer ribbed plates has demonstrated both qualitative and quantitative deviation of the experimental stresses from existing theoretically calculated values of the critical load of a local loss of stability. According to the existing theory, the critical stresses triggering a local loss of stability should increase as the physical characteristics of a trilayer structure's materials increase. Experiments have shown that actual critical stresses do not in fact obey this law. Analysis of experimental research on the stability of the skin of trilayer structures has revealed that destruction of the skin results from a loss in its local stability referred to as "transient buckling" or "snapping." This type of loss of stability is known to be associated with the effect of disturbances (in this case deformations) directed opposite to the bending of the skin. Deformation of the middle layer is in fact the source of disturbances of the compressed skin of a trilayer structure. In order to determine the actual theoretical laws governing the critical force of the loss of stability of the skin of a trilayer structure with different boundary conditions, it is necessary to examine the equilibrium of its elements in a half-space. The author of this article has worked to develop a mathematical method of finding the actual values of the critical forces triggering a loss of the stability of the skin of a trilayer structure. First, an equation of equilibrium in motions, i.e., a Lamé equation, is used as an input equation to find the movements of the filler or, in other words, to find the disturbances in the half-space. When no body forces are in play, the body deformation satisfies a Laplace equation (i.e., it is a harmonic function). Next, boundary conditions and tangential stresses are found for the case of buckling where the two opposite sides of the trilayer structure are hinged and the other two are free. The differential equations derived for this scenario are solved by the method of separating variables. Next, a differential equation of the bending of an orthotropic plate with consideration for the reverse deformation of the filler is then used to find the critical forces of the skin's loss of stability. Analysis of experimental research on the separation of the skin and filler of a trilayer structure has demonstrated that calculating the critical forces triggering a loss of local stability requires a high degree of precision. The main reason for this fact is the extremely small value of the disturbing deformations of the filler. Obtaining reliable results therefore requires consideration of at least three terms of each series of respective functions in the equations used. For this reason, the system of nonlinear

equations presented must be solved by numerical iteration. A program has been developed in Fortran that makes it possible to determine the values of the critical forces of a local loss of stability and the site of the separation. The results of calculations performed by using the new program have been found to be in both quantitative and qualitative agreement with experimental data. References 3 (Russian).

The Load-Bearing Capacity of Laminar Composite Shells and Plates at an Elevated Temperature

927F0175B Kazan IZVESTIYA VYSSHIKH UCHEBNIKH ZAVEDENIY: AVIATIONNAYA TEKHNIKA in Russian No 2, Apr-Jun 91 (manuscript received 28 May 90) pp 11-13

[Article by E.S. Sibgatullin; UDC 539.3:539.4]

[Abstract] As the temperature rises, the region of safe stressed states applied to a composite material narrows. In view of this fact, the author of this article proposes a method of determining the load-bearing capacity of composite shells and plates with consideration for the effect of temperature. Specifically, he uses Drucker's postulate and assumptions about the law governing the change in the kinematic characteristics of a bundle of layers by thickness as a foundation for deriving parametric equations of a boundary surface in the space of internal forces and moments. The problem of the load-bearing capacity of a cylindrical shell is solved as an example. The proposed method is said to be useful for constructing the boundary surface of different composite structures at different working temperatures by using a minimum required amount of experimental data for the individual layers. Figures 2; references 3 (Russian).

Discontinuous Control of Manipulator With Inertial Drives. Part I

927F0176A Kazan IZVESTIYA VYSSHIKH UCHEBNIKH ZAVEDENIY: AVIATIONNAYA TEKHNIKA in Russian No 3, Jul-Sep 91 (manuscript received 21 Feb 90) pp 13-20

[Article by A.S. Meshchanov; UDC 681.516.7]

[Abstract] The control systems of manipulators mounted on board spacecraft, aircraft, or other moving objects (including self-contained moving robots servicing spacecraft) are subject to damage due to various uncertain parametric and external effects. Included among these undetermined sources are changes in the mass of the loads carried by the robot or in the control system's parameters from product to product, vibrations of the craft itself, winds, dry friction in hinges, and unforeseen small deviations from ideality. The author of this article proposes a method of controlling an aircraft manipulator in a sliding mode. The proposed control method is a qualitative method that is invariant to various sources of

uncertainty and other disturbances and selectively invariant. Throughout the course of the mathematical analysis presented herein the author examines equivalent transformations of a nonlinear system of differential motion equations specifying the motion of the spacecraft manipulator being controlled. Unlike familiar methods of designing discontinuous manipulator control systems, the methods proposed herein give consideration not only to the aforesaid sources of uncertainty but also to the inertia of the drives of the manipulator's individual links. References 6: 5 Russian, 1 Western.

An Experimental Investigation of Heat Transfer in Model Nozzles

927F0175J Kazan IZVESTIYA VYSSHIKH UCHEBNIKH ZAVEDENIY: AVIATIONNAYA TEKHNKA in Russian No 2, Apr-Jun 91 (manuscript received 22 Nov 90) pp 96-99

[Article by V.G. Zubkov; UDC 621.45:533.6]

[Abstract] The author of this study conducted a series of experiments measuring the heat fluxes in two model supersonic nozzles. A solid fuel-fired gas generator with a constant flow rate was used in the tests. The shape of the charge was such that the combustion surface remained constant over the entire operating time. The combustion products were virtually free of condensed phase and had a deceleration temperature of 2,160 K. The primary research object was a removable nozzle unit made of M1 copper disks 1.5 mm thick. The heat resistance of the contact between the disk made it possible to consider each of them to be an annular calorimeter. To measure the temperature state of the nozzle units, two thermocouples were caulked to each other at distances of 0.015 and 0.025 m from the inner surface. The two types of conical nozzles investigated differed from one another in terms of their angles of half-dissolution in the subcritical and supercritical ranges. Their inner circuits were configured so as to achieve accelerations of 5×10^{-6} and 2.5×10^{-6} in the subsonic range for the two nozzles (designated No. 1 and No. 2), respectively. A nonlinear inverse heat conduction problem was solved to determine the heat fluxes acting on the surface of the nozzle units based on the known temperature state of the structure. The regularization method was used to obtain a numerical solution to the problem. The calculations performed established that the maximum heat flux is, in both cases studied, located in the vicinity of the nozzle's critical section. A second, much smaller maximum was observed close to the cylindrical gas passage. It was especially pronounced in the case of the nozzle with the elongated entrance. The effects of the flow resulting from the unprofiled entrance to the confuser section of the nozzle and the sharp change in wall temperature had a significant influence on the intensity of heat transfer. A comparison of the results of the experiments conducted with previously published findings demonstrated the reduced intensity of heat transfer in accelerated flows. The reliability of laminarization of the current was found to increase as the degree

of acceleration of the flow increased, thus indicating that the intensity of heat transfer in real structures may be reduced significantly by the appropriate profiling of their flow paths. The studies further indicated that in geometrically similar nozzles, the effects of laminarization are most likely in the case of profiles whose critical section has a smaller diameter. Figures 2; references 4: 3 Russian, 1 Western.

An Analog Model of the Three-Dimensional Circulation of a Maneuvering Helicopter

927F0175D Kazan IZVESTIYA VYSSHIKH UCHEBNIKH ZAVEDENIY: AVIATIONNAYA TEKHNKA in Russian No 2, Apr-Jun 91 (manuscript received 18 Dec 90) pp 36-40

[Article by L.N. Makarov, I.N. Rodionov, A.V. Shorichev, ; UDC 629.7.015.3:533.6.072]

[Abstract] In a previous publication, the authors of this article presented an algorithm for constructing an analog model of the circulation of the system helicopter rotor-fuselage in a steady horizontal flight. The algorithm is said to be convenient in that during the process of designing a quasi-analog model of the rotor, the meeting of the boundary conditions at the enclosures and the conditions in the wake are separated into successive operations. Because of this feature, the algorithm may, with slight modification of the model's structure and boundary conditions, also be used to calculate the disturbed velocity field around a maneuvering helicopter. Specifically, the model must be modified to give consideration to the curvilinear nature of the helicopter's motion. In this article, the authors develop an analog method of calculating a disturbed velocity field around a rotor-fuselage combination. A sample computation is presented that illustrates the effect of the magnitude and direction of banking velocity on the velocity field along a rotor in the presence of a fuselage. Figures 3; references 2 (Russian).

The Execution of a Method for Calculating a Rotor's Characteristics With Consideration for Vibrations of the Shaft

927F0175H Kazan IZVESTIYA VYSSHIKH UCHEBNIKH ZAVEDENIY: AVIATIONNAYA TEKHNKA in Russian No 2, Apr-Jun 91 (manuscript received 11 Sep 90) pp 78-81

[Article by A.Yu. Liss; UDC 539.3:629.7.015.4.035]

[Abstract] The author of this article has used a method detailed in his previous publications as a basis for developing an algorithm to design a rotor on an elastic helicopter fuselage. The author confines himself to consideration of the vibrations of a helicopter with an initial transfer frequency of $\Omega = z_b \omega$ (where z_b is the number of blades and ω is the angular velocity of the rotor's rotation). Consequently, in one vibration period, each blade moves one position forward to take the place

previously occupied by the blade in front of it. This means that all of the blades pass through each azimuth in an identical phase and that, consequently, the dependence of a blade's vibrations on the azimuth is identical for all of the blades. This fact in turn makes it possible to restrict his calculations to a single blade. His method follows published programs for designing helicopter rotors but features several additions, including refinement of the blade's deformations with consideration for the additional forms of the shaft's vibrations, refinement of the aerodynamic and inertial loads and deformation equations, and introduction of a harmonic analysis at the end of each rotation of the rotor coupled with a determination of the coefficients c_n the fundamental transfer harmonic for the forces and moments acting on the rotor's shaft. The results obtained for 10 rotations of the rotor are averaged to increase the precision of the calculations. The program developed to execute the algorithm allows for one calculation with a stationary rotor shaft and 12 calculations in which one of the components of the vector of the rotor's reaction to shaft vibrations equals 0. Sample calculations were performed for a two versions of a helicopter with an eight-blade rotor with a diameter of 32 m, a thrust of about 50 t, and a fundamental transfer frequency of 17.2 Hz. The calculations were performed for a flight speed of 250 km/h. The calculations demonstrated that considering the vibrations of the rotor's shaft resulted in a change in the amplitude of the variable portion of the load on the shaft with respect to the transfer harmonic by as much as a factor of 4 in the first design version analyzed and by as much as a factor of 9 in the case of the second design version. Table 1; references 5 (Russian).

The Nonlinear Deformation of Discretely Stiffened Thin Shells

927F0175G Kazan IZVESTIYA VYSSHIKH UCHEBNIKH ZAVEDENIY: AVIATIONNAYA TEKHNKA in Russian No 2, Apr-Jun 91 (manuscript received 24 Dec 90) pp 70-74

[Article by B.A. Antufyev; UDC 539.3:629.7.02]

[Abstract] The author of this article has performed a mathematical analysis of the problem of the two-dimensional strained state of flexible shells with small elastic arbitrarily shaped stiffening members in a plane. The stiffening members were considered to be sections of the shell's surface with a locally changing thickness. The deformations of the structure were assumed to be small, and the displacements were assumed to be finite. These assumptions are said to be consistent with the simplest version of the theory of flexible shells that gives consideration to nonlinear terms in a quadratic approximation in Cauchy relationships. The least squares method was used to solve the problem formulated because it permits the use of finite elements as a way of approximating accumulations of any shape in a plane. The matrix of the geometric stiffness of the finite elements was constructed. The principle used to construct the matrix was examined by way of the example of a

plane triangular element subjected to extension-compression and bending. An algorithm was developed to investigate geometrically nonlinear deformation of discretely stiffened shells. The said algorithm is designed to be executed on a computer in the form of an object-oriented suite of programs. Sample calculations performed by using the algorithm are presented. Figures 3; references 9: 6 Russian, 3 Western.

Determining the End Losses in Turbine Cascades With Consideration for the Effect of Inlet Boundary Layer

927F0175F Kazan IZVESTIYA VYSSHIKH UCHEBNIKH ZAVEDENIY: AVIATIONNAYA TEKHNKA in Russian No 2, Apr-Jun 91 (manuscript received 17 Jul 90) pp 54-60

[Article by Ye.N. Bogomolov; UDC 621.438]

[Abstract] The author of this article has examined the problem of determining the end losses in turbine cascades with consideration for the effect of the inlet boundary layer. He constructs a model of the inlet eddy and then proceeds to use the model as a basis for deriving a formula for calculating the secondary losses in a turbine cascade in the presence of an initial boundary layer on the face wall. The hydrodynamic properties of the inlet eddy are examined without consideration for the change in velocity throughout the thickness of the outer part of the boundary layer swirled into an eddy. From a structural standpoint, the inlet eddy formed is assumed to conform to a Rankine eddy. The acceleration of the fluid inside the eddy due to the effect that the pressure gradient arising on the deceleration line at the leading edge of the blade and directed along the normal to the face wall has on the eddy is also given consideration. The elevated pressure arising in the vicinity of the deceleration of the flow at the leading edge is also considered in that it is a factor causing the eddy formed to fan out of the deceleration region along the normal to the velocity vector of the oncoming flow in the plane of the currents. Friction-induced losses are also considered. The secondary losses occurring in the channel between the blades and after the cascade are added together to obtain the total secondary losses. The author concludes by stating that the main shortcoming of the methods of calculating secondary losses is the elevation of the values of ζ_{sec} in the case where the cascade heights are relatively low (which leads to the phenomenon of the joining of secondary flows originating from the cascade's opposing face walls). He explains that the respective necessary corrections to the mathematical formulas may be derived from an analysis of the conditions of the joining of secondary currents in a cascade. Figures 2, table 1; references 5 (Russian).

The Axial Turbine Stage With the Greatest Peripheral Work

927F0175E Kazan IZVESTIYA VYSSHIKH UCHEBNIKH ZAVEDENIY: AVIATIONNAYA TEKHNKA in Russian No 2, Apr-Jun 91 (manuscript received 12 Mar 90) pp 49-53

[Article by A.A. Sergiyenko; UDC 621.438.2.081]

[Abstract] The author of this article has examined the problem of determining the parameters of the gas flow in an optimized axial turbine stage with the highest peripheral work value given specified parameters of the working medium at the turbine's inlet. The flow rate of the gas and density of the axially moving current are the problem's constraints. Solved next is the problem of finding those gas dynamic parameters of the flow at the outlet from the nozzle and the turbine wheel that result in the highest peripheral work values for the said axial turbine stage given the specified constraints. Formulas are presented for calculating the main geometric dimensions of the turbine wheel of an optimized stage. Five independent variables (λ_u , λ_1 , α_1 , λ_{w2} , and β_2) resulting in the extremum of the objective function presented are found given specified conditions at the turbine's inlet (namely, p_{00} , T_{00} , R , γ). The solutions obtained are analogous to those solutions to the problem of optimizing the parameters of a turbine that the author published in 1989. The calculations performed indicate that the highest peripheral work values are obtained for a turbine stage with supersonic velocities both at the outlet from the nozzle and in the relative motion at the outlet from the turbine wheel. These supersonic flows are characteristic in that the waves of the propagation of weak disturbances are parallel to the fronts of the blade cascades of the nozzle and turbine wheel. When this type of flow exists, the disturbances from the turbine wheel blades are "locked" in the turbine wheel and do not reach the nozzle blades, and the oblique shear of the nozzle blades does not come into play. In order for an axial turbine stage to have the highest peripheral work values, the Mach numbers for the axial components of the flow velocities should equal 1. In a stage with the highest peripheral work values, as much as 20 to 50% of the thermal energy of the turbine wheel at the inlet to the turbine may be converted into mechanical energy. Figures 2; references 2 (Russian).

The Synthesis of Nonlinear Controllers To Stabilize Objects Damaged by Parametric and External Effects

927F0175C Kazan IZVESTIYA VYSSHIKH UCHEBNIKH ZAVEDENIY: AVIATIONNAYA TEKHNKA in Russian No 2, Apr-Jun 91 (manuscript received 7 May 90) pp 18-22

[Article by B.V. Ulanov; UDC 62-50]

[Abstract] The author of this article has worked to synthesize nonlinear controllers to stabilize objects damaged by external effects. The damage may be measurable or immeasurable. The parameters of the object and an exogenous dynamic model of the external effects are assumed to be unknown and may vary within broad bounds, as is characteristic of flight control problems. Methods are proposed for designing a system with a variable structure where the said limits are known, as well as for designing a controller with parameters that may be adjusted based on adaptation laws when the bounds of their variation are not known. A system with

discontinuous control without sliding modes is also considered. References 7 (Russian).

Effect of the Scale of the Inhomogeneity of an Oncoming Flow on the Characteristics of Combustion in the Afterburner of a Bypass Engine

927F0176C Kazan IZVESTIYA VYSSHIKH UCHEBNIKH ZAVEDENIY: AVIATIONNAYA TEKHNKA in Russian No 3, Jul-Sep 91 (manuscript received 17 Oct 90) pp 35-39

[Article by V.N. Gruzdev and I.Ye. Kuznetsov; UDC 533.6.35]

[Abstract] To date, the main emphasis when designing mixers for bypass engine afterburners was on reducing the pressure loss of the internal path of the mixers and afterburner overall. The problem of matching the parameters of the mixer and the characteristics of combustion in the afterburner was largely ignored. The authors of this study conducted an experimental study of the effect that the type of lobed mixers and cavity width have on the completeness of the burnup of a fuel-and-air mixture in a model afterburner. Most such research has examined homogeneous mixtures so as to exclude the additional effect of fuel distribution. The study reported herein, however, examined the case of a heterogeneous (i.e., kerosene and air) mixture. The unit in which the studies were performed contained two channels and featured separate control and measurement of the air flow rate and independent heating of the air in each channel. The working section of the unit consisted of three compartments. The first contained a lobed mixer; the ratio of the total area of the cavities of the outer and inner loops amounted to $f = 1.22$. The second compartment (length, 0.2 m; cross section, 110 x 210 mm²) contained a flame stabilizer with flanged edges located along the normal to the flow axis. The stabilizer was mounted on the center line along the cavities' height at a distance of 110 mm from the mixers' edge. For the nonisothermal case involving heterogeneous fuel mixtures in the second compartment, fuel was fed to the injectors from three lines: to the carburetor, to the stabilizer walls, and to the flow. Stream-type injectors were used. The third compartment was a combustion chamber 1.1 m long. Its walls were cooled with water. Mixers with characteristic cavity sizes were studied (i.e., $b = 30, 47.5$, and 95 mm). The mixers had corrugated components with the depth of the corrugation increasing along the direction of the flow. The mixers were also provided with straightening segments in the form of corrugations of a constant height equal to the height of the corrugations at the mixer's outlet. This was done to reveal the effect of secondary eddy currents. The completeness of heat release was determined by the method of gas analysis by using a single-point gas sampler. Gas samples were taken at eight points along the combustion chamber's cross section at a distance of 1.2 m from the mixer's edge. The ratio of the velocities of the streams of the "outer" and "inner" loops was varied: ratios of 1 and 1.5 were used. The ratio of the temperatures for the

nonisothermal case was 1.64. The coefficient of excess air ranged from 0.8 to 3.5, the average mass velocity of the oncoming flow amounted to 80 m/s, and the average mass temperature amounted to 623 K. Equipment manufactured by DISA was used to measure the turbulence characteristics. The experiments performed established that the average intensity of the turbulence beyond the mixer's edge increases as the size of the mixer cavity increases. This same pattern was discovered in the cases of both an even velocity field and a nonuniform velocity. A velocity shift in the mixing chamber was found to result in an increase in the level of the average values of turbulence intensity regardless of the mixer's geometry. The maximum completeness of burnup occurred when the coefficient of excess air was between 1.3 and 1.4. The presence of a velocity nonuniformity was found to result in a marked increase in the coefficient of the completeness of heat release for mixers with straightening segments. The effect of the ratio of the flow speeds in the inner and outer loops on combustion characteristics was much less pronounced in the said mixers. The completeness of fuel burnup turned out to be much higher after short mixers without straightening segments regardless of whether the air flow rate was uniform or not. Increases in mixer cavity size were, contrary to expectations, found to result in an increase in the values of the mean integral completeness of burnup in the cases of both short and elongated lobed mixers. The overall level of total burnup of the oncoming flow for the kerosene-and-air mixture and specific chamber design studied was found to range from 58 to 92%. The maximum total burnup was achieved when the coefficient of excess air (α) was between 1.6 and 1.8. When α approached the stoichiometric value, there was a marked decrease in completeness of burnup. Depleting the mixture all the way to $\alpha = 3$ had an insignificant effect on the completeness of burnup. On the basis of the studies performed, the authors concluded that from the standpoint of achieving maximum completeness of burnup in an afterburner, mixers with small cavity dimensions must not be used. The configuration of the air flow of the mixer cavities must be such that the formation of secondary eddy currents is not suppressed. The authors further concluded that their results are well explained from the standpoint of the theory of turbulent combustion with consideration for the effect of the characteristics of the turbulence of an oncoming flux. Figures 4; references 3 (Russian).

Problems in Designing Pyrolytic Drives

927F0176D Kazan IZVESTIYA VYSSHIKH
UCHEBNIKH ZAVEDENIY: AVIATSIONNAYA
TEKHNICA in Russian No 3, Jul-Sep 91 (manuscript
received 14 Jan 91) pp 87-90

[Article by A.B. Kondratyev, V.A. Chashchin; UDC
629.7.062]

[Abstract] The authors of this study use the term "pyrolytic drive" to refer to a system consisting of a solid-propellant compressed gas source and a piston pneumatic engine with unilateral action. They present a mathematical analysis of the main problems that must be considered when designing pyrolytic drives for aircraft automation systems. First, they consider the problem of ensuring that the pyrolytic drive will have a stable activation time and will perform a specific amount of mechanical work. A series of six dependences are introduced as a starting equation system for describing the process of the movement of the drive's piston and loading. The equations presented make it possible to use iteration methods to find the time dependence of the pyrolytic drive's components given known parameters, as well as to find those parameters that will satisfy specified performance requirements. An approximation solution of the formulated problem is examined. The pyrolytic drive design examined is said to result in the maximum moving-part velocity at the end of the piston's course while reaching a stop. The case where damping springs are required to reach a stop without impact in the same fixed activation time is also examined. The equations presented for the latter case may be solved numerically. Figures 3; references 3 (Russian).

The Problem of Diagnosing the Operating Mode of Aircraft Engine's Air Intake

927F0176F Kazan IZVESTIYA VYSSHIKH
UCHEBNIKH ZAVEDENIY: AVIATSIONNAYA
TEKHNICA in Russian No 3, Jul-Sep 91 (manuscript
received 13 Mar 91) pp 105-107

[Article by S.V. Puzach, Yu.A. Polyakov, Yu.M. Markvit, and N.N. Zakharov; UDC 629.7.062.3]

[Abstract] The authors of this study conducted an experimental study to determine the possibility of using a film thermal converter as a transducer providing information about the operating mode of an aircraft engine's air intake. Unlike conventional receivers, the said thermal converter reacts to a change in the coefficient of heat emission, which may be used to fix the position of the closing normal shock wave. The proposed method is based on the known principle that the interaction of a closing normal shock wave and turbulent boundary layer on a wall at Mach numbers of 1.3 or less results in separation of the flow and the formation of an eddy zone in which heat transfer at the wall changes sharply versus that in the case of an attached flow. The experimental stand included a module with a film resistance thermometer that in turn included a thermometric recording unit, digital voltmeter, and electromagnetic oscillograph. The film resistance thermometer's operation was modeled mathematically in terms of the heating of an unbounded plate that was in thermal contact with a half-space. The sensitive element of the film resistance thermometer was made of a metal (platinum) film by cathode sputtering. The thickness of the sensitive element (about 0.1 μm) was such that its heat-accumulating capacity could be ignored. The working area of the sensitive element's

surface ranged from 0.4 to 1.6 mm². The sensitive element had a linear static calibration function $R = f(T)$ all the way to $T \approx 700$ K (R being the film's resistance). The film resistance thermometer was mounted flush with the air intake's wall. During the course of the experiments, a choke was used to move the closing normal shock wave from a mode of exiting the air intake to a pumping mode. For each mode, measurements were taken of the braking pressure before the air intake and at its output and the distribution of static pressure along the air intake's length. Measurements were taken by means of DMI pressure transducers and by film resistance thermometers. During the experiments, the low-ohm film resistance thermometer ($R = 45$ ohms at $T = 293$ K) was heated to about 100 K. The characteristics of the film resistance thermometer remained unchanged during the 2 hours of experiments performed. The position of the closing normal shock wave at each moment in time was determined from the distribution of static pressure along the length of the air intake. When the said value decreased to a specified point, a signal was issued indicating that the closing normal shock wave had moved from the air intake's outlet to its neck. The studies performed revealed that the output signal from the film resistance thermometer was more distinct and provided earlier tracking of the position of the normal shock wave in the channel than did the DMI sensors used. On the basis of their experiments, the authors concluded that film resistance thermometers may fulfill two functions in an air intake control system. First, they may be used to signal an emergency stop (surge). Second, they may be used to monitor the conditions of the establishment of the flow before the combustion chamber. The film resistance thermometers tested were found to possess three significant advantages over sensors reacting to a change in pressure pulses: The film resistance thermometers were faster, they were unaffected by random fluctuations of the pressure in the flow, and they were not noticeably affected by noise. Further testing of the proposed method of using film resistance thermometers to monitor the operation of an aircraft engine's air intake over a broad range of flow parameters (Mach and Reynolds numbers and braking temperatures, etc.) was recommended. Figures 2; references 2 (Russian).

Optimizing the Startup of Mobile Power Plants

927F01751 Kazan IZVESTIYA VYSSHIKH
UCHEBNIKH ZAVEDENIY: AVIATIONNAYA
TEKHNIKA in Russian No 2, Apr-Jun 91 (manuscript
received 12 Nov 90) pp 91-91

[Article by L.S. Vernovskiy, V.N. Kashin, and M.A. Edelshteyn; UDC 621.311.28:629.7.064]

[Abstract] Mobile power plants consisting of an electric generator, turbodrive, and gas supply system are enjoying wide-scale use in the national economy. The authors of the study reported herein have examined the problem of optimizing the startup of mobile power plants. The term "optimal startup" is understood to

mean achieving the minimum startup time and minimum consumption of fuel components while still adhering to safety requirements. Startup time is defined as the time required for the turbodrive's rotor to achieve its minimum permissible rotation frequency. It is known that the rate of change in the rotor's rotation frequency is directly proportional to the power imbalance between the turbodrive and electric generator. Two possible methods of increasing this imbalance between the turbodrive and electric generator during startup of a mobile power plant are considered. The first method considered is boosting the turbogenerator's power, and the second method is reducing the power required by the electric generator. The experiments performed established that the startup regimen that is considered optimal from the standpoint of reducing both startup time and unproductive consumption of fuel components is that of starting the mobile power plants with an imbalance between power of the turbodrive and the electric generator when the electric generator's excitation current is switched off. Doing so reduces the startup time by 50%. Figures 3; references 4 (Russian).

An Analysis of the Trajectories of an Energy Model of an Aircraft's Motion

927F0176B Kazan IZVESTIYA VYSSHIKH
UCHEBNIKH ZAVEDENIY: AVIATIONNAYA
TEKHNIKA in Russian No 3, Jul-Sep 91 (manuscript
received 5 Feb 91) pp 20-25

[Article by K.A. Pavlov and A.A. Gorelov; UDC 629.735.33.016]

[Abstract] The authors of this study have performed a mathematical analysis of a family of extremal trajectories of an energy model of motion, as well as the properties and characteristic features of the said trajectories. The analysis is based on the assumptions that the mass of the aircraft and the number of rotations of its engines are both constant and that the aircraft's thrust, air drag, and fuel consumption are all known functions of the flight velocity and altitude. The qualitative study of a family of extremal trajectories that is presented is general in nature. The results of the theoretical analysis are illustrated and confirmed by a numerical analysis based on values conforming to a typical aircraft maneuver. The analytical research presented provides a qualitative pattern of a family of extremal trajectories for an entire set of boundary conditions. These trajectories may be used as an initial approximation when solving optimization boundary value problems, and the results of the research presented may be used when developing automatic trajectory control systems. Figures 4; references 6: 4 Russian, 2 Western.

Calculating Heat Transfer in Model Nozzles

927F0176E Kazan IZVESTIYA VYSSHIKH
UCHEBNIKH ZAVEDENIY: AVIATIONNAYA
TEKHNIKA in Russian No 3, Jul-Sep 91 (manuscript
received 3 Dec 90) pp 90-94

[Article by V.G. Zubkov; UDC 532.5]

[Abstract] The author of this study has proposed a method of calculating the parameters of a flow in thermal power plants that is based on a mathematical model of a boundary layer for a wide range of turbulent Reynolds numbers. By directly solving boundary value equations, the author is able to discover local characteristic features in the flow and the role of the prehistory of the boundary layer's development. He is also able to establish a link between the flow's parameters by considering the temperature and pressure dependence of the properties of the working medium. The boundary layer is assumed to be stationary, and the effect of body forces and body sources on the processes of heat and pulse transfer are not considered. A semiempirical modified ϵ - ϵ model of turbulence is used for closure of the system of Reynolds and energy equations. The main differences between the said model and the basic model as published elsewhere lie in (1) the form of the representation of the equations of the intensity of the turbulence (ϵ) and dissipation (ϵ) and in (2) the closing relationships. The proposed model does not use several of the terms used in the basic model. A corrective function is introduced, however, to allow for the characteristic features of turbulent transfer in the near-wall region of the flow, where turbulence is anisotropic in nature. The purpose of introducing this term was to restrict the growth of the term for degradation of dissipation close to the wall from 0 to 1. The specific form of the said function is determined by a numerical experiment proceeding from the conditions of the best fit of the average velocity profiles and the intensity of turbulence with the experimental data for different flow modes. The proposed model makes it possible to discover the effect of the dissipation of kinetic energy on the nature of the flow without the introduction of any correcting function. A computer experiment confirmed the model's validity. The studies conducted and presented herein indicate that the proposed method may be used as an engineering method when designing or checking the designs of the nozzle units of thermal power plants. When the method is used for such purposes, the flow outside the boundary layer is

considered to be one-dimensional, and no allowance is made for the effect of the boundary layer. Figures 4; references 12: 9 Russian, 3 Western.

A Second Type of Steady Motions of Two Gravitating Bodies: Axisymmetric and Spherical-Symmetric

927F0174A Leningrad VESTNIK LENINGRADSKOGO UNIVERSITETA: MATEMATIKA, MEKHANIKA, ASTRONOMIYA in Russian No 3, Jul 91 (manuscript received 30 Aug 90) pp 92-97

[Article by S.N. Kirpichnikov; UDC 521.12:531.55]

[Abstract] This article is a continuation of the author's work on the subject of the possible types of steady motion of two gravitating bodies in relation to one another. In this article, the author turns his attention to coplanar steady motions of the second type. Such motions are characterized by the fact that the gravity center O of the axisymmetric body M is the center of the circular orbit of the spherically symmetric body (M_0). The said motions are a generalization of the motions of an "arrow," "quasi-arrow," and arbitrary axisymmetric body M . By rejecting the generally accepted very specific models of the gravitational field of the body M , the author is able to arrive at qualitatively new results. Specifically, he presents five theorems related to the classification and conditions of the orbital stability of the axisymmetric and spherically symmetric steady motions of two gravitating bodies in relation to one another. Through these theorems he is able to demonstrate that an axisymmetric body that is asymmetric relative to the equatorial plane can effect the motion of an "arrow" and that the motion of a "quasi-arrow" and its generalizing motion in the noncoplanar case may also be effected by the symmetric body relative to the equatorial plane of the axisymmetric body. The author states that these results may, with only slight modification, be applied to the random potential interaction of bodies with an axisymmetric potential. References 7 (Russian).

The Reflectivity and Refractivity of ZnS-Based Mono- and Polycrystalline Materials

927F0153A Leningrad OPTIKO-MEKHANICHESKAYA PROMYSHLENNOST in Russian No 7, Jul 91

(manuscript received 14 Mar 90) pp 3-5

[Article by N.A. Nazarova, Leningrad Institute of Precision Mechanics and Optics; UDC [535.312+535.32]:681.7.03]

[Abstract] The author of the study reported herein investigated the variance of the refractivity $n(\lambda)$ and reflectivity $R(\lambda)$ of zinc sulfide-based mono- and polycrystals. The following materials were studied: KO-2 (produced by hot molding), KO-2V (also produced by hot molding), PO-2 (produced by vacuum sublimation), and ZnS monocrystal (grown by the Bridgman method). The key parameters of elementary cells of the study specimens were determined from roentgenograms taken by using a DRON-5 diffractometer ($\Delta a = \pm 0.003$ Å), their densities were determined by hydrostatic weighing ($\Delta d = \pm 0.001$ g/cm³), and information regarding their grain size was obtained from microscopy (MIK-4) surface studies. The variance of $n(\lambda)$ was measured in the spectral range $\lambda = 0.8$ to 12 μ m at a temperature of $T = 20^\circ\text{C}$ on prisms by the least deviation method as described elsewhere. The reflection spectra $R(\lambda)$ were measured at room temperature in the range $\lambda = 0.2$ to 2.5 μ m on a model 330 Hitachi spectrophotometer and in the range $\lambda = 2.5$ to 50 μ m on a model 580 Perkin-Elmer spectrophotometer. The error of the reflectivity measurements did not exceed ± 0.01 . Analysis of the experimental data (which are summarized in table form) revealed satisfactory pairwise agreement ($\Delta n \leq \pm 0.0002$) of the measured values in monocrystals and the material PO-2 on the one hand and the materials KO-2 and KO-2V on the other hand. The discrepancies of the experimental data from material to material did not exceed the bounds of the experimental error. Further analysis revealed that the data obtained in the study reported herein were in good agreement with data regarding the hot-molded material KO-2 that were published by Bogdanov in 1987. The observed increase in the refractivity of the hot-molded specimens as compared with monocrystals or sublimates was found to be negative and amount to $\Delta n \approx 13 \times 10^{-4}$. Δn was found to increase in the short-wave region of the spectrum as a function of radiation wavelength; however, the monotonic nature of the dispersion dependence $\Delta n(\lambda)$ was maintained through the entire region of the spectrum investigated. The observed increase in Δn is in good agreement with the characteristic features of the study reflection spectra $R(\lambda)$ and indicates that the edge of intrinsic absorption is shifted to the short-wavelength range in the case of KO-2 (as compared with its monocrystalline counterpart). Figure 1, tables 1; references 7: 4 Russian, 3 Western.

Using a Rough Surface To Improve the Characteristics of Neutral Light Filters

927F0153Q Leningrad OPTIKO-MEKHANICHESKAYA PROMYSHLENNOST in Russian No 7, Jul 91 pp 66-68

[Article by M.A. Validov, candidate of technical sciences, G.S. Belous, R.T. Galyautdinov, and V.L. Tonkov, State Institute of Applied Optics, Kazan, and L.M. Rykova, Orion Scientific Production Association, Moscow; UDC 681.7.064.42-408.8]

[Abstract] The authors of this study have examined a new method of manufacturing neutral optical light filters entailing the combined use of a scattering surface and a metallic chromium film with a transmissivity unevenness in the spectral range from 5 to 12 μ m. Type ERKh electrical chromium was vaporized from a debiteuse made of tungsten foil 0.05 mm thick. Germanium substrates were placed a distance of 260 mm from the vaporizers and were subjected to planetary rotation during the vaporization process. The substrates were heated by a nichrome spiral located above them. The substrates' temperature was kept between 200 and 250°C . The coatings were deposited at a pressure of 1.33 to 2.66×10^{-3} Pa, and the vaporization time ranged from 10 to 60 seconds depending on the required transmission of the neutral optical filters. The thickness of the metal coatings was monitored based on the change in the transmission of a control specimen at the wavelength of an He-Ne laser ($\lambda = 0.63$ μ m). The spectral coefficient of neutral optical filters manufactured based on a chromium coating was found to decrease as the wavelength increased in the range from 5 to 12 μ m. The unevenness of transmission in the given region was also observed to increase as the density of the neutral optical filters increased. Further tests revealed that using a rough surface in neutral optical filters significantly improves the evenness of the transmissivity of filters with a chromium coating. Optimal surface roughness was found to result in neutral optical filters with a transmission of 0.3 to 5% , with the unevenness of the said filters not exceeding 10% in the spectral region from 5 to 12 μ m. Neutral optical filters manufactured by the new process were found to withstand the following test conditions without any change in their optical properties: a relative humidity of $95 \pm 3\%$ at a temperature of $30 \pm 2^\circ\text{C}$ for 3 days and a temperature change from -60 to $+85^\circ\text{C}$ in three cycles. The mechanical strength of the neutral optical filters produced was at a level of at least group 1 according to branch standard OST 3-1901-85. Figures 3, tables 2; references 3 (Russian).

The New Titanium Flint TF14: Its Composition, Properties, Advantages

927F0153N Leningrad OPTIKO-MEKHANICHESKAYA PROMYSHLENNOST in Russian No 7, Jul 91

(manuscript received 9 Jan 90) pp 50-52

[Article by V.Ye. Galant, candidate of technical sciences, V.N. Polukhin, doctor of technical sciences, and L.N.

Urusovskaya, candidate of chemical sciences, State Optics Institute imeni S.I. Vavilov VNTs; UDC 666.221.4]

[Abstract] The USSR produces five titanium flints (LF8, LF9, LF12, F9, and TF11) with refractivities of 1.543 to 1.654. Until recently, the only one of the heavy titanium flints to be used was TF11, which has a refractivity of 1.6536. The new titanium flint TF14 was developed in an effort to meet the increasing demand for high-quality optical systems. The glass TF14 is unrivaled among optical glasses both in the USSR and abroad. It is the only titanium flint with a refractivity of about 1.7, and it is distinguished by its high mass content of titanium dioxide (25%). It also contains germanium and niobium oxides and potassium bifluoride. This unusual composition is responsible for the unique properties of TF14 titanium flint. TF14 is an analogue of TF8 from a refractivity standpoint, but it has a lower Abbe number (by 2.0), and its relative scattering in the dark blue region of the spectrum is increased to the level of titanium fluoride flints. Another big advantage of TF14 is its low density (3.00 g/cm^3) versus that of its analogue TF8 (density, 4.23 g/cm^3). It is significantly more resistant to the effects of radiation than other existing heavy flints. TF14 also boasts a high chemical stability (it is a grade A material with respect to stability in a humid atmosphere, and it is a group 1 material with respect to susceptibility to spotting). Because TF14 contains a significant amount of titanium dioxide, it has high annealing number values, and like all titanium-containing glasses, it changes its scattering upon annealing. It has a quenching temperature of 615°C and a quenching number of 101×10^{-4} . TF14 may be manufactured in blanks up to 250 mm in diameter. Table 2; references 7 (Russian).

An Analysis of the Illumination Engineering Characteristics of the Viewfinder of a Reflex Still Camera

927F0153G Leningrad OPTIKO-MEKHANICHESKAYA PROMYSHLENNOST in Russian No 7, Jul 91
(manuscript received 14 Mar 90) pp 26-28

[Article by A.V. Gitin, candidate of physical and mathematical sciences, State Optics Institute imeni S.I. Vavilov VNTs; UDC 771.371.5]

[Abstract] A method is described for analyzing the illumination engineering characteristics of the viewfinder of a reflex still camera that makes it possible to use the illumination engineering characteristic as a basis for estimating the indicatrix of a mat focusing screen. The method makes use of the concept of the aperture ratio of a reflex camera's viewfinder that the author introduced in a previous publication. After processing the illumination characteristics of several main foreign reflex cameras in accordance with the proposed method, the author determined that the indicatrix of the mat focusing screens of the Pentax-LX, Nikon-F, and Contax-137 is 2

arctg $1/8$, while that of the Canon-new-F1, Nikon-F3, and Minolta-XC is 2 arctg $1/5.6$. Figures 4; references 7 (Russian).

The Scattering of Surface Electromagnetic Waves on the Rough Surface of a Metal Grating

927F0153B Leningrad OPTIKO-MEKHANICHESKAYA PROMYSHLENNOST in Russian No 7, Jul 91
(manuscript received 28 Jun 90) pp 5-8

[Article by S.P. Surov, candidate of physical and mathematical sciences, and V.A. Sychugov, candidate of physical and mathematical sciences, General Physics Institute, USSR Academy of Sciences; UDC 539.211:537.874]

[Abstract] The authors of the study reported herein conducted an experimental study of the scattering of visible and near-IR surface electromagnetic waves on rough (corrugated) aluminum and silver photolithographic gratings. First, they modified the existing formulas that have been derived to determine the roughness parameters of diffraction gratings to allow for the characteristic features of a corrugated grating. Next, they performed a series of experiments to determine the roughnesses of photolithographic diffraction gratings sprayed with silver or aluminum films $0.15 \mu\text{m}$ thick. Various grating periods ($\Lambda = 3,500$ to $7,800 \text{ \AA}$) and depths ($2\sigma = 400$ to $1,100 \text{ \AA}$) were used. RN-27 and SK-17 photoresists were used. Surface electromagnetic waves were excited by an LG-126 He-Ne laser at wavelengths of 0.63 and $1.15 \mu\text{m}$, and the radiation was recorded by FEU-62 and FD-10g detectors, respectively. The measured values were as follows: $Q = 0.5 \pm 0.05 \mu\text{m}$, and $\delta = 110 \pm 20 \text{ \AA}$. The value obtained for Q from the dependence $S(K)$ in accordance with the modified formula derived by the authors was found to be in good agreement with values published elsewhere. During the course of the experiments, the authors discovered an effect that is possibly the surface analogue of intensification of the backscattering of radiation. Specifically, the authors observed a strong scattering corresponding to surface electromagnetic waves propagated in the direction opposite to the initial wave propagation. Figures 2; references 6: 5 Russian, 1 Western.

Optimization of a Channel Amplifier Based on Noise Factor

927F0153D Leningrad OPTIKO-MEKHANICHESKAYA PROMYSHLENNOST in Russian No 7, Jul 91
(manuscript received 13 Oct 89) pp 11-14

[Article by V.N. Yevdokimov, candidate of physical and mathematical sciences (Severo-Osetinsk State University), Vladikavkaz, A.M. Tyutikov, doctor of physical and mathematical sciences, Yu.A. Flegontov, doctor of

physical and mathematical sciences, and A.V. Shiman-skaya (Kiev Polytechnic Institute, Chernigov), State Optics Institute imeni S.I. Vavilov VNTs; UDC 537.533.3]

[Abstract] The main flaw of systems with microchannel amplification is their high noise factor. In the case of discrete dynode systems, other researchers have emphasized the need to increase the coefficient of secondary electron emission of the first dynode in order to reduce the amplification noise of the system overall. The authors of the study reported herein have conducted a theoretical investigation of the effects arising when a layer with increased secondary emission is formed at the channels' entrance. Specifically, they developed a theoretical model of the following scenario: The electrons of a parallel monochromatic flux fall onto the entrance plane of a microchannel amplifier. The electrons entering the channel collide with the walls at different angles with various incidence coordinates and knock out the secondary electrons, which are amplified before the channel exit. A conductive contact layer with a high coefficient of secondary electron emission is sprayed onto the channel amplifier's entrance, and an effective emitter is applied to the said layer. Because there is no drop in potential along the conductive layer, the conditions of the motion of the secondary electrons in this region are very different from motion in a homogeneous field. The process of electronic amplification thus has characteristics that are different from those conventionally examined in a homogeneous field. Both the Monte Carlo and a generalization of Burgess' theorem are used to model the processes of electronic amplification occurring in the channel. The mathematical analysis presented demonstrates the effectiveness of the method (developed here and in previous articles) of sequential and parallel stages in statistical calculations. The calculations performed indicate that the noise factor is an extremal function of the depth of spraying and the angle of incidence of the primary electrons. The results presented make it possible to use adjusted nomograms as a basis for selecting microchannel amplifier operating modes for specific systems that are optimal from a noise factor standpoint. Figures 3; references 8; 6 Russian, 2 Western

Low-Noise Avalanche Photodiodes To Record Laser Signals in the Spectral Range From 1.5 to 2.5 μm

92⁷F0153F Leningrad OPTIKO-MEKHANICHESKAYA PROMYSHLENNOST in Russian No. 7, Jul 91
manuscript received 26 Jun 90; pp 19-23

[Article by I.A. Andreyev, A.N. Baranov, candidate of physical and mathematical sciences, M.P. Mikhaylov, doctor of physical and mathematical sciences, Physics Technology Institute imeni A.F. Io. fe, Leningrad, and M.V. Voznitskiy, B.A. Yermakov, doctor of technical sciences, professor, and general director, T.N. Sirenko,

and Yu.P. Yakovlev, candidate of physical and mathematical sciences, State Optics Institute imeni S.I. Vavilov VNTs; UDC 621.383.52:621.373.826]

[Abstract] The authors of this study worked to develop low-noise avalanche photodiode structures with separate absorption and amplification regions. In the structures developed the absorption region was made of a solid solution of n-GaInAsSb ($E_g = 0.52$ eV), and the amplification region was made of a solid solution of n-Ga_{1-x}Al_xSb of resonance composition ($x = 0.04$ and $E_g = 0.76$ eV). Grown on top of this layer was a wider-band layer of the solid solution Ga_{1-x}Al_xAsSd_{1-x} ($x = 0.34$ eV, $E_g = 1.2$ eV). Its purpose was to ensure that radiation would enter the structure efficiently. The avalanche photodiodes with separate absorption and amplification regions were produced by liquid-phase epitaxy on n-GaSb substrates in accordance with a method detailed elsewhere. The concentration of charge carriers ranged from 5 to $7 \times 10^{15} \text{ cm}^{-3}$ in the absorption region and amounted to $8 \times 10^{16} \text{ cm}^{-3}$ in the amplification region. The mesa diodes were $260 \mu\text{m}$ in diameter. The breakdown voltage of the said structures was between 10 and 20 V, and the avalanche gain factors ranged from 30 to 45 at $T = 300$ K. The time constant of the avalanche photodiode, as measured with illumination through a lightguide fiber by light pulses of a semiconductor laser with $\lambda = 1.3 \mu\text{m}$ at a load of $R = 50$ ohms, was less than 1 ns. The spectral characteristics of the structure at $T = 300$ K were found to be typical for heterophotodiodes, and a current sensitivity of $> 0.6 \text{ A/W}$ was provided in the spectral range from 1.6 to 2.2 μm with a maximum in the region from 2.0 to 2.1 μm ($S_A = 1 \text{ A/W}$). The new avalanche photodiodes with separate absorption and amplification regions were also found to be characterized by a low coefficient of excess avalanche amplification noise ($F = 1.6$ at $M = 10$ ($b = 0.2$)). These and other findings presented confirm that the new GaInAsSb-GaAlAsSb avalanche photodiodes are promising for use as pulsed radiation detectors for laser detection and ranging systems in the wavelength range from 1.7 to 2.5 μm . Figures 6, tables 2; references 14; 8 Russian, 6 Western

Induced Absorption in Interference Filters

92⁷F0153H Leningrad OPTIKO-MEKHANICHESKAYA PROMYSHLENNOST in Russian No. 7, Jul 91
manuscript received 5 Apr 90; pp 29-32

[Article by V.A. Proshin, Siberian Institute of the Earth's Magnetism and Radio Wave Propagation, Siberian Department, USSR Academy of Sciences, Irkutsk; UDC 535.345.67]

[Abstract] The key parameters of interference filters are known to fluctuate over the course of time for various reasons. Their wavelength of maximum transmission and half-width and transmission at the maximum all change under the effect of atmospheric moisture, for example. The wavelengths of maximal transmission also

change under the effect of UV radiation and temperature. These changes are irreversible and due primarily to changes in the layers of the interference filters. The author of this study has discovered fundamentally new and reversible changes in the parameters of interference filters. During the course of his research, he observed that the location of the interference filter in relation to the light source, monochromator, and photoreceiver all have a significant effect on transmission at the maximum and on half-width. He compared the measurements taken when two different optical trains were used. In the first case, the filter being measured was placed in front of the monochromator's inlet slit and illuminated with white light. In the second case, the filter was placed after the outlet slit and illuminated with monochromatic light. A comparison of the two sets of results revealed that interference filters' half-width and transmission at a maximum both change when the filter is struck by the short-wave component of light (wavelength, <450 nm). Experiments conducted by using stacks of eight quarter-wave $\text{ZnSO}_3\text{Na}_3\text{AlF}_6$ films on four identical substrates and a half-wave ZnS film established that the change in half-width decreases as the order of the interference filter increases. This in turn was taken as evidence that absorption increases not in the separating layer but rather in the first layers of the interference filter constituting the reflector. This finding is in agreement with the fact that layers of ZnS and ZnSe are highly absorbent in the range of wavelengths shorter than 450 nm so that the short-wave light never even reaches the separating space because it has already been absorbed by the first ZnS (ZnSe) layers. The author concludes by stating that these reversible changes must be taken into consideration when narrowband interference filter are filters are used by designing the optical system so that short-wave light does not fall directly on the interference filter. In other words, a filter cutting off the short-wave light should be placed before the main interference filter. Figures 4, table 1; references 3: 1 Russian, 2 Western.

The Aperture Characteristics of Corner Cat's Eyes

927F0153L Leningrad OPTIKO-MEKHANICHESKAYA PROMYSHLENNOST in Russian No 7, Jul 91
(manuscript received 1 Aug 90) pp 42-46

[Article by S.V. Protsko, candidate of physical and mathematical sciences, and A.D. Titov, candidate of physical and mathematical sciences, Applied Physics Problems Scientific Research Institute: UDC 681.7.062.7]

[Abstract] Corner cat's eyes reflect the light falling on them backward regardless of their orientation in space. The magnitude of the luminous flux reflected by them depends on the sighting direction, however. The characteristic features of the effect of corner cat's eyes ($\pi/2$, $\pi/2$, $\pi/2$) that change their spatial position relative to the incident radiation have been examined in a number of publications. There is a family of corner cat's eyes in the form of trihedral angles: $\pi/2$, $\pi/2$, π/s , where s is some even integer (with the right-angle cat's eye representing

just one particular case, i.e., the case where $s = 2$). The authors of the study reported herein worked to examine the aperture characteristics of corner cat's eyes ($\pi/2$, $\pi/2$, π/s). First, they derived analytical formulas for cat's eyes with equal lateral edges. Next, they found those cat's eye designs that are optimal for various size conditions from the standpoint of their working aperture areas. Finally, they have presented three tables of data that may be used in selecting a cat's eye with specified aperture characteristics. The relationships presented are said to be valid for hollow corner cat's eyes. When prismatic cat's eyes are being dealt with, consideration must be given to the refraction at the frontal face. In other words, exterior rather than interior angles of incidence must be considered. Figures 4, tables 3; references 10: 9 Russian, 1 Western.

The Effect of Changes in Laser Recorders' Operating Mode Parameters on Image Quality

927F0153E Leningrad OPTIKO-MEKHANICHESKAYA PROMYSHLENNOST in Russian No 7, Jul 91
(manuscript received 29 Mar 90) pp 14-19

[Article by A.A. Brazhnik, Siberian Scientific Research Institute of Optical Systems, Novosibirsk; UDC 621.373.826]

[Abstract] The author of this study has examined the effect that changes in the operating mode parameters of laser recorders have on the quality of the images they record. The effects that defocusing and changes in laser power level have on the size d of the smallest resolvable pixel are examined for the cases of recording by means of moving and nonmoving beams. For both recording methods, the author determines the dependence of the maximum permissible defocusing and changes in laser power level (when both are used together) on the specified pixel size tolerances. He also finds the average power and laser beam construction radius required for the aforesaid. The expressions and graphs presented are recommended for use in developing devices to record graphic and half-tone images based on a CO_2 laser and the method of moving-beam recording with pulse width modulation. Figures 5; references 4: 3 Russian, 1 Western.

Calculating the Aberrations of Laser Beam Area Converters

927F0153K Leningrad OPTIKO-MEKHANICHESKAYA PROMYSHLENNOST in Russian No 7, Jul 91
(manuscript received 16 Apr 90) pp 37-42

[Article by S.I. Klimentyev, candidate of physical and mathematical sciences, V.I. Kuprenyuk, candidate of physical and mathematical sciences, and I.V. Khloponina, State Optics Institute imeni S.I. Vavilov VNTs: UDC 535.317]

[Abstract] The development of lasers with an active medium having an annular cross section has necessitated the use of converters to convert the beam cross section from a ring to a circle. This conversion is accomplished by a system of two coaxial reflecting conical surfaces of revolution that together are termed a conical converter. Numerical methods of calculating the aberrations of a conical converter have been published elsewhere. The authors of this study worked to develop analytical methods of analyzing the aberrations of a conical converter. Through a series of calculations for converters with rectilinear or cofocal parabolic cone rulings, the authors derived explicit expressions for the primary errors in the manufacture and adjustment of the said cones that result in a specified reduction in the Strouhal number of the said conical converters. Tables are presented detailing 1) the parameters of conical converters, 2) the wave front $\Phi(r, \varphi)$ at the outlet of conical converters with aberrations, and 3) the values of the primary errors of conical converters when $S_k = 0.85$. In their concluding remarks, the authors state that the relationships presented may be used to estimate the manufacturing quality and tuning precision requirements for conical converters used in amplifier circuits, whereas in cavity circuits, the said relationships should only be used as a first approximation and cannot replace numerical methods. In the HEX-DARR resonator, for example, a conical converter with non-cofocal parabolic rulings is used that converts a collimated beam into a beam with a toroidal wave front. In such cases the use of numerical methods to calculate aberrations is unavoidable. Figures 2, tables 3; references 18; 12 Russian, 6 Western.

Liquid Optical Media With a Unique Dispersing Action

92*F01530 Leningrad OPTIKO-MEKHANICHESKAYA PROMYSHLENNOST in Russian No 7, Jul 91 (manuscript received 21 Aug 90) pp 53-58

[Article by V.M. Volynkin, candidate of chemical sciences, M.V. Petrova, G.T. Petrovskiy, corresponding member USSR Academy of Sciences, and M.N. Tolstoy, doctor of physical and mathematical sciences, State Optics Institute imeni S.I. Vavilov VNTs, and A.A. Tokarev, candidate of technical sciences, Krasnogorsk Machine Plant; UDC 535.324:535.328]

[Abstract] In a 1990 publication, the authors of the study reported herein recommended that lenses made of ultradispersing liquid media be used to create apochromatic lenses (systems without a secondary spectrum). In a continuation of the same line of research, they have worked to determine the physicochemical principles of creating the new class of liquid optical materials that they term ultradispersing liquid media. They began their analysis by plotting a diagram linking the relative particular dispersion ($v_{g,e}$) of optical materials with their dispersion coefficients (v'_e). A straight line conditionally termed the "normal" line was drawn through the points corresponding to the optical glasses K8 and F1. This is the line along which most of the points corresponding to

conventional optical glasses lie. The diagram illustrates that the optical constants of liquids do not satisfy the equation of the "normal" line. The unique optical properties of various media examined may be determined on the basis of the distance along the abscissa, $\Delta v'_e$, between the point corresponding to the given medium and the "normal" line given equal values of $v_{g,e}$. Different classes of organic liquids are shown to be characterized by a positive deviation from the "normal line" (i.e., $\Delta v'_e / g > 0$), whereas water and aqueous solutions of mineral acids, salts, and bases are shown to be characterized by a negative deviation (i.e., $\Delta v'_e < 0$). The authors proceed to determine the maximum absolute values of $\Delta v'_e$ that may be achieved in crown and flint ultradispersing liquid media. Next, they indicate the physicochemical factors dictating the selection of liquids with the required values of $v_{g,e}$ and v'_e in both classes. Fluorinated hydrocarbons and nitrile compounds are noted to be particularly promising as a basis for developing crown liquid media possessing high transparency in the UV region of the spectrum. The large value of $\Delta v'_e$ for particular crown liquids is said to confirm the fact that it is truly possible to create materials that can serve as a basis for the design and construction of thermally non-disarranging optical systems with liquid elements. Figures 3; references 9; 8 Russian, 1 Western.

The Effect of Glasses' Luminescence on the Results of Measuring Fiber-Optic Wafers' Light Transmission

92*F0153J Leningrad OPTIKO-MEKHANICHESKAYA PROMYSHLENNOST in Russian No 7, Jul 91 (manuscript received 26 May 89) pp 34-37

[Article by G.Ya. Konayeva, candidate of Technical Sciences, and K.P. Pecherskaya, State Optics Institute imeni S.I. Vavilov VNTs, and D.A. Pyatsi and N.K. Sokolov, Rudgeofizika Scientific Production Association, Leningrad; UDC 681.7.068.4.535.247.4]

[Abstract] The authors of this study examined the effect that the luminescence of the glasses of the original lightguides and spatial integrators have on the precision of measurements of the light transmission of fiber-optic wafers. They propose a new method of measuring light transmission based on suppressing the contribution of luminescence to the measurement results by means of spectral selection of the radiation passed through the fiber-optic wafer and integrator. They examined the equipment and technique generally used to measure the inherent luminescence of glasses in the ultraviolet range. Specifically, they studied the luminescence spectra of the MS23 milk glass and fiber-optic wafers generally used and estimated the UV boundary of light transmission. The measurements were made on a KSVU-23 spectral system that included an MDR-23 monochromator that in turn included an FEU-100 detector and digital voltmeter. A 15-IPG-128 computer system included as a component of the KSVU-23 was used to control the

monochromator and collect the test information. The studies performed indicated that errors associated with the luminescence of the spatial light integrators and starting glasses of the fiber-optic wafer can indeed result in errors in measurement of the spectral light transmission of fiber-optic wafers close to its UV boundary. The source of the distortion is an increase in light transmission in the short-wave portion of the spectrum, which is especially apparent when glass spatial integrators are used. The studies also confirmed that, because the luminescence encompasses a broad spectral range whereas the light transmission is measured at specified wavelengths, it is possible to suppress the effect of the luminescence by spectral selection. It was further demonstrated that the best method of suppressing the effect of the said luminescence is through spectral selection of the light passed through the fiber-optic wafer rather than the light falling onto it. This makes it possible to reduce the luminescence addition to the measured transmission by more than two orders of magnitude. Figures 4; references 2: 1 Russian, 1 Western.

The Effect of Machining Regimens on the Structural Changes in the Material of a Reflector's Surface Layer

927F0153R Leningrad OPTIKO-MEKHANICHESKAYA PROMYSHLENNOST in Russian No 7, Jul 91
(manuscript received 4 Jul 90) pp 71-73

[Article by I.V. Ruban and V.M. Ruban, candidate of technical sciences, Podmoskovsk Affiliate, Tractor Scientific Research Institute, Chekhov, and P.D. Dudko, candidate of technical sciences, Kharkov Economics and Engineering Institute; UDC 681.7.062:621.922.02]:620.192.4]

[Abstract] The authors of this study examined polycrystalline specimens of MOB copper to determine the interconnection between structural distortions of a mirror's surface layer and the machining technique used to produce it. The test specimens were subjected to preliminary machining on a lathe with diamond cutters and then annealed at a temperature of 600°C for 1 hour. They were then subjected to finishing treatment on a special stand with a suspension based on artificial corundum powder (grain size, M5) and machine oil in a 1:6 ratio. The technique of turning the individual specimen workpieces in relation to the stationary lapping disk and the pressure of the specimen workpieces against the lapping disk were varied from specimen to specimen. The stand used was capable of modes in which the workpieces could be moved along the lapping disk at constant and variable speeds. Cyclical speed variations were also possible. The surface material was removed by electrochemical etching in an electrolyte (a 60% solution of orthophosphoric acid) at a working voltage of 1.6 V with a linear current density of 10 A/dm. The solution temperature was held between 293 and 295 K, and the etching speed was kept at 1.0 μm/min. The degree of structural distortions on the machined reflector surfaces was measured by the change in the half-width of the

diffraction line throughout the depth of the removed layer. An analytical expression was proposed that satisfactorily describes the dependence of the half-width of the diffraction line on the depth of the removed layer for different machining modes. The nature of the change in polishing speed (i.e., whether the workpiece was moved along the lapping disk at a steady or variable speed) had little effect on the build-up of pressure of the test workpiece against the lapping disk. It was discovered that as the pressure of the workpiece against the lapping disk was increased, the half-width of the diffraction line close to the reflector's surface increased sharply because that was where the main structural changes occurred. Because of these changes it became necessary to remove more material from the surface of the workpiece in order to restore the material's starting structure. These findings underscored the need to avoid increasing the pressure of the workpiece against the lapping disk during finishing abrasive treatment of reflectors made of MOB polycrystalline copper. Figures 2; reference 1 (Russian).

The Impact of Thermal and Mechanical Effects on the Properties of a Sapphire Hollow Waveguide of IR Waveguide Lasers

927F0153I Leningrad OPTIKO-MEKHANICHESKAYA PROMYSHLENNOST in Russian No 7, Jul 91
(manuscript received 25 Sep 90) pp 32-34

[Article by Ye.R. Dobrovinskaya, candidate of physical and mathematical sciences, and L.A. Litvinov, candidate of technical sciences, Monokristallreaktiv Scientific Production Association, Kharkov, and Yu.A. Rubinov, candidate of physical and mathematical sciences, State Optics Institute imeni S.I. Vavilov VNTs; UDC 681.7.068.4]

[Abstract] Sapphire waveguides are enjoying increasing use in waveguide CO₂ lasers. Sapphire is particularly well suited for use in waveguides because of its high heat conduction and low losses in a hollow waveguide at lasing wavelengths in the spectral range from 9 to 11 μm. Waveguides with opening diameters of 2 to 4 mm make it possible to use CO₂ lasers in heterodyning, they expand the range of radiation tuning frequencies, and they increase the power of single-mode, single-frequency lasers. In view of these facts, the authors of the study reported herein studied the effect that different thermal and mechanical effects have on the structural perfection of sapphire waveguides and on their optical properties. A profilometer-profilograph was used to study the surface roughness of waveguides that had been put through various stages of machining and heat treatment. The techniques of layer-by-layer chemical polishing and selective etching were used to measure the depth of the defect layer on the study specimens. The specimens were subjected to grinding by bonded diamond with a grain size of 80/63, 60/53, and 40/28 and were then polished with a free abrasive (ASM 14/10 and 5/3) on a buffing polisher. The polished and buffed specimens were then annealed for 2 hours at a temperature of 1,950°C. The

defective layer in the ground specimens was four- to fivefold deeper than in the polished specimens. Heat treatment was found to improve the surface quality of the ground specimens significantly and to sharply reduce the depth of the defective layer and density of the dislocation on the surface. The height of the irregularities was reduced, and the average distance between them was increased. The machining class increased as well. An entirely different pattern was observed in the case of the polished specimens that had been heat-treated. Although the density of the dislocations on the surface turned out to be equal to the bulk density and although the layer with an elevated dislocation density virtually disappeared, the surface roughness of the said specimens increased. The studies performed established that producing sapphire waveguides with acceptable losses requires that they be subjected to no less than class 11 machining and that they not be subjected to heat treatment after mechanical polishing. Figures 2, table 1; references 7: 4 Russian, 3 Western.

Technology and Equipment for Precision Machining of Glass Wafers for Liquid Crystal Screens

927F0153P Leningrad OPTIKO-MEKHANICHESKAYA PROMYSHLENNOST in Russian No 7, Jul 91
(manuscript received 25 Jan 91) pp 59-62

[Article by V.S. Kondratenko, doctor of technical sciences, V.P. Strekalov, candidate of technical sciences, V.D. Kolesnik, and Yu.V. Kotlvarov, Kristall Plant, Zheleznogorsk; UDC [666.151.1:532.783]:621.923.4]

[Abstract] The authors of the study reported herein have reported on efforts to develop a technology and equipment for the precision machining of high-quality glass wafers 0.7 to 1.2 mm thick for liquid crystal screens. The technology developed consists of the following three main stages: 1) preliminary grinding by a bonded diamond tool in order to form a single-center surface, removing the defects existing on the glass surface, and trimming most of the allowance (amounting to 100 to 200 μm or more); 2) fine or finishing polishing by means of a bonded diamond tool based on an organic binder to prepare the glass surface for polishing by reducing the surface roughness to a value of $R_a \approx 0.12 \mu\text{m}$ and to finish shaping the working surface; and 3) paste-free polishing by means of elastic combination polishers to remove the discontinuous layer, obtain a class II to class III surface cleanliness depending on the given requirements, and obtain a surface micron-planarity up to $0.05 \mu\text{m}/\text{cm}$. A new type of diamond tool capable of providing a high cutting capacity at low specific pressures from 0.01 to 0.03 MPa in a self-sharpening mode was developed for use with the new technology. An epoxy-dian resin with polyethylenepolyamine as a hardener was used as the binder, and a three-component multifunctional additive was used as the

filler. An array of grinding-polishing machines in the Kristall series (the Kristall-1A, Kristall-1M, Kristall-2, and Kristall-2M) was also created for precision machining of glass plates ranging in size from 178 x 178 mm (the Kristall-1) to 350 x 350 mm (the Kristall-2). Type ZShP-320 and ZShP-350 grinder-polishers were also used in support of the new technology after their basic circuits were modified to allow for planetary machining. The technology and equipment developed made it possible to produce qualitatively new products with a surface roughness of about $0.12 \mu\text{m}$ and with a single-center working surface. Tests performed on experimental batches of plates for liquid crystal screens performed by leading enterprises in the USSR and abroad (Philips in Holland, LCD in the United States, and Samsung in Korea) confirmed that the glass plates were of a quality sufficient for use in manufacturing liquid crystal display screens based on the "supertwist" effect. Figures 4, table 1; references 5 (Russian).

Using Geometric Optics Methods To Calculate the Function of Energy Concentration in the Image of an Axial Point

927F0153M Leningrad OPTIKO-MEKHANICHESKAYA PROMYSHLENNOST in Russian No 7, Jul 91
(manuscript received 20 Feb 90) pp 47-50

[Article by V.I. Peysakhson, doctor of technical sciences, and T.A. Cherevko, State Optics Institute imeni S.I. Vavilov VNTs; UDC 535.317]

[Abstract] The authors of the study reported herein worked to develop a method of using the tools of geometric optics to calculate the concentration of energy in the polychromatic image of a point. The method presented makes it possible to model optical systems with different aberration corrections. Another advantage of the new method is that only four rays need to be calculated for each wavelength. It is moreover possible to calculate the function of energy concentration in the image of a disk of finite dimensions. Using their new method as a foundation, the authors developed a program for BESM-6 computers that could be used to calculate the function of the concentration of energy in the image of an axial point for different optical systems. Calculations performed with consideration for diffraction as well as in a geometric approximation demonstrated that in the case of wave aberrations of 2 to 3 wavelengths or more, geometric methods are sufficiently effective for an approximate estimate of optical system quality. A comparison of the results of calculations performed by using methods of wave and geometric optics confirmed that the new method yields results that are in satisfactory agreement with results obtained by using the conventional method. Figures 3, table 1; references 2 (Russian).

Superisocon With a Sensitivity in the Near-UV Range of the Spectrum and Its Use in Photometric Research in Astrophysics

927F0153S Leningrad OPTIKO-MEKHANICHESKAYA PROMYSHLENNOST in Russian No 7, Jul 91 (manuscript received 11 Apr 90) pp 76-79

[Article by A.N. Abramenko, L.G. Bogacheva, K.I. Osminkina, Ye.P. Pavlenko, V.V. Prokofyeva, doctor of physical and mathematical sciences, and L.M. Sharipova, Krymsk Astrophysics Observatory, USSR Academy of Sciences, and A.Ye. Verkhoshentsev, Vacuum Tube Plant, Nalchik; UDC 520.344.6:520.82]

[Abstract] Systems consisting of various types of television systems combined with computers are being widely used in the practice of astronomy. The development of isocons in the 1970's made it possible to create television systems capable of astrophotometric measurements with a precision that was three- to fivefold greater than by the photographic method of TV image recording. Because of absorption in the glass of the tube's entrance pupil, the region of wavelengths shorter than 400 nm still remained inaccessible for observation, however. A new superisocon with a uvio faceplate and a new photocathode with maximum sensitivity (about 400 nm) was first tested in May 1987 at the Krymsk Astrophysics Observatory. The new superisocon, which was made by using components from an LI-804 transmission tube, has been used since 1987 for regular observations of weak stars and galaxies in a TV system including the observatory's MTM-500 half-meter telescope. The new telescope has made it possible to receive the spectrum of weak stars up to 15^m with a resolution of 8 to 16 nm and to measure the brightness of stars to 18-20^m. During observations the temperature of the transmission tube is kept at around 0°C by a special unit that blows dry cold air around the tube. This low temperature reduces the thermal noise coming from the incoming photocathode, reduces the splatter of the potential relief on the target (thus improving its accumulation properties), and helps in achieving stable photometric measurements. An estimate of the DQE for the superisocon yielded a value of 0.02 ± 0.01 and a value of 0.04 ± 0.02 for the matrix. Figures 4, references 11, 9 Russian, 2 Western

New KM145 Magnetic Ship Compass With Latitude Compensator

927F0162A Leningrad SUDOSTROYENIYE in Russian No 9, Sep 91 pp 22-23

[Article by L.A. Kardashinskii-Braude and V.F. Ulanov, UDC 629.12.053.11]

[Text] The UKP-M visual magnetic compass and KMO-T magnetic compass with optical transmission are currently used on ships with an unlimited navigation range.

The most significant flaw of these magnetic compasses is that they lack latitude compensators to compensate for variations in hemispheric deviation, which depend on

the magnetic latitude of navigation. Compensation for quadrantal deviation due to the inductive magnetization of quadrantal deviation compensators by the magnetic field of the compasses' sensitive elements is also required. A flaw unique to the UKP-M compass is the fact that its parameters do not conform to the requirements of operation under conditions of a humid tropical climate or under Arctic conditions. The UKP-M also has a very low vibration resistance.

The KM145 and KM145-S magnetic compasses, which meet international standards, have been developed in an effort to eliminate these flaws. They have been tested and approved by the USSR Registry and are now being series-produced commercially. The new compasses are available in the following versions: visual, with optical course transmission, with electric course transmission, and with combined (optical and electrical) course transmission.

The magnetic compass' magnetic sensitive element contains a system consisting of six needle-magnets with a float located in the magnetic compass' case. The magnetic sensitive element's scale (coil) is 145 mm in diameter, which explains the numeral 145 in the new compass' name. The period of the magnetic sensitive element's natural vibrations is 40 seconds under Leningrad's conditions, which is a factor of 1.5 to 2.0 greater than the periods of the vibrations of the UKP-M and KMO-T. This made it possible to reduce compass error caused by pitching.

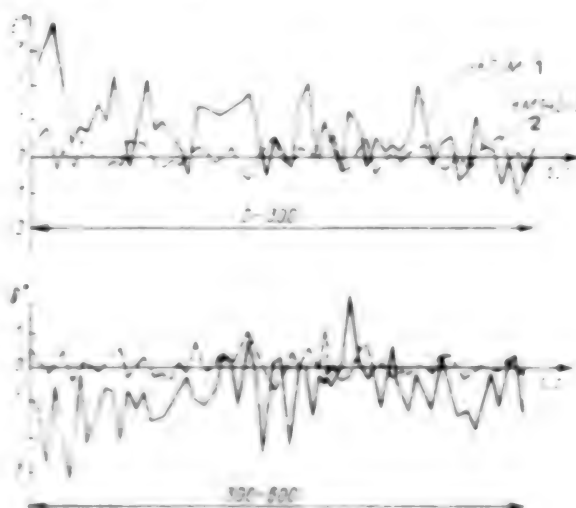


Figure 1. Results of Tests of the Magnetic Compasses Under Conditions Involving Rolling

Key: 1, UKP-M; 2, KM145-S; the x-axis represents time in seconds

Figure 1 presents comparative data from tests of the KM145-S and UKP-M magnetic compasses under conditions involving pitching. The tests were conducted on the vessel Ivan Polzunov and involved rolling with an

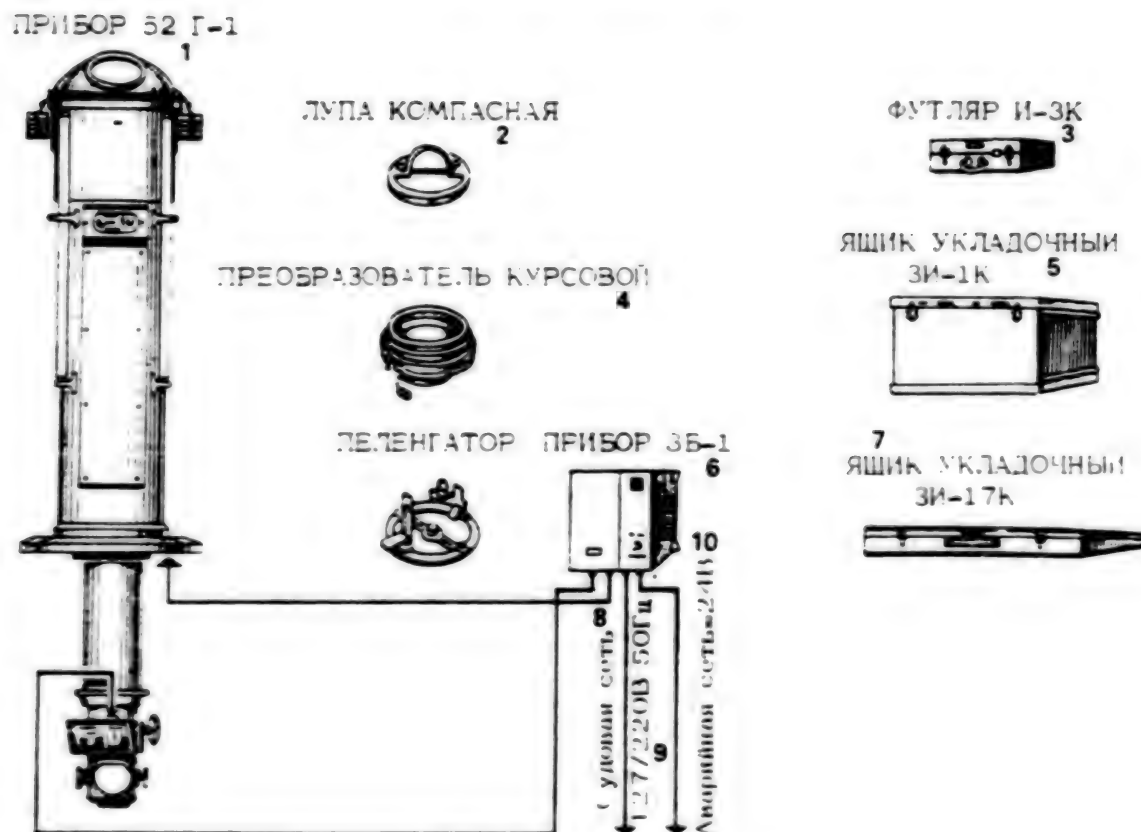


Figure 2. The KM145-S1 Compass

Key: 1. instrument (52 G-1); 2. compass magnifying glass; 3. I-3K case; 4. course converter; 5. storage box; 6. 3B-1 direction finder; 7. 3I-17K storage box; 8. ship power supply system; 9. 127/220V (50 Hz); 10. emergency power supply system (24 V)

amplitude of 15° in the Mediterranean Sea. The compasses were mounted on the top of the vessel's pilot-house. The tests made it evident that the amplitude of the vibrations of the magnetic sensitive element of the KM145-S was only a third that of the vibrations of the magnetic sensitive element of the UKP-M. The KM145-S1 (Figure 2) is the most popular version of the KM145 magnetic compass.

The compass's binnacle is equipped with a double inductionless latitude compensator that makes it possible to compensate for the Poisson vessel parameter from 0 to 0.2. Figure 3 illustrates its capability of compensating for changes in hemispheric deviation with a change in latitude. The method used to test the compensator was as follows. The hemispheric deviation of the KM145-S and UKP-M was compensated for in the Gulf of Finland (magnetic latitude, 73.5°). The Ivan Polzunov then sailed down the Volga to the latitude of Samara (magnetic latitude, 68.5°). The changes in hemispheric deviation were determined at the Kuybyshev Water Reservoir, and the latitude compensator of the KM145-S was used to

compensate for the changes. In the case of the UKP-M, a standard hemispheric deviation compensator was used. The residual deviation (curves 1) was then determined. Next, the vessel returned to the Gulf of Finland. The changes in deviation are shown in the curves designated by the numeral 2. The deviation of the UKP-M magnetic compass increased from 2° to 8° . The deviation of the KM145-S remained virtually unchanged, thus confirming the superiority of magnetic compasses equipped with a latitude compensator.

The type KM145 and KM145-S magnetic compasses are equipped with quadrantal deviation compensators consisting of two sets of plates located on the magnetic compasses' binnacles. The plates do not create induction-induced quadrantal deviation. The number of plates needed to compensate for quadrantal deviation is selected by the deviator during the process of deviation operations along the vessel's route based on a table contained in the compass' operating documentation. The compensation may be performed during the first voyage of a newly constructed vessel. There is no need to

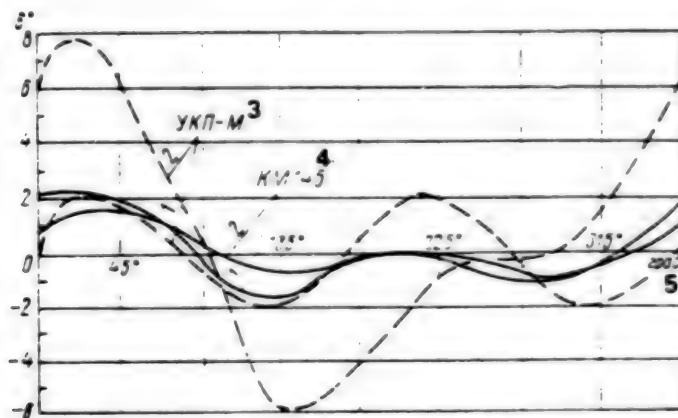


Figure 3. Nature of the Change in the Compasses' Deviation With Changes in Magnetic Latitude

Key: 1. residual deviation; 2. changes in deviation; 3. UKP-M; 4. KM145; 5. degree

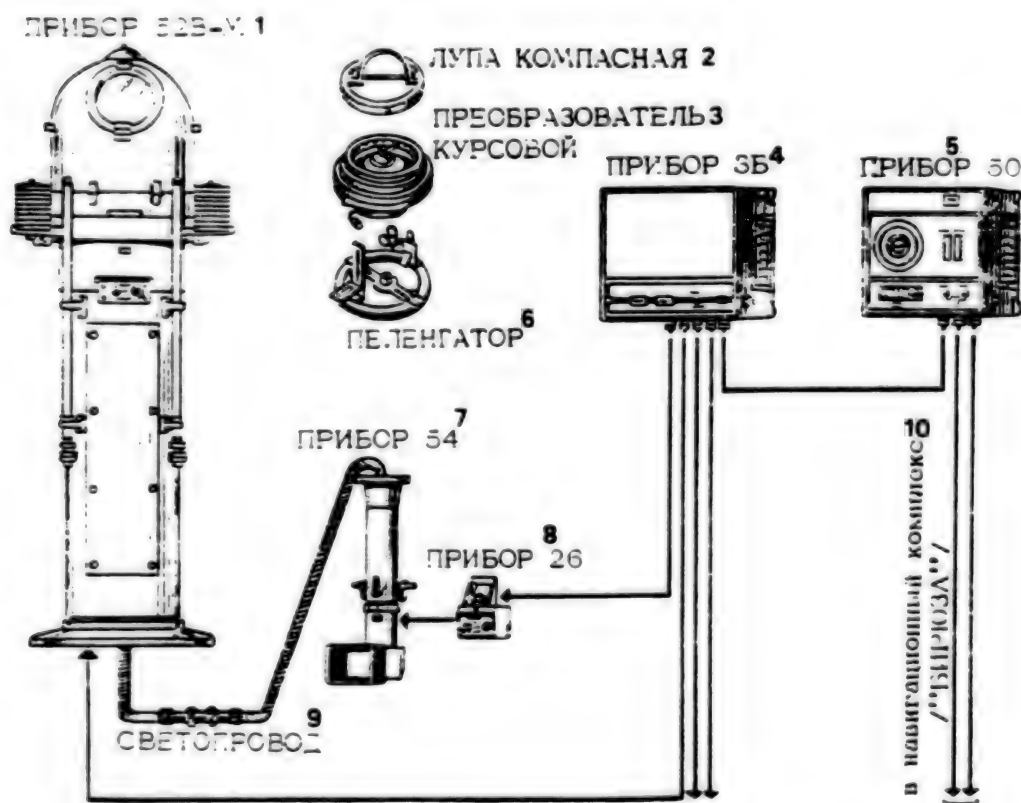


Figure 4. The KM145-S4 Compass

Key: 1. instrument (52V-M); 2. compass magnifying glass; 3. course converter; 4. instrument (3B); 5. instrument (50); 6. direction finder; 7. instrument (54); 8. instrument (26); 9. lightguide; 10. to the navigation system (Biryuz)

remove a compass from a vessel after its first voyage to perform onshore deviation work on it, nor is there any need for any deviation work after a repeat voyage, as there is in the case of the UKP-M compass. Figure 4 shows the instruments of one version of the KM145-S (the KM145-S4), which has both electrical (the instruments designated 3B and 50) transmission of readings to the Biryuz navigation system and optical transmission of readings to the ship's pilothouse (the instruments designated 54 and 26) by means of a fiberglass lightguide. The use of a flexible lightguide in the KM145 and KM145-S compasses has made it possible to locate the compass' binnacle in the vessel's diametral plane in cases where the rudder control compartment is shifted in relation to the diametral plane. An image of the sector of the magnetic sensitive element's scale and the course indicator is not sent to a mirror as in the case of the KMO-T and KM145-S1 compasses but rather to a mat screen. This permits not one but two operators (the operators at the rudder and watch posts) to see the course readings simultaneously.

The KM145 compasses are widely used by special design offices responsible for designing new ships. The UKP-M and KMO-T compasses are not used in new designs, and commercial production of the two compasses is gradually being curtailed.

COPYRIGHT: Izdatelstvo "Sudostroyeniye", 1991

An Investigation of the Structures of Mirrors Made of Silicon Carbide

927F0153C Leningrad OPTIKO-MEKHANICHESKAYA PROMYSHLENNOST in Russian No 7, Jul 91 (manuscript received 5 Apr 90) pp 8-10

[Article by V.A. Alekseyev; candidate of technical sciences, V.V. Bokov and V.N. Yegorov, candidates of physical and mathematical sciences; G.I. Yermeyev, E.A. Narusyev, and N.L. Tkachenko, candidate of geological and mineralogical sciences; and A.I. Filippov; Astrofizika Scientific Production Association, Moscow; UDC 681.7.062]

[Abstract] The authors of this study examined the structures of telescope laser system mirrors made of silicon carbide. All four mirrors studied were of identical size, and all were made of self-bound silicon carbide. The only difference between the different mirrors was in their structure. Mirror 1 was manufactured by pressing in the form of a monolith without any measures to reduce its weight; it weighed about 18.6 kg. Mirror 2 was a hexagon with ordered structural elements in the form of stiffening ribs. It was manufactured by the technique of hot slip casting and weighed about 14.5 kg. The weight of mirror 3 reduced by manufacturing it in the form of honeycombs without any plates attached from the back, and it weighed about 12.7 kg. Mirror 4 was also manufactured in the form of honeycombs. Unlike mirror 3, however, the honeycombs of mirror 4 were coated from the back with a thin plate about 10 mm thick. Mirror 4 weighed about 13.5 kg. For the sake of comparison, the authors

also tested a mirror made of AL24P aluminum alloy; its structure and overall dimensions were analogous to those of mirror 4. The tests were designed to characterize the mirrors' stiffness in terms of the extent of elastic deformation at their centers due to the effect of an identical load that was evenly distributed under identical conditions. Of the different mirror structures tested, the one with honeycombs coated with a thin plate from the back was the most rigid. The said structure resulted in a rigidity that was a factor of 1.9 greater than a monolithic mirror of the same weight. The rigidity of the mirror made of AL24P aluminum alloy was much less rigid (by a factor of 5.2) than its silicon carbide counterparts. Figures 3, table 1; references 5: 2 Russian, 3 Western.

Acoustooptic Optical Beam Coordinate Meter

927F0157E Novosibirsk AVTOMETRIYA in Russian No 5, Sep-Oct 91 (manuscript received 7 Sep 90) pp 110-113

[Article by V.A. Komotskiy and M.V. Kotyukov, Moscow; UDC 53.082.4/5:531.71:531.74]

[Abstract] In a previous publication, the authors of this article proposed a new device to measure the coordinates of an optical beam. In this article they describe its operating principle and present results of tests performed on a prototype coordinate meter. The new coordinate meter's acoustic line features an amplitude-modulated signal (F_A) with a carrier and harmonic frequency modulation (F_M) (modulation depth, 90-100%). The new meter also includes a reference grating, carrier frequency generator, modulator, power amplifier, photodetector, measuring amplifier, demodulator, phasemeter, modulating frequency generator, optical radiation source, and phase detector. Besides making it possible to measure static displacements, the new instrument also makes it possible to observe the dynamics of a beam's motion. A prototype of the new coordinate meter was created for test purposes. Its acoustooptic scale had a period of 100 μm . The tests conducted confirmed that the new instrument can measure the displacement of the gravity center of an optical beam relative to the instrument's acoustooptic scale with a resolution on the order 1 to 10 microns. The new acoustooptic optical beam coordinate meter appears promising for use in several areas, including measurement of the following: angular fluctuations of an optical beam, vibrations of mechanisms' components, objects' shapes, and the refraction of light beams. Figures 3; references 5: 4 Russian, 1 Western.

Precision Laser Thermographic Image Generator

927F0157A Novosibirsk AVTOMETRIYA in Russian No 5, Sep-Oct 91 (manuscript received 17 Dec 90) pp 3-12

[Article by S.G. Bayev, V.P. Bessmeltsev, L.V. Vydrin, A.I. Zhilevskiy, I.G. Maksimov, Novosibirsk; UDC 681.6-3:621.373.8]

[Abstract] A new precision laser thermographic image generator has been developed on the basis of a drum scanner and a CO_2 laser with an output power of up to 25 W. The new image generator produces photocopies of circuit boards on silver-free carriers with no need for

further development and with a resolution of at least 10 lines/mm and an accumulated error of no more than 15 μm throughout the entire recording field. The hardware capabilities of the new thermographic device make it possible to use existing laser thermography processes to produce slides and graphic and half-tone images on paper carriers, as well as circuit boards themselves, and photosensitive plates for offset printing. Tests conducted on the new image generator established that it has the following characteristics: maximum carrier format, 600 x 500 mm; maximum recording area, 590 x 480 mm; recording speed, 5 m/s (96,000 pixels/s); maximum total recording time, 60 minutes; digitization increment, 25, 50, and 100 μm ; error, 2 μm /increment or 15 errors per 300 mm; no. reproducible half-tones, >16; type of carrier, heat-sensitive carriers and polymer films with a maximum coating thickness of 5 μm ; and carrier substrate thickness, 0.1 to 0.5 mm. The new image generator is capable of receiving input data from three sources: magnetic tape, floppy disk, and an RS-232 serial channel. It has a power requirement of 220 V, 50 Hz, and 1,500 W. A prototype of the new device is now in the middle of a trial operating period tested in the circuit board section of the Automation and Electrometry Institute of the Siberian Department of the USSR Academy of Sciences. In 1990 it produced more than 200 photocopies for multilayer circuit boards. Figures 8; references 7: 6 Russian, 1 Western.

Mirrors for High-Power UV-Range Argon Lasers

927F0157D Novosibirsk AVTOMETRIYA in Russian
No 5, Sep-Oct 91 (manuscript received 21 Dec 89)
pp 108-110

[Article by N.D. Goldina, Novosibirsk; UDC 535.39:621.373.826]

[Abstract] The author of the study reported in this concise report examined the possibility of using plasmasion coatings of $\text{Ta}_2\text{O}_5/\text{SiO}_2$ for mirrors of high-power continuous-wave argon ion lasers operating in the ultraviolet range. The study coatings were produced by cathode sputtering of targets (Ta, Zr, Hf, Y, and Si) in a reactive medium (a mixture of argon and oxygen). Multilayer interference mirrors of the said materials were sprayed onto quartz substrates. The $\text{Ta}_2\text{O}_5/\text{SiO}_2$ mirrors were found to increase the laser's power by a level twice that of the other materials tested. Consequently, $\text{Ta}_2\text{O}_5/\text{SiO}_2$ mirrors were compared with $\text{ZrO}_2/\text{SiO}_2$ mirrors manufactured by electron beam vaporization. The absorption factors of the best mirrors produced by cathode sputtering and electron beam vaporization equaled 0.1%. The beam strength of the cathode-sputtered mirrors amounted to 3.5 MW/cm^2 (versus >8.1 MW/cm^2 for the mirrors produced by conventional electron beam vaporization). When examined under a microscope, the cathode-sputtered $\text{Ta}_2\text{O}_5/\text{SiO}_2$ mirrors were found to contain craters with even fused edges several microns deep and 100 to 200 μm in diameter. For the sake of comparison, the beam strength of K8 crown glass was determined to equal 1.5 MW/cm^2 .

Further tests revealed that when the mirrors were used inside a laser's discharge tube, the beam resistance of the coatings was not directly linked to their beam strength as measured in a focused beam. In fact, when the mirrors' performances inside an actual discharge tube were compared, it was discovered that the electron beam-vaporized coatings were more susceptible to damage than the cathode-sputtered mirrors were. The electron beam-vaporized mirrors were also more likely to change color due to short-wave UV radiation discharges. The tests performed thus indicated that cathode-sputtered mirrors are competitive with conventional mirror coatings produced by electron beam vaporization. Table 1; references 7: 3 Russian, 4 Western.

A Geodesic Information-Measuring System Based on Acoustooptic Sensors

927F0157B Novosibirsk AVTOMETRIYA in Russian
No 5, Sep-Oct 91 (manuscript received 23 Nov 90)
pp 12-17

[Article by M.A. Bokov, A.N. Maksimov, K.G. Shumilov, and V.I. Yurlov; UDC 621.376.52]

[Abstract] The authors of this study examined the prototype of a geodesic information-measuring system based on an acoustooptic linear displacement converter and intended for precision automatic measurement of objects' positions relative to one another. The model geodesic information-measuring system studied consisted of a reference light beam generator and two geodesic acoustooptic linear displacement converters. Each acoustooptic linear displacement converter included a two-coordinate acoustooptic modulator, two photoreceivers, and two electronic units. The new system was studied under conditions of a straight leg of a subway tunnel 102 m long. The equipment of the geodesic information-measuring system was mounted on five stable metal tripods with special sleeves to center the instruments and ensure that the instruments would be positioned correctly with an error not exceeding ± 0.006 mm. The diameter of the reference light beam was calculated as measuring 8 mm in the center of the tunnel distance and 12 mm at the beginning and end. The instrument precision of the acoustooptic linear displacement converters themselves were calculated under laboratory conditions before the tests began: The calculations revealed that as the beam spread, the error would increase to about 15 μm for a reference light beam width of 8 mm and about 25 μm for a reference light beam width of 12 mm. During the tests of the prototype geodesic information-measuring system the No. 1 acoustooptic linear displacement converter was placed consecutively at the first, second, and third points of the test path, while the No. 2 acoustooptic linear displacement converter was always kept on the fifth tripod. At each of test points, 10 readings were taken of the simultaneous measurements of the phase shifts made by the No. 1 and No. 2 acoustooptic linear displacement converters. Analysis of the test data revealed that using an "error elimination" regimen involving simultaneous measurement of the phase shifts by the first and second acoustooptic

linear displacement converters made it possible to reduce the geodesic information-measuring system's maximum mean square measurement error by a factor of 3 and to thus reduce it to a value on the order of 50 μm in the middle of the 100-m test distance. Figures 4; references 8 (Russian).

The Principles of Creating Integrated-Optics Multichannel Associative Correlators for Computer Systems and Circuit Engineering Problems in Designing Them

927F0157C Novosibirsk AVTOMETRIYA in Russian No 5, Sep-Oct 91 (manuscript received 3 Sep 90) pp 27-34

[Article by A.A. Verbovetskiy, Moscow; UDC 681.3.01:681.7]

[Abstract] The author of this article has proposed principles and circuit engineering approaches to designing multichannel associative correlators based on integrated and fiber optics. Three possible versions of optical systems for integrated-optics multichannel associative correlators with parallel input of attributes are discussed and diagrammed. In the first version discussed, the bits of associative attributes are represented in a forward Reed-Muller code while the inquiry attributes are represented in a reverse Manchester code. This is done to ensure that the indication of a coincidence of attributes will have a high noise immunity. The remaining two multichannel associative correlators with parallel attribute input are distinguished by their use of a multi-color photoreceiver array to indicate coincidence. Each photoreceiver registers each spectral component of an n-color signal separately. Optical systems of integrated-optics multichannel associative correlators with sequential input of attributes are also discussed. Next, the author discusses the optical train of an integrated-optics multichannel associative correlator based on retunable laser diodes. According to the author's estimates, the said correlator can simultaneously process up to 10^{12} attributes with a coincidence determination time on the order of 100 ns. Next, the author discusses the creation of a fiber-optic interprocessor communication and switching system with associative information retrieval that may be used with supercomputers. The new system, which is based on spectral multiplexing, is capable of operating in two modes. In the first, i.e., a switching mode, it can send information from any central processor to any memory unit. In the system's second operating mode, i.e., associative retrieval from memory, the laser diodes of all n central processors of the given supercomputer represent associative attributes in terms of optical signals with a wide spectral range containing all of the spectral components in which information may be sent in the system's switching mode. These optical signals represent associative attributes in a Reed-Muller code. The said system should be able to switch about 1,000 central processors with 1,000 memory units at a frequency of about 1 GHz and perform associative retrieval from them with a response time of about 2 ns.

which is significantly faster than the speed of electronic switches. Figures 6; references 5 (Russian).

The Kristall-2 Goniometer Unit With an Automated Control System

927F0155G Moscow PRIBORY I TEKHNIKA EKSPERIMENTA in Russian No 3, May-Jun 91 (manuscript received 11 Jun 90) pp 188-193

[Article by V.N. Berezka, V.B. Ganenko, N.G. Golovko, V.G. Gorbenko, V.A. Gushchin, Yu.V. Zhebrovskiy, L.Ya. Kolesnikov, V.D. Ovchinnik, A.L. Rubashkin, and P.V. Sorokin, Kharkov Physics Technology Institute, Ukraine Academy of Sciences; UDC 539.122.2:681.3]

[Abstract] The Kristall-2 is a new goniometer unit that is intended for use in producing quasi-monochromatic linearly polarized photons by the method of coherent bremsstrahlung in monocrystals in the beam of the Kharkov linear accelerator (which accelerates electrons with an energy of 2 GeV). The monocrystalline target is oriented in the goniometer by turning it around two mutually perpendicular axes with an angle readout precision of 5×10^{-5} radians. The monocrystal is placed under the beam by turning it around the azimuthal rotation axis in the range from 0 to 22° . The direction of the photon polarization vector is changed by turning the target around the electron beam's axis with a precision of 0.1° . The Kristall-2 goniometer is mounted in a CAMAC rack containing Elektronika 60 microcomputer with a VTA 2000-3 display terminal and CAMAC crate. The CAMAC rack is connected to a higher-level CM-4 that is in turn used to prepare programs and load the absolute versions of the systems for storage and processing of the experimental data. The Kristall-2 goniometer's capability of changing the direction of the photon polarization vector in modes of discrete or continuous rotation around the beam axis makes it possible to eliminate system experiment errors associated with possible fluctuations in the parameters of the electron beam and detection equipment. This is very important when studying photoprocesses. Figures 4; references 10: 5 Russian, 5 Western.

A Space Conditions Simulation To Study the Properties of Materials

927F0155F Moscow PRIBORY I TEKHNIKA EKSPERIMENTA in Russian No 3, May-Jun 91 (manuscript received 1 Jun 90) pp 180-181

[Article by M.N. Mikhaylov and Yu.A. Rylkin, Tomsk Polytechnic Institute; UDC 535.59]

[Abstract] A new unit that simulates space conditions has been developed for use in studying the changes occurring in the properties of various materials when they are exposed to the conditions of outer space. In other words, the new unit makes it possible to study the effects that low-temperature plasma and electromagnetic radiation with a close-to-solar spectral component have

on a material's integral absorption factor, mass loss, and gas evolution. The ion source developed makes it possible to simulate the ionic composition and ionic energy of ionospheric plasma and to generate an ion flux of up to 10^{13} ions/cm²/s. In essence, the ion source is a coaxial gas discharge chamber with a cold cathode. The ions in the plasma discharge created in a magnetic field are pulled out and accelerated to about 5 keV, thus creating the necessary flux density. Next, the ions are decelerated to the specified energy. In the ion source's optimal operating mode (discharge current, 50 mA; discharge voltage, 700 V; magnetic field intensity, 200 Oe), the ions' energy is regulated from 0 to 400 eV. Mass spectrometry analysis of the oxygen ion flux generated by the new ion source established that it consists of 62% O⁺ and 12% O₂⁺ plus N⁺, N₂⁺, and NO⁺. Even when the discharge current was increased significantly, the ion flux was found to contain only small quantities of metal ions and other undesirable impurities. At a discharge current of 100 mA, the relative content of copper ions appearing due to sputtering of the electrode material amounted to only 0.2%. Figures 2; references 3: 2 Russian, 1 Western.

Two-Coordinate Electrooptical Deflector Based on a Cooled DKDP Crystal

927F0155E Moscow *PRIBORY I TEKHNIKA EKSPERIMENTA* in Russian No 3, May-Jun 91 (manuscript received 24 Jul 89; after revision 16 Feb 90) pp 143-145

[Article by A.B. Vankov, V.M. Volynkin, A.A. Chertkov; UDC 621.376]

[Abstract] A new two-coordinate prism feedthrough electrooptical deflector has been created on the basis of DKDP crystals cooled to a temperature 4 K above the Curie point. The deflector is based on a two-prism cell that has been immersed in an immersion fluid that does not change its physical and optical properties all the way to a temperature of -70°C. The angle of the deflector's deviation relative to the specified angle is established to within values amounting to single percentage points by means of temperature stabilization and additional self-adjustment of the control voltage as a function of deflector temperature. Deviation angles up to $\pm 4 \times 10^{-2}$ radians are obtained in the case of dipolar control of the deflector with respect to both coordinates, which corresponds to a resolution of 350 x 350 pixels for $\lambda = 1.06 \mu\text{m}$ and a beam diameter of 5 mm. Thus, in the case of a scanning duration of 10 ns, 30 ps is required to switch the deflector's directional pattern. The minimum scanning duration in the deflector is dictated by the capacity of the deflector cell, which amounts to about 200 pF at the working point. Scanning durations of about 2 ns have been achieved in deflectors based on cooled KDP crystals, which makes it possible to hope that the speed of the deflector described herein will be improved in the future. Figures 2; references 5: 4 Russian, 1 Western.

New Photocathodes for Radiation With a Wavelength of About 100 Angstroms

927F0155D Moscow *PRIBORY I TEKHNIKA EKSPERIMENTA* in Russian No 3, May-Jun 91 (manuscript received 25 May 90) pp 137-139

[Article by A.L. Andrushchenko, A.M. Pavlov, V.N. Shchemelev, V.A. Podvyaznikov, A.M. Prokhorov, and V.K. Chevokin, General Physics Institute, USSR Academy of Sciences, Moscow; UDC 621.383]

[Abstract] The authors of this study worked to develop new metal photocathodes to record low-energy x-ray and UV radiation (i.e., radiation with a wavelength of about 100 angstroms). They developed a model of the operation of an x-ray photocathode and used it as the basis for calculating the emitter thickness. Next, they manufactured a complex metal photocathode (consisting of Au, Sn, Cu, Al, Pb, and Au on a nitrocellulose substrate). The width of the test photocathodes was kept at $< 100 \mu\text{m}$, and each region of the cathode was 2 mm long. The test photocathode was placed in a small x-ray image-converter tube and irradiated with laser plasma formed by focusing a laser pulse (wavelength, $1.06 \mu\text{m}$) with a duration of 100 ps and an energy of 50 mJ onto the surface of a nickel target located in a vacuum chamber. The power-flow density amounted to $3 \times 10^{11} \text{ W/cm}^2$, and the temperature of the laser plasma reached 40 to 50 eV, which conforms to the spectrum lying in the range of wavelengths to 120 angstroms. After conducting a series of comparative tests, they concluded that aluminum and copper photocathodes provide the greatest quantum yield (as opposed to gold photocathodes, which are widely used). The Cu photocathodes were determined to have theoretical and experimental quantum yields of 5.6 and 4.6, respectively, and the Al photocathodes were found to have theoretical and experimental quantum yields of 6.6 and 5.6, respectively. The optimal thicknesses of the photocathodes were also calculated and confirmed experimentally (80 angstroms in the case of the copper photocathodes and 110 angstroms in the case of the aluminum photocathodes). Figures 3; references 4: Russian, Western.

A High-Power Electron and Ion Beam Source With Periodic-Pulse Action

927F0155C Moscow *PRIBORY I TEKHNIKA EKSPERIMENTA* in Russian No 3, May-Jun 91 (manuscript received 13 Aug 90) pp 130-134

[Article by A.G. Berkovskiy, V.G. Guselnikov, N.Ye. Semenova, T.V. Smirnova, and A.N. Sushchenko, Electrophysics Institute, Ural Department, USSR Academy of Sciences, Sverdlovsk; UDC 621.383.292]

[Abstract] A source of high-power electron and ion beams with a periodic-pulse action is described. The new electron-ion source features a plasma emitter based on a low-pressure arc with a screened cathode spot. Because the device is based on a periodic-pulse discharge mode with a pulse duration of 1.2 ms and a pulse-repetition

frequency of 0.1 to 50 s⁻¹, it may be used to produce beams with a broad range of pulsed and average currents. Tests have confirmed that the pulsed and average currents of electron beams produced by the new source range from 5 to 40 A and 0 to 1 A, respectively, at energies up to 25 keV. The flow of argon, nitrogen, and oxygen ions in a pulse produced by the new source has been found to reach 0.1 to 2 A, with the average beam current amounting to 0.1 A at an ion energy up to 50 keV. The new electron-ion source's multiaperture electrode system is capable of shaping both wide beams with a cross section of about 100 cm² and convergent beams with a crossover of about 2 cm². The new electron-ion source has been used in research on the formation of nitride layers by implantation of nitrogen into titanium, in studies of nonthermal phase transitions in model alloys under the effect of ion bombardment, and in experiments on electron-beam surface hardening of steels and cast iron. The new sources may also be used to develop a process to modify the surfaces of various workpieces and tools. Figures 3; references 11: 2 Russian, 9 Western.

Electron Beam Sources at Energy Up to 1 keV

927F0155B Moscow PRIBORY I TEKHNIKA
EKSPERIMENTA in Russian No 3, May-Jun 91
(manuscript received 24 Apr 90) pp 124-127

[Article by A.A. Borovik; UDC 621.384]

[Abstract] The author has described the designs and parameters of two electron guns and a monochromatic electron source that are all intended for use in making spectrometric measurements. The first electron gun described is capable of producing beam intensities ranging from 0.03 to 3 mA in the energy range from 2 to 1,000 eV. It contains two lenses (a two-electrode immersion lens and a three-electrode single lens). In tests conducted in the energy range from 2 to 20 eV, the energy inhomogeneity of the electrons in the beam produced by the gun did not exceed 0.8 eV. The fluctuations in beam intensity, as measured over the course of 10 hours, amounted to only 1% in the energy range from 2 to 10 eV and was less than 0.5% at high energies. The second electron gun described is capable of maintaining a constant beam geometry throughout a broad energy range. The gun is based on three axisymmetric diaphragm lenses. The volt-ampere characteristic of the gun reaches a plateau at a current of 25 A and an energy of 150 eV. The gun features an energy inhomogeneity of ≤ 0.8 eV for energies of about 90 eV or less. The gun's collimation properties were determined by measuring the ratio of the currents at the receiver and guard cylinder (which were located 40 mm from the exit) at different beam energies. The diameters of the entrances of the receiver and guard cylinder amounted to 10 and 6 mm, respectively. Beginning at an energy of 20 eV, the ratio of the currents amounted to 100:1 or more, which corresponds to a beam divergence of about 2°. The monochromatic electron beam source described includes two main nodes: an electron gun (the primary electron source) and a 127-degree cylindrical electrostatic

Hughes-Rojansky selector. The gun provides an electron beam intensity of ≥ 55 μ A at the entrance to the selector at an energy of 10 eV. Tests have revealed that the beam's angular divergence does not exceed 4° and that the monochromator has a relative energy resolution of 2.2%. The monochromator's volt-ampere characteristic reaches a plateau at a beam energy of 15 eV. The beam's intensity and cross section remained virtually unchanged as the energy was increased to 500 eV. The beam was found to measure 1.3 x 5.0 mm² at a distance of 10 mm from the monochromator's outlet, and its energy inhomogeneity did not exceed 0.2 eV in the energy range from 16 to 500 eV. The intensity fluctuations measured at beam energies of > 15 eV did not exceed 5%. Figures 3; references 9: 2 Russian, 7 Western.

A Pulsating Device To Discharge a Quasi-Continuous Electron Beam Into Dense Gas

927F0155A Moscow PRIBORY I TEKHNIKA
EKSPERIMENTA in Russian No 3, May-Jun 91
(manuscript received 13 Apr 90) pp 122-124

[Article by V.S. Zhivopistsev, A.O. Ikonnikov, S.A. Ilchenko, A.T. Kunavin, D.V. Sapozhnikov, and V.Ye. Yakovlev, High Temperatures Institute, USSR Academy of Sciences, Moscow; UDC 537.533 7]

[Abstract] The authors of this article have described a device to produce a quasi-continuous concentrated electron beam. The new device consists of two electromagnetic pulse valves separated by an evacuated damping space. The beam is discharged from an accelerator chamber into an experimental chamber as both valves are opened simultaneously. The damping space is evacuated by a 2NVR-5DM forepump to a pressure of 10⁻¹ torr. The geometric dimensions of the damping space are selected so that the pressure within it does not exceed ≈ 1 torr during the time required for actuation of the valves given a pressure of 1 atm in the experimental chamber. Each of the two valves has identical power supply and control units. Each power supply and control unit in turn consists of a stabilized power source, accumulator, and control circuit. The stabilized power source has a maximum charging rate of 1 A, a controlled voltage range of 600 to 1,200 V, and a voltage stabilization of at least 1%. The accumulator (capacity, 1,000 μ F) consists of five parallel-connected K75-27-200 μ F capacitors and has an operating life of $\geq 10^4$ charge-discharge cycles. Tests performed on the new device indicated that it can produce an electron beam with an energy of 300 keV, a duration as long as 500 μ s, a current as high as 15 A, and a beam diameter of 10 mm in the range of gas pressures from 10 torr to atmospheric pressure. Tests have also confirmed that the angular deviation of the electron beam from the path axis amounted to ≤ 0.005 radians. Figures 2; references 3 (Russian).

Impairment of the Adhesion of Protective Mirror Coatings

927F0177A Moscow *POVERHNOT: FIZIKA, KHIMIYA, MEKHANIKA* in Russian No 11, Oct 91 (manuscript received 21 May 90; after revision 5 Dec 90) pp 34-40

[Article by G.M. Kudinov and V.M. Kostin; UDC 535.2:621.575.826]

[Abstract] The authors of this study conducted a series of experiments on the impairment of the adhesion of ThF_4 protective mirror coatings on copper under conditions of a laser effect with luminous fluxes not resulting in a change in the films' optical properties. For a substrate material the researchers selected cold-rolled oxygen-free copper (type MoB) that had been annealed for 1 hour at temperatures of 150 and 800°C. The substrates were coated (by using the optimum technology) with a transparent coating of thorium tetrafluoride. Coating thicknesses of 0.1, 0.4, and 1 μm were used. The study specimens measured 60 x 8 x 2 mm³. A GOS-1001 laser operating in a free lasing mode at a wavelength of 1.06 μm with a pulse duration of 10⁻³ s and an energy of up to 1 kJ was used to produce a spot 3 mm in diameter. An electron microscope was used to inspect the condition of the coating. Microplastic deformation of the mirror substrate was found to initiate adhesion instability. The damage incurred on the coating specimens under conditions of mechanical compression occurred in the form of peeling from the substrate. The films 0.1 μm thick were generally not destroyed after the peeling, whereas the thicker (0.4 and 1 μm) films broke and sloughed off of the substrate surface. The damage and destruction of the protective layer was found to occur as early as in the stage of plastic flow of the substrate with a marked deformation relief on the surface. The coating was found to have only an insignificant effect on the microplastic deformation of the base. The critical plastic deformations ϵ_0 causing the coating to peel off were reduced from 0.55-0.6 to 0.4-0.45% as the film thickness was varied from 0.1 to 1 μm . The structural state of the substrate material was found to have virtually no effect on ϵ_0 . The initial damage to a film applied to a substrate annealed at a temperature of 800° and then subjected to laser irradiation appeared in the form of local instances of peeling from the substrate. As the density of the heat flux increased, the size of the peeling zone increased. The sequence of the development of damage to the protective layer was generally preserved as the coating thickness was decreased. A trend toward brittle spalling during the laser-induced destruction process was also noticed. The authors proceeded to develop a theoretical model of the process of the impairment of the adhesion of protective mirror coatings under the effect of laser irradiation.

They then used the model as a basis for deriving an analytical expression for the critical heat flux leading to exfoliation of the film as a function of pulse duration and the characteristics of the substrate and coating material. Figures 3; references 8: 6 Russian, 2 Western.

Double-Crystal X-Ray Diagnosis of Impaired Near-Surface Layers of Silicon Subjected to a Laser Effect

927F0177B Moscow *POVERHNOT: FIZIKA, KHIMIYA, MEKHANIKA* in Russian No 11, Oct 91 (manuscript received 15 Mar 90; after revision 5 Oct 90) pp 46-51

[Article by A.P. Petrakov, V.I. Punegov, and N.A. Tikhonov, Syktyvkar State University; UDC 548.732:621.315]

[Abstract] The authors of this study used the method of double-crystal x-ray diffractometry to investigate impaired near-surface layers of silicon subjected to pulsed millisecond laser radiation. A DRON-UM1 x-ray diffractometer was used. Nearly perfect Si (111) monocrystals served as the monochromator. The near-surface structure of the Si monocrystals was disturbed by pulses of a GOR-100M laser ($\lambda = 694$ nm, flux density = 25 to 130 J/cm²) in a free-lasing mode. The pulses had a spike shape, with each spike lasting about 1 μs and each pulse lasting about 500 ms. The studies were performed with both single and multiple pulses on segments of the study crystal surfaces measuring 5 x 5 mm² that were bounded by a mask. The single-pulse irradiation was performed with energy flux densities of 25, 55, 90, and 130 J/cm², and the multipulse irradiation was performed with an energy flux density of 100 J/cm². After the first through fourth cycles of irradiation, the maximum diffraction peak intensities amounted to 0.7, 0.9, 0.8, and 0.6 of the maximum peak before irradiation, respectively. The half-widths of the curves of diffraction reflection before and after the four cycles of irradiation equaled 9, 13, 11, 12, and 13° respectively. Changes in the profile of the diffraction reflection curves were also noted. Asymmetric distortions in the "tails" of the curves of diffraction reflection appeared initially from the large-angle side (the first irradiation) and then from the smaller-angle sides (the second and third irradiations). Next (i.e., after the fourth irradiation), distortions appeared from both sides of the curves of diffraction reflection and the "pedestal." A numerical calculation of the curves of diffraction was performed based on a statistical dynamic theory of diffraction on unidimensionally distorted crystals. A comparison of the results obtained from the theoretical calculations and the experiments substantiated the validity of the numerical calculations. Figures 4; references 23: 19 Russian, 4 Western.

Country of the Nuclear Bumpkin

927F0166A Moscow ROSSIYA in Russian No 12 (71).
18 to 24 Mar 92 p 10

[Article by Sergey Brusin under the "Warning" rubric: "Country of the Nuclear Bumpkin"; first paragraph is boldface ROSSIYA introduction]

[Text] How do you select a spot for a nuclear power plant? Do you entrench yourself in geological and other studies? We will do it more simply: We will take a contour map of Russia and map out the network of all existing power systems. Do you see a gap? Right there! There is a gap between the Center and Northwest systems. They have a power shortage there. Splendid. Let's build! Do you think we are exaggerating? Not a bit. That is how the act regarding selecting of the site for construction of the Kalinin Nuclear Power Plant [KAES], the first unit of which began operation in 1984, was compiled on 12 November 1970. According to local legend, the matter was even more anecdotal. The station was designed for a different region altogether, but that did not phase the first secretary of the Kalinin obkom. He made arrangements for the capital designers at the bank, and the next day the "scientific substantiation" was changed.

But look at the fantastic place that we stumbled into by accident. Little Lake Udomlya of the Tver Oblast. There are many such lakes here. The lake's water flows along a route encompassing the Syezha River, the Msta River, Lake Ilmen, the Volkhov River, and farther on to the Ladoga and Neva and then onward to the Baltic Sea. Four kilometers from Lake Udomlya is Lake Kubych, which is just as small, and water flows from it to the Volchina River and then onward into the Volga and the Caspian Sea. It is a miracle of nature that water from a single point flows along a flat area the size of half a continent called the Russkaya plane and ends up on opposite sides! This miracle of nature is the Volga-Baltic watershed. And the plan's creators did not notice it!

Neither did they notice that the surface waters join the ground waters at this very spot, which by the way was not the case at Chernobyl. If it were, God forbid, the catastrophe would have reached all the way to the Caspian and the Baltic and all the space in between.

But then the Japanese have been operating nuclear power plants on islands with a risk of earthquakes! Build, but safeguard at the level of modern technology.... But then we switched to a market economy. The plants and factories fell into a tailspin. And what about the nuclear power plant?

It should, in good conscience, remain a peaceful oasis of the controlled economy, where everything it needs "comes down" from above in the required amount. Alas. You need materials, spare parts, tools, and equipment? Barter for them using consumer goods, meat, and currency. Pay 10 or 20 times what they're worth.

"But please, from where?" exclaims Gennadiy Shchapov, general director of the plant. "We cannot trade electric power, we do not set the prices for it, we cannot store it. You can see for yourself that the excess is sent via electric power lines to industrial areas and everywhere else!"

Well if you cannot barter, you are left with nothing. That is what they are saying today.

By logic, the power plant's long-time master, namely, the state as embodied in the government, is obligated by governmental decree to provide materials, foodstuffs, and so on. How? Who can be given the order to provide these things? Nobody is listening anymore. Or else pay for everything that the power plant needs. But the state is itself bankrupt. How this will affect nuclear power plant safety is unclear.

Each component of the government is obliged to create its own, figuratively speaking, level of safety around the nuclear power plants in its own part of the Russian territory. And the contribution of Ye. Gaydar's government to the world cashbox should evidently be called the "Safety of Nuclear Power Plants in the Transition From a Controlled Economy to a Market Economy."

There is no alternative to nuclear power where there is no social tension. But if an operator cannot wait until the end of his shift to run off from his section to plant potatoes out of fear that his family will not have enough to eat in the coming winter? And if he lives in a communal flat and cannot rest before the night shift? And so on. In Europe conflicts between the population living alongside nuclear power plants and plant workers on the grounds of a difference in privileges are unknown. It has not happened in Udomlya, but it has happened in our country. There have been cases where crowds of agitated citizens in one of the nuclear power plant towns blocked the plant entrance and kept a shift of operators from the control panel!

Alas, once a plant is put into operation, the city does not get anything else. The schools are overfilled, and two shifts turn into three shifts. One store is added each year when two are needed. And there are no preventoriums. For 3 years now it has been impossible to get a sports complex. The maternity hospital, antenatal clinic, and medical and sanitary unit have only been half built. There are no residential homes, and no pharmacy has been built for 5 years. The city is on the wane, and its social culture has been underbuilt by 36 million rubles in 1991 prices.

But the main alarming factor that is tearing away at the safety of nuclear power is the critical phenomenon that was heretofore unknown in the world: a vacuum of governmental attention.

Russia is a powerful and all-mighty bureaucracy. That is how it always was. Chernobyl was an accident, but it was also a piece of luck. After it, Ryzhkov's Council of Ministers made a whole series of top-level decisions that

created a whole space of precedents for raising issues of nuclear power generation in the government, and the whole pyramid of bureaucrats from bottom to top was educated. Wherein lies the strength of the apparatus bureaucrats? In their ability to guess the mood of those in charge. And they all knew the position to take regarding nuclear power. And Pavlov was trained so well in the government corridors that he even had the following decree written after the number 1 on his office: "Concerning Measures To Increase Interest on the Part of Local Bodies and the Public in Locating Nuclear Power Facilities in Their Territory." And so it was!

[Boxed item: Wherein lies the strength of the apparatus bureaucrats? In their ability to guess the mood of those in charge. And they all knew the position to take regarding nuclear power.]

And suddenly there came the collapse! When the union structures were eliminated, absolute uninitiated people came. Some were entirely without any experience in the workings of the apparatus, while others realized how convenient it is to "rush" matters related to reforms. When V. Pleshakov, administrative head of the Udomlya Oblast, and G. Shchapov, the plant's director, were in Moscow going from reception room to reception room not knowing to whom they could pose their questions, they came to the Russian Ministry of Finance (true, it is the same as always) to clear up the matter of material support of local territorial bodies in areas with a nuclear power plant, they were told that the document they had was not a Russian document and so Russia would not honor the financial commitments made in it. And they were told that their audience was over. A brick wall has been reached when the apparatus will not even pay attention to the person at the top. (Interestingly, the government of a European country can change once a month, and the change will not be reflected in nuclear power generation.)

What will sustain us now? The old reserves. Under the controlled economy the city was built, and the personnel discipline was set. A highly professional collective was assembled. Today the prestige of the specialty of nuclear power engineer is plummeting (down to the level of merchant!), but operators still must have completed higher education and a 5-year probationary period.

As strange as it may seem, the explanatory work of the Udomlya "greens" is stabilizing the situation. In their digging down to the roots, the "incompetent agitators" have led the public from unconscious fear to the mature social consciousness that should exist in a region with a nuclear power plant.

And finally, we are being sustained by engineering innovations, namely, by systems for diagnosis and early detection of flaws in critical equipment and by a system consisting of three independent safety levels. Experts from the IAEA have given it an OK.

In a word, the plant is still operating normally. On 6 January 1990 there was an accidental emission: 20 tons

of radioactive water ended up on the plant's roof. The incident was cleared immediately without consequences, and the protective and preventive measures taken received a positive evaluation by experts throughout the world. But that first warning bell! One that must never be forgotten about a nuclear power plant is that an atom is an atom.

The government is clearly obligated to the station and the region. This must be remembered for more than cheap journalistic pluralism. We simply cannot implement reforms first and take care of nuclear power plant second. We will go up in smoke.

The special situation of the population living next to a nuclear power plant has long been reflected in the Russian Law on Nuclear Power Generation. It remains to be passed. Without it there are almost none of the promised advantages. People have grown tired of waiting for it. The road to Vyshniy Volochek is another source of worry. It will not handle the evacuation of the forty-odd thousand persons living in the region. A road to Bologoye is also needed. Twelve hours down the water's path down the Syezha from Udomlya is the city of Borovichi with its population of 90,000. The people must have a drinking water source that is independent of the Msta River. This may be done by drilling artesian wells. But who will do it?

The rayon administration has remained extreme, that is, in all its responses to the public, although it is without resources in general. For comparison, the region around the Kola AES is receiving 13% of the total sum realized from the power generated by the plant, whereas for some reason the Udomlya region is only receiving 1%, which the administration then has to beg the plant for.

As in an incomplete phrase, there is no sense in the stagnant third unit. The problem is that hairline cracks may develop somewhere in the steam generators installed in the first two units in several years. Then they will yell Stop the machines! The machines will have to be stopped at once. Replacing the equipment will require half a year at a minimum, which means that the power from the central commercial zone will have to be disconnected for half a year. The loss to the national economy will be unthinkable. The third unit should be finished as a stand-by unit....

That is the suggestion that the general director received from his Western colleagues. They view us and our nuclear power system as a monster that is best helped regardless of the cost so that they themselves will be safer. And so they made the following proposal: Decide what equipment you need and we will obtain it, give it to you, and help you install it, start it up, and adjust it. But we will not give you dollars. We do not trust you. It is shameful of course, but what choice is there?

Is the Russian government in any condition to take care of its nuclear power plants after having been warned, or must it wait for the "bang"?

A Period of Half-Decay: Subjective Comments About the Rostov AES

927F0146C Moscow PATRIOT in Russian No 9
Mar 92 p 3

[Article by L. Mazyrin, PATRIOT correspondent.]

[Text] Several times each day Rostov radio broadcasts an announcement to the industrial enterprise directors. The announcement contains a request to adhere to operating regimens. At the end there is the ominous warning: Violators will have their electric power cut off.

The strict warnings of the Elektronadzorrostovenergo do not emanate from a good life. According to modest estimates, the Don is today experiencing a shortage of a million kilowatts. There had been hope that it would have its own nuclear power plant, but more than once a wave of meetings attended by several thousand protesting the start-up of its No. 1 unit swept through the oblast and drowned this hope.

I happened to attend one of these "measures." What generally motivates a protest by popular masses? Why are people prepared, as they say, to hold a candlelight vigil just to keep the Rostov AES from starting operation? Did the Chernobyl tragedy scare them?

Evidently so. People have an enormous lack of faith in the reliability of nuclear power plants. Many have mentioned the fact that about a hundred buildings in Volgogradsk have begun to sway and that others have even fallen. And yet the nuclear power plant has been built on the same site and by the same hands...

And in fact, how has it been built? I recall a distant conversation with the a former worker of the KGB administration [UKGB] for our oblast who is now a lieutenant in the reserves. He said a great many curious things. It turns out that since the beginning of the construction work the Politburo of the CPSU Central Committee and USSR Council of Ministers had received signals indicating that the Rostov AES must not be built on the selected site and that forcible arguments had been raised. But someone from the Central Committee Politburo secretaries came and told the people "The Party has spoken—Build!"

But who built it? At first there were the agreed-upon workers, and then there were military builders. And only later was the facility turned over to civilian special organizations. Was that level of strength and reliability that would guarantee the plant's safe operation achieved in this "drawn-out construction process?" The commissions working at the facility by popular demand did not give any such guarantee. Indeed, except for the assurances of the plant directors, there was not one argument in favor of the safety of the Rostov plant.

Therefore, a half-year ago, after demands from area residents, the session of the oblast Soviet passed a resolution halting construction of the Rostov AES and calling for its inactivation.

It is easy to say "halt construction and inactivate it!" But what happens next? The plant and its first unit have been 98% completed. Only the final finishing work remains. And what is to be done with the uninstalled equipment that cost almost 300 million and is now sitting in the plant's warehouse.

No matter how you reckon things, what could have been a profit is now a loss. According to estimates, the Rostov AES should provide a billion rubles' worth of electric power each year.

But there are questions and more questions... What is to become of the specialists? The moment construction of the plant was halted more than 2,000 persons left. They left for cooperatives and small business. In general, they left for places where they could earn a good living. And for the most part, they were highly qualified people. They had been trained for years, they were entrusted with a big construction project, and now they have flown off all over the country like swallows.

"Suddenly it will be needed, don't go," sighed N. Shilo, the disappointed head of the plant's construction, evidently still entertaining hopes that the plant will be started up.

E. Mustafinov, the plant's director, has not lost hope, however. He is convinced that unit No. 1 will become operational.

I don't know what they are basing their hopes on. I, for one, think that the public opinion that has been created around the Rostov AES will hardly change in favor of the "peaceful atom" any time soon. What fate awaits the nearly ready nuclear power plant in which the hopes of not only the Rostov Oblast but all South Russia have been placed? What fate awaits the plant on which hundreds of hundreds of millions of the people's resources have been spent?

No matter which directors you talk to on the matter, there is no clarity. Some suggest mothballing the plant, while others suggest preserving it and then dismantling the equipment and selling it if the plant is not put into operation. They say that buyers will be found in the third-world countries. The prospects are, to put it bluntly, dubious. Moreover, the equipment is becoming obsolete right before our eyes, and much of it may fail.

Should the nuclear power plant be reprofiled for another type of fuel? Igor Kovalev, a Rostov resident who is also a candidate of technical sciences and specialist in matters of power generation, touched on this problem. Other specialists, however, have negated the possibility even in principle. And if it were to happen, the redesign effort would cost more than construction of a new plant. And the cost of the operations required to inactivate the plant are estimated at nearly a billion...

Operations to inactivate the plant are nevertheless under way. For what? So that at one splendid moment, when

the energy shortage reaches the critical mark, it can be un-inactivated and put into operation? There are no other explanations.

To use the language of the physicists, the AES is now in a period of half-decay. And the same goes for the collective and builders are as well. It is, as I see it, a dangerous period. Where it will lead is difficult to say.

Those who are fighting for start-up of the Rostov AES now have a powerful trump card in their hands: the conclusion of the Ecocenter of the International Fuel and Energy Association, which includes dozens of leading specialists from various countries throughout the world. After studying the matter in detail, they have concluded that start-up of the Rostov AES will not harm the ecology. The conclusion has convinced many people. In Volgogradsk, however, they have nevertheless decided to hold a referendum to, as they say, consult the people. The referendum will decide the question "Are you for banning construction of the nuclear power plant?" Why are they holding a referendum now after having spent more than a billion in rubles and currency and after having delivered the first phase of the plant? This is, of course, just our opinion.

Perhaps the people's fears are wrong. Perhaps the plant is really being built for a good cause. Nevertheless, a hundred checks are needed. The OK to start up the plant must not be given as long as any doubts remain. And there are doubts. Will a referendum dispel them?

Without the Peaceful Atom There Is Nowhere To Go

927F0146B Moscow PATRIOT in Russian No 10.
Mar 92 p 5

[Text] Moscow professor Armen Abalyan, one of the most renowned specialists in the field of nuclear power plant operation was called in for the immediate work to restore the Armyansk Nuclear Power Plant. He heads the industrial institute in Moscow. Together with English scientist Lord Marshall, he visited Yerevan and met with republic president Levon Ter-Petrosyan.

A. Abalyan has based his categorical conclusions on examples from the world practice, noting that the Armyansk plant is fundamentally different from the Chernobyl plant. And the technology proposed from the English side will make the nuclear power plant even more reliable than its analogues in Bulgaria, Finland, and even Japan, where, as in Armenia, there is a rather large amount of seismic activity.

As is known, in view of the fuel shortage, Armenia is experiencing a most acute energy crisis. Its entire industry has been practically shut down. Not only is the nuclear power plant capable of eliminating the shortage, but it can also reap a profit from selling its surplus electric power.

Do You Wish To View Some Uranium?

927F0146A Bishkek SLOVO KYRGYZSTANA
in Russian 8 Feb 92 pp 8-9

[Article by Yu. Gruzlov; boldface as published in source]

[Text] In the first moments, the handful of yellow powder in a human hand caused a shock. Hiroshima, Chernobyl, the x-ray, and death—all those words hammered in my brain, muddling my thoughts. And in the pit of my stomach and in my heart there were fear and curiosity.

This is no fragment from some fantastic story but rather a chronicle of reality. The year was 1992, and the place was Kyrgyzstan, specifically, one of the enrichment plants in the now-broken uranium production chain of the former union nuclear weapons complex. A. Belyusenko, head of department No. 6 at the Gorkiy Metallurgy Plant (GMZ), was smiling and holding real uranium in his hand. In the language of the specialists it was 3-Oh-8, mixed oxide.

Just yesterday at the ball of the Main Administration for Safeguarding State Secrets in the Press (Glavlit), hardly any of the journalists could imagine anyone who could speak about something similar. Of course, they all knew of the secret production. It was gossiped about in kitchens. But to talk directly about what kind of uranium is being produced, about how it is produced or the degree to which it is enriched, about where it is being shipped, and for how much, or about how the specialists are working—God save us!

The pictures drawn by the average person successfully compensated for the lack of information, and because the fantasies were urged on under the stamp of "complete secrecy," their plots were even stranger: Those who work at the plant die before reaching 50. Two atom bombs were built in short order during the events in the Osh Oblast in Kara-Balta. The stories cannot even be counted.

FROM THE OFFICIAL RECORDS:

The GMZ, which was created based on a USSR Council of Ministers decree dated 13 June 1952, is working continuously to process recovered ores and concentrates. Besides producing uranium products, the plant has begun processing molybdenum-containing wastes and by-products from various sectors of industry. The metal, which is produced in accordance with unique technologies, has made it possible to recoup the costs of all of the plant's fixed capital. In addition to uranium and molybdenum, the plant is currently producing rhenium—the metal of the future. No more than 20 tons of it are produced annually throughout the world. From a secrecy standpoint, the plant has been classified as a class 2 plant. It still has not been declassified today.

Nevertheless, it is no secret that practically only one-third of the plant's capacity is being used, although it is

capable of processing up to 1.5 million cubic meters of ore yearly. To be more precise, in connection with the switch to underground leaching, another two-thirds of the production chain car dumping-crushing-enrichment has been shut down.

When it unexpectedly became clear that need of the CIS for a nuclear shield had diminished to the extent that nuclear power plants would have to be shut down despite the energy programs of the countries of Western Europe, the United States, and Japan and that the daughter enterprises of the Yuzhpolimetall Production Association should be nationalized by order of Kazakhstan's president, the prospects began to look extremely gloomy. The specialists were not excluding the complete shutdown of the plant due to the absence of raw materials. Of course, way back in the fifties hardly anyone could have imagined that the mining combine created with the resources of the entire country would begin to be divided between Kazakhstan and Kyrgyzstan.

FROM THE OFFICIAL RECORDS:

On 24 October 1950 the USSR Council of Ministers adopted the Decree Regarding Construction of a Large Mining Enterprise. The first ore mines were created in the territory of Kyrgyzstan, i.e., in Kavak, Kadzhi-Say, and Mayli-Say. As the deposits were assimilated, ore enrichment plants, hydrometallurgy plants, and TETS were built along with auxiliary subdepartments and residential settlements with all the facilities of a social infrastructure. The intensive processing of the deposits prospected in the territory of Kyrgyzstan resulted in depletion of the ore reserves and made it necessary to activate geological prospecting operations in the territory of Kazakhstan. An open-pit mine and an enrichment plant and set of shops and services at the Kurday deposit were the first to begin operation. They were followed by enterprises and residential settlements at the Eastern, Western, and Karasay deposits.

The paradox is that practically all of the independent states in the CIS have come to think that the civilized world should help us. But the level of technologies in nuclear power is such that currency can be earned by normal labor without begging or humiliation. It is the unanimous opinion of nuclear power specialists that the position of the leaders of the independent states is entirely incomprehensible. Indeed, the thing that can save each republic and the CIS overall is collapsing before our eyes.

We are moreover prepared for this turn of events. A conversion program has been developed.

Says V.I. Pirogov, general economics director of the Yuzhpolimetall, "With respect to our basic production operations, it will develop as follows: 'The recovery and processing of gold-containing ores, the extraction of rare earth metals, the production of artificial zeolites, the development of a scheme to reprocess molybdenum and tungsten-molybdenum raw materials and products, the recovery and enrichment of barite ores, and the recovery and processing of granites. The matter of introducing a

series of processes producing means for personal protection has been resolved. The production of microwave ovens by license with the firm Goldstar has been set up, as has joint production of household electric motors with the plant Kyrgyzelektrodvigatel and the production of agroindustrial equipment for farmers. In the area of the construction industry, the production of bricks, roof tiles, and tiles has been set up."

"We are already producing purely civilian-use products in the amount of 400 million rubles," says V.A. Kuzmin, director of the GMZ. "Even if production of our main products must be curtailed, the plant and association will survive. And not just by refining gold. We have other innovations as well and will soon begin producing basalt fibers. Basalt is a stone—a rock mass. But we will use it to produce an ultrathin fiber. Then, down the technological chain, it will be turned into fabric, computer boards, and heat insulation material. All of the countries of Western Europe, North and South America, and South-east Asia are ready to buy these products for currency."

The plant bosses' main hopes are still tied to gold production, with the highest specimen measuring in at three-tenths. But not all is well there either. The essence of the problem lies in the raw material. Previously, the problem lay in the short-sighted policies of the former Soviet socialist republics. The problem now lies in the policies of the directors of the oblast and sector in an independent state. Despite the decision of the Kyrgyzstan cabinet ministers to transfer the gold-bearing deposit in the Talas Valley to the Yuzhpolimetall Association, both the Kyrgyzzoloto and oblast Soviet do not consider it necessary. The reasons are understood, and the analogy is obvious. It is undoubtedly much more advantageous for Kazakhstan to build its own hydrometallurgy plant and trade "mixed oxide" than to give its neighbors the raw material without charge. Neither is the management of the Kyrgyzzoloto against bringing in foreign capital and creating an SP (not further identified) to process the gold-bearing raw material. The oblast would receive a percentage of the profits in its budget. And so it turns out that practically no one needs the modern technologies of the hydrometallurgy plant in Kara-Balta.

And so, if you have not seen uranium before, look at it while it is still in A. Belyusenko's hand. Indeed, the head of department No. 6 of a plant of category 2 secrecy does not share detailed information with everybody every day:

"What does a person feel when he holds uranium in his hand?"

"Our product is best termed uranium salt. It is a low-activity product, there is no hard radiation. Ordinary working clothes and cigarette paper can protect you from this uranium."

"But atomic bombs are made from this uranium!"

"We only produce uranium salt. Everything else depends on the buyer."

"Which countries do you sell it to?"

"To England and the United States through the Vneshtekhsport."

"How many years have you been producing it?"

"Since 1966, but the mines began operation in 1959."

"So much uranium has passed through your hands! How many atomic bombs have been produced from it?"

"A bomb is enriched uranium. Only 0.7% of ^{235}U goes for a bomb, which means 7 kilograms per ton. As far as the entire technology of bringing the uranium to the proper metallic state goes, it isn't even worth mentioning. Read your physics."

"Have your specialists been invited to work abroad?"

"No."

"Would you like to go?"

"But why not? I would gladly go if it were useful to me and the state."

"How would you be useful there?"

"As a specialist in purification."

"Could you take uranium from the plant and, let us say, sell it?"

"We have none. And who needs it?"

And so, no matter what twists are taken, everything will turn out. The one path for the Yuzhpolimetall is to run to conversion.

Control and Protection Systems of VVER Nuclear Power Reactors

927F0145A Moscow ELEKTROTEKHNIKA in Russian No 9, Sep 91 pp 60-62

[Article by V.K. Kalashnikov, engineer, Yu.N. Olshevskiy, candidate of technical sciences; UDC 621.039.538.001.5]

[Abstract] One of the most critical scientific-technical problems entailed in creating a nuclear power plant is that of developing the reactor control and protection system (RCPS). The All-Union Scientific Research of Electromechanics (VNIEM) has been working on the creation and development of RCPS since 1956 and developed the first domestic RCPS for VVER reactors. The said RCPS was put into operation at the Novovoronezh AES in 1964. Since that time, the VNIEM has developed RCPS for more than 30 nuclear power plants in the USSR and with USSR participation abroad. The VNIEM has developed three generations of series RCPS

reflecting continuing progress in nuclear power generation and control equipment. The scientific-technical activity of the VNIEM is proceeding in four main directions: development of thermal radiation-resistant submersible electric motors that can be operated in the medium of the primary loop to actuate the reactor's control elements; development of low-frequency semiconductor converters for control element actuators and for the systems used to control and monitor the actuators; development of emergency and preventive reactor protection; and R&D of the dynamics of automatic reactor power level control systems. The third-generation RCPS, which was developed for VVER-1000 reactors, features stepper motors for the control elements designed in accordance with a two-level hierarchical structure that is in turn based on the principles of multichannel interactive majority systems for the top level and multichannel distributed structures with individual redundancy for the power devices of the bottom level. The extensive R&D conducted by the VNIEM in the area of the dynamics of control and synthesis of equipment to control a reactor's power level have resulted in the creation of a highly reliable multichannel (three-channel) controller with majority time-pulse output. Each of the power level controller's channels has its own sensors so that a failure of one channel will not affect operation of the remaining two channels. The channels each have automatic zeroizing of their initial conditions, which permits shock-free startups of each channel, shock-free switching from mode to mode, and individual reliability checks of the channels. The controller also has a system to automatically diagnose the channels and disconnect failed channels from the control loop. The reactor power level controller can operate in two basic modes: a mode of stabilizing the reactor's neutron flux-determined power at a specified level and a mode of astatic maintenance of the pressure in the secondary loop (also known as a unit control mode). The VNIEM has also been conducting research directed toward developing a new generation of RCPS for VVER-1000 reactors. These new RCPS will be based on microprocessors and will make VVER-1000 reactors safer. To date, this research has indicated that the new RCPS should have a two-level hierarchical structure with self-contained standardized multicontroller majority systems (including in-depth diagnostic support) at the top level, a microcontroller network to collect and process information regarding the status of all of the system's control elements (there will be about 120 in all), and static converters at the lower level that are controlled directly by special single-board microcontrollers. Figures 2.

The Technical and Economic Feasibility of Using Asynchronized Turbogenerators in an Asynchronous Mode at Electric Power Plants

927F0165B Minsk IZVESTIYA VYSSHIKH UCHEBNYKH ZAVEDENIY ENERGETIKA in Russian No 11, Nov 91 (manuscript received 3 Apr 91) pp 117-121

[Article by A.S. Minyaylo, candidate of technical sciences and docent, N.P. Shmatyuk, candidate of technical

sciences, and R.V. Pylypyuk and K.B. Pokrovskiy, engineers, Lvov Polytechnic Institute imeni Lenin Komsomol; UDC 621.311:621.313.17.001.5]

[Abstract] The advantages of using large synchronous turbogenerators in an asynchronous mode as a means of increasing the operating reliability of electric power plants and reducing interruptions in the supply of electricity are well known. The main problem in operating synchronized turbogenerators in an asynchronous mode is the need for deep discharge of the turbine-generating unit to 40% of its rated active power level for 15 minutes. Using asynchronous turbogenerators at electric power plants has been shown to eliminate the need to shut power generation units down due to a loss of excitation. This is because the reduction in active load (up to 20%) required in order to operate asynchronous turbogenerators in an asynchronous mode does not cause any process or operational problems at a thermal electric power plant (TES) regardless of the type of equipment and type of fuel (including nuclear) involved. Asynchronous turbogenerators are more complex and contain more components than do synchronized turbogenerators; specifically, they require the use of two excitation systems. Despite this fact, asynchronous turbogenerators operating in an asynchronous mode have been found to possess a higher inherent reliability than synchronized turbogenerators do and are thus less likely to fail. The main reason for this is that asynchronous turbogenerators contain two identical field windings on a rotor that is symmetrical from a magnetic standpoint and two reversing exciters for each winding. This increased reliability results in cost savings and consequently higher technical and economic feasibility on two counts: 1) the additional costs of fuel equivalent entailed in repeated start-ups of units after turbogenerator failures are reduced, and 2) the emergency stand-by power systems required as a reserve in the event of a turbogenerator failure do not need to be as large as the stand-by system required with synchronized turbogenerators. Calculations performed by the authors confirm the close interrelationship between the reliability and technical and economic feasibility of asynchronous turbogenerators. The question of the comparative reliability of asynchronous turbogenerators and synchronized turbogenerators will be fully resolved after long-term commercial operation of asynchronous turbogenerators. Tests of ASTG-200-2UZ asynchronous turbogenerators in an uncontrolled asynchronous mode have already established that they are fully capable of maintaining a power level that is considered acceptable during conventional operation in synchronous modes. When their field windings or switches are damaged, asynchronous turbogenerators operating in an asynchronous mode may be operated with open field windings. The long-range permissible load in this mode is only 60% of the rated load, however, and the maximum asynchronous moment can hardly reach the rated moment. For this reason, such asynchronous modes can only be considered acceptable in extreme emergency situations. In conclusion, the authors reiterate that the improved reliability indicators

of asynchronous turbogenerators make it possible to eliminate the practice of installing additional stand-by electrical generator dynamo units at electric power plants and thus eliminate the costs of the said units. Tables 3; references 11 (Russian).

Improving the Operating Efficiency of Steam Turbine Units at AES by Using Multistage Moisture Separation

927F0165A Minsk IZVESTIYA VYSSHIKH UCHEBNYKH ZAVEDENIY: ENERGETIKA in Russian No 11, Nov 91 (manuscript received 16 Jul 91) pp 62-65

[Article by V.M. Borovkov, doctor of technical sciences and professor, A.G. Kutakhov, candidate of technical sciences, and N.N. Davidenko, V.K. Myasnikov, N.I. Zhuk, and N.E. Molodkina, engineers, Leningrad State Technical University and Kalinin AES; UDC 621.165:621.039.5]

[Abstract] The thermal circuits of the turbine units at all modern AES are equipped with external moisture separation and steam-steam reheating systems. The reheaters were added because the threshold moisture levels in the low-pressure section, while in and of themselves useful from the standpoint of improving the operating efficiency of the turbine's flow path, reduce the overall thermal economy of the cycle. The reheaters are themselves a source of inefficiency, however, because of the large amounts of metal required to make their surfaces and because they often experience failures. Others have researched the possibilities of eliminating the use of reheaters while still maintaining acceptable moisture levels in the last stage of the low-pressure casing. The study reported herein was conducted in continuation of this line of research. Specifically, the researchers examined a circuit involving multistage moisture separation for the K-1030-60/1500 turbine of the No. 2 unit of the Kalinin AES. Comparative studies were performed to determine the turbine's efficiency in two different operating modes. In the first circuit tested, moisture was removed in the main moisture separator/reheater unit at the outlet from the high-pressure casing. The second circuit tested was based on the principle of multistage moisture separation. Four additional separators were used along with the main separator. One of the additional separators was placed after the medium-pressure casing, another was placed in the turbine's flow path after the second stage of the medium pressure casing, and the two remaining additional separators were placed after the second and third stages of the low-pressure casing. Special separator-stages mounted on their own bearings in the flow path were used as the additional separators. Calculations were performed for identical turbine power levels during a discharge to 700 MW for four circuits: the plant's existing circuit, the plant's circuit with the reheater disconnected, a circuit involving multistage separation with a moisture removal factor (k) of 50%, and one with $k = 70\%$. Throughout the entire load range tested, thermal economy increased by

1% for the circuit without a reheater and with single-stage separation. A 1.16% increase in efficiency was achieved in the case of the circuit involving multistage separation with $k = 50\%$, and a 1.2% increase in efficiency was achieved with $k = 70\%$. Disconnecting the reheater while maintaining single-stage separation increased the moisture level at the turbine outlet to 17%. Using the circuit entailing multistage separation not only made it possible to maintain the moisture level at its previous level but also made it possible to significantly improve the operating conditions of the last stage of the low-pressure casing by decreasing the moisture level at the turbine outlet to 8% with $k = 50\%$ and to 6% with $k = 70\%$. The power level throughout the entire range of operating modes studied was higher than that obtained for the plant's existing operating mode. Multistage separation thus made it possible to achieve a significant power-level increase while simultaneously providing greater operating economy and reducing the deleterious effects of moisture on the various turbine stages. Further detailed studies of the effect of internal and external moisture separation on turbine efficiency should make it possible to select concrete types of separation devices and decide precisely where to place them in the turbine flow path. Figures 3; references 6 (Russian).

70-MW Floating Electric Power Plant for the North

927F0147A Moscow FIZIKA I KHIMIYA OBRABOTKI MATERIALOV in Russian No 9, Sep 91 pp 8-10

[Article by V.K. Kovalenko and V.K. Tarasov; UDC 629.12.066:[621.039]

[Abstract] The Aysberg Special Design Office and Technical Supervisory Office of the Murmansk Steamship Agency developed a joint technical proposal for a two-reactor 70-MWe floating nuclear power plant. The keynote of the proposal was the idea of combining a new-generation power plant with a nuclear icebreaker. A ship monounit nuclear power plant with internal safety has been proposed as the steam generator. All of the radioactive equipment, including the reactor and liquid and solid waste repositories, are to be located inside a sealed containment designed for a maximum emergency pressure of 5 bar. The jackets of each of the reactors are to be

self-contained. An additional protective enclosure is to surround the containment and all systems servicing the steam generating unit. A special room over the containment will be provided to make it possible to refuel the reactor without having the fuel come into contact with the atmosphere. The core is to have a power supply sufficient to keep it in operation for 4 years with an average power utilization factor of 0.7. Two main turbogenerators with a capacity of 37 MW each are to be provided. Together, these two generators will generate a total of 70 MW of electricity for use by consumers. The remaining power generated will be for the plant's auxiliary needs. An auxiliary turbogenerator with a capacity of 3.2 MW (380 V) will be provided to service internal users in the event that the main turbogenerator is shut down. Standby and emergency generators will also be provided. The station will be designed to cover both base and peak loads. In extreme cases, the power output will be able to be increased to the maximum at a rate of 1%/s. The main turbines will have up to three steam bleeds, thanks to which steam will be available for heat or hot water, depending on customers' specific needs. High-purity water will be available in amounts ranging from 240 to 400 t/s. Control of the entire plant will be concentrated at a central station. The plant vessel will be 120 m long and 28 m wide and will have a submersion of 4.5 m and a water displacement of 16,000 t. Eight specific provisions have been developed to ensure that 1) the new floating nuclear power plant will be ecologically pure throughout its entire life cycle and 2) the likelihood of design and hypothetical accidents will be kept to a minimum. From start to finish, construction of the plant will be handled by specially trained workers at the specially prepared Baltiyskiy zavod Production Association. The containment, steam generator unit, and reactor and power generation compartments will be constructed under closed-shop conditions to ensure that they are manufactured with the highest quality. The plant will be brought to its operating site in finished form. The plant's automation and design will be such that there will be no need to enter the containment for an entire year of normal failure-free operation. Refueling of the core will take place entirely within the confines of the containment. Work is currently under way to refine the technical proposal and gain a more precise understanding of the specific needs of the plant's intended customers. The floating power plant will be able to operate under the conditions of both the Far North and Antarctica. Figure 1.

Underground-Type GAES: Problems and Solutions

927F0163A Moscow PROYEKTIROVANIYE I
INZHENERNYYE IZYSKANIYA in Russian No 5.
Oct 91 pp 10-12

[Article by G.L. Sarukhanov, Ya.Z. Zaslavskiy, and L.B. Sheynman, engineers, Gidroproyekt Association imeni S.Ya. Zhuk; UDC 621.311.21]

[Text] It is known that water storage power plants [GAES] accumulate the surplus energy of thermal and nuclear power plant units during "trough" hours in their load curves. They do this by pumping water to ponds located at higher levels. They then return energy to the system by releasing the water through turbines during the period of greatest power consumption. GAES also keep the voltage levels and frequencies of the electric current in power systems constant by functioning as a fast-acting reserve.

Thanks to their high demand adaptability, GAES react quickly to all load fluctuations in power systems. They switch on automatically when critical situations arise.

Construction of GAES is widespread in the United States, Japan, Germany, Italy, and other countries. More than 200 GAES with a total capacity of about 75 million kW are now in operation abroad, and about 50 are in the construction state. The maximum heads of GAES now in operation reach 1,500 to 1,600 m.

The power system of the European territory of the USSR is based on the operation of large thermal and nuclear power plants that may be operated reliably and economically at constant loads. This fact, coupled with the increasing unevenness of power systems' daily load curves, has made it necessary to construct GAES primarily in the central, northwestern, and southern regions of the European territories of the country.

The experimental Kiev GAES, which has a capacity of 225,000 kW, is now in operation, and the Zagorsk GAES is partially on line (at a capacity of 800,000 kW versus its design capacity of 1,200,000 kW). The Kayshyadoris GAES is being built in Lithuania, the Kanev (capacity, 3,600,000 kW) and Dnestrovsk (capacity, 2,700,000 kW) GAES are being constructed in the Ukraine, and a number of additional plants are in the design stage. The head of domestic GAES is between 100 and 160 m.

GAES include two artificial or natural water reservoirs that are located at different levels and connected by aqueducts, turbines with generators, and pumps with electric motors. Compact reversible machines, specifically turbine-pump and engine-generator sets, with high efficiencies have mainly been used in recent years. When the energy-accumulating capacity of two GAES are equal, the volumes of their ponds are inversely proportional to the head of each of the installations. Increasing the head of a GAES helps reduce the area of the lands that must be dispossessed and also reduces the facility's

impact on the environment. We will note that the territories involved are rather large: the ponds of the Zagorsk GAES (head, 100 m) occupy about 700 hectares.

In a search of the European part of the USSR for sites on which to construct conventional-type GAES with all of their structures located above ground, it was established that the relief of most of the possible sites identified was such that the heads of the plants could only reach 100 m. Furthermore, the said sites were all in areas with complicated geologic engineering conditions.

These facts have dictated the feasibility of designing a new type of GAES at which heads are created artificially by sinking all of the principal structures of the GAES except for the upper pond in stable rock to a depth of 300 to 1,000-1,200 m. This includes the aqueducts, buildings (rooms) housing the mechanical equipment, and the lower pond. Assuming that the height difference between ponds (i.e., the head of the GAES) equals 700 m, the area of the lands permanently dispossessed under such a GAES would be reduced by a factor of 6 as compared with the lands required for the Zagorsk GAES.

The idea of erecting underground GAES is also being developed in the United States, Canada, the Netherlands, and in other countries.

From a geostructural standpoint, the Russkaya platform is the most promising site for GAES in our country. It consists of a complexly constructed rock foundation made up of strong crystalline rock of Precambrian age covered by thick seams of weakly dislocated sedimentary rock. The rocks of the crystalline foundation form a monolith with high physicomechanical properties.

Because of its ancient geological age, the crystalline rock of the Russkaya platform has endured numerous destructive changes—breaks, thrusts, etc. Consequently, the process of selecting a site suitable for erecting an underground GAES and locating its structures at the optimum depth is a complex engineering task.

Outcroppings of the crystalline foundation at the surface have been noted in the northwestern portion of the country's European territory (the Baltic crystalline craton) and in the south (the Ukraine crystalline craton). The Belarus and Voronezh anticlines are regions where the foundation is raised but has not reached the surface.

The Gidroproyekt has examined GAES with two types of structures located underground: with specially created ponds and with recovery of the depleted industrial workings under these ponds.

The said GAES include the following facilities: shaft-type aqueducts with tunnels feeding water to the hydroelectric generating units; the buildings (rooms) housing the valves of the upper and lower ponds; the lower pond, which consists of a system of hydraulically interconnected large-cross section tunnels; aqueducts connecting the plant units with the lower pond; and bus, cargo, and ventilation shafts. Approximately 90% of all of the mining and excavation

work is concentrated in development of the underground pond. Natural ponds (lakes) or specially constructed small water reservoirs located in direct proximity to the GAES are used as the upper ponds.

One of the main factors determining the technical and economic indicators of a GAES is its mechanical equipment. The domestic industry has recently begun production of turbine-pump units designed for heads of 100 m and motor-generator units with a unit capacity up to 250 MW.

Equipment is now being developed for domestic GAES providing heads of 190 and 440 m and units with a unit capacity up to 400 MW. Different types of hydrogenerators designed for heads up to 1,600 m and with unit capacities up to 400 MW are being manufactured in the United States, Italy, France, Germany, Japan, and other countries.

On the basis of the foreign experience, the following types of units may be recommended for the following heads:

- up to 700 m: single-stage reversible hydraulic machines with controlled guide vanes;
- from 700 to 1,000 m: two-stage reversible hydraulic machines with controlled guide vanes;
- from 1,000 to 1,200 m: multistage uncontrolled reversible hydraulic machines;
- above 1,200 m: three-machine units with Pelton turbines and multistage pumps.

Two types of GAES are described below.

The first type is the GAES with a specially created lower pond. The Voronezh Oblast was selected as a region where stable crystalline rocks lie close to the earth's surface and where there is need for a GAES.

The site for construction of the GAES is located on the shore of the Don River 10 km below the mouth of the Voronezh River. The nearby Lake Pogonovo has been proposed for use as the upper pond. The geologic structure of the territory where the Voronezh GAES is to be located has been explored by numerous wells up to 1,200 m deep. One is in direct proximity to the site. The region's tectonic structure may be judged from existing space photographs. The region in which the site is located is a part of the vault section of the Voronezh anticline, which represents a large uplift of the Precambrian crystalline foundation of the Russkaya platform formed of complexly dislocated and metamorphosed crystalline rocks of Archean and Early Proterozoic age intersected by a sedimentary cap of Paleozoic, Mesozoic, and Cenozoic rock up to 150 m in thickness.

The electric power plant's six units have an installed capacity of 1,200 MW. It is planned that water will be supplied to the units via two shafts with three branches/tunnels each (depending on the number of units).

Development and comparison of different versions of GAES have revealed that the version of a GAES in which the lower basin is constructed at a depth of about 700 m (Figure 1) is preferred.

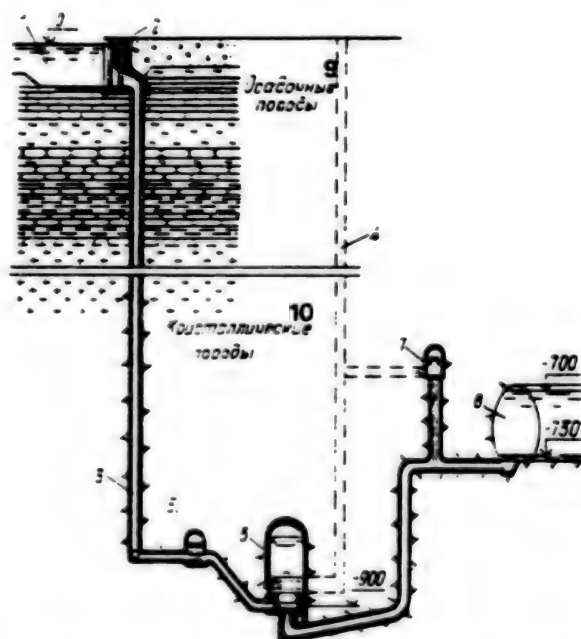


Figure 1. Diagram of an Underground-Type GAES:

Key: 1. upper pond; 2. water intake; 3. pressure shafts; 4. bus, ventilation, and cargo shafts; 5-7. rooms housing the gates of the upper pond, units, and lower pools; 8. lower pond; 9. sedimentary rocks; 10. crystalline rocks

A second type of GAES is that with its lower pond located in industrial workings. The GAES structures are slated to be located in the zone of the Kursk magnetic anomaly in the vicinity of the city of Gubkin.

The Gubkin GAES (which is to have a capacity of 1,200 MW) is being designed in four units that will be supplied with water via two shafts passing through four turbine tunnels/aqueducts.

It is planned that the depleted workings of the iron ore mine imeni Gubkin (located at a depth of about 300 m) will be used for the lower pond and ventilation shafts of the GAES. The turbine building of the GAES, as well as the buildings housing the gates, cargo shaft, and intake and discharge tunnels will be built from scratch. All of the underground structures of the GAES will be located in ferrous quartzites and shales of the Korobkov suite of the Early Proterozoic period that are intersected by sandstones, clays, sands, chalks, and marl with a total seam thickness of 150 m. Lying above this level are

Quaternary sediments—argillaceous sands, sandy loams, and sands with a thickness up to 50 m.

A portion of the Korobkov deposit has been virtually depleted. Its ore reserves have been developed by the underground method based on what is termed a staged-chamber system. This has left an open cleared space that is supported by a system of interchamber and interpanel pillars on which a ceiling pillar at least 70 m thick rests.

The ceiling is 60 m high, and the cleared area is 30 m wide and 55 m long. One chamber has a volume of 100,000 m³. When the chambers are used as the lower pond of the GAES, they will be interconnected by tunnels into a single hydraulic system.

The upper pond may be situated in direct proximity to the underground complex of the GAES.

Table 1 presents the key indicators of the GAES examined.

Table 1.

Indicator	Voronezh GAES	Gubkin GAES
Installed capacity, MW	1,200	1,200
Head, m	700	260
No. units	6	4
Water flow rates, m ³ /s:		
in turbine mode	198	520
in pump mode	167	380
Useful pond capacity, millions of m ³	3.5	10
Cost of 1 kW of installed capacity, rubles	387	294

The authors suggest that GAES with underground lower ponds are more competitive from an economic standpoint than are GAES that have their primary structures located at ground level. The specific capital investments required for the numerous developments of the latter average about 350 rubles/kW.

Underground GAES have the least disruptive effect on the environment and economy of the region in which they are constructed, which makes them promising power generation facilities.

COPYRIGHT: Sroizdat, zhurnal "Proyektirovaniye i inzhenernyye izyskaniya", 1991

The Heat Transfer and Drag of a Cylinder Coated With a Layer of Magnetic Fluid and Surrounded by a Transversal Flow

927F0156A Riga MAGNITNAYA GIDRODINAMIKA in Russian No 3, Jul-Sep 91 (manuscript received 27 Sep 90) pp 39-42

[Article by V.G. Bashtovoy, Nguyen Quyet Thang, and V.A. Chernobay; UDC 537.84:536.2]

[Abstract] The authors of the study reported herein conducted an experimental study of the effect of a magnetic fluid coating on the heat transfer and drag of a cylinder circulated by a transversal flow. The experiments were performed in a closed-type circulation loop with transformer oil as the active medium. The working segment, which was made of acrylic plastic, had a rectangular cross section of 60 x 60 mm and a length of 1,500 mm. A grid of lengthwise-circulated tubes 5 mm in diameter and 100 mm long and two fine-cell meshes were placed in front of the entry to the working section so as to equalize the velocity profile in the working section and reduce its turbulence. The velocity field in the channel was measured by Pitot tubes; the average velocity profiles were rectilinear in all of the experiments conducted. The average flux temperature was measured by thermocouples and laboratory thermometers. The study cylinder was placed a distance of 120 mm from the entry to the working section. The cylinder had a diameter of 7 mm and a length of 44 mm. A permanent cylindrical magnet magnetized across its axis ($H_{max} = 18$ kA/m) was placed inside a fluoroplastic tube. A heater made of constantan wire 0.1 mm in diameter was attached from without. A 0.1-mm-thick copper foil coating on the heater was used as a heat exchange surface. Measures were taken to eliminate the step voltage of the thermocouples' voltage on the heat exchange surface. During the experiments, a steady heat flux was supplied to the heat exchange surface by maintaining a constant heater power level. Measurements were taken of the force of the total drag of the cylinder mounted on a holder whose axis was mounted on point supports. A cathetometer was used to measure the thickness of the magnetic coating at a Reynolds number of ≤ 23.2 . The total hydraulic drag across a circulated cylinder without a magnetic fluid coating was also measured. The experiments conducted established that if the cylinder surface is covered with a layer of poorly viscous magnetic fluid (i.e., if the ratio of the viscosity of the oil to that of the magnetic fluid is 7.96), the reduction in hydraulic drag will reach 15.5% and the intensification of heat transfer will reach 70%. Heat transfer was demonstrated to improve as the thickness of the magnetic fluid coating increased. Drag reduction was only observed at coating thicknesses of $r \leq 1.5$ mm. Figures 4; references 13: 12 Russian, 1 Western.

Dynamics of the Operation of a Pneumatic Shock Absorber With Magnetic Fluid

927F0156B Riga MAGNITNAYA GIDRODINAMIKA in Russian No 3, Jul-Sep 91 (manuscript received 12 Feb 91) pp 107-111

[Article by V.A. Boguslavskiy; UDC 62-567.7:537.84(088.8)]

[Abstract] Pneumatic shock absorbers with magnetic fluid operate on the principle of retaining the pressure difference between cavities separated by magnetic fluid located in the region of the magnetic field's gradient. In a pneumatic shock absorber gas is passed through the magnetic fluid at a constant pressure differential. The authors of the study reported herein have conducted a mathematical examination of the dynamics of the operation of pneumatic shock absorbers with magnetic fluid. Specifically, they have used numerical methods to graph the change in the working gap and pressure difference over time. They considered the case where three media (a magnetic fluid, a nonmagnetic fluid, and a gas separated from the fluid by flexible membranes) are located inside the shock absorber. A system of two nonlinear equations was solved on a computer for the following parameter values: $d = 0.07$ m; $l = 0.005$ m; $l_2 = 0.1$ m; $a = 0.05$ m; $B = 1$ tesla; $I_n = 10^5$ A/m; $p_0 = 10^5$ Pa; $\mu_n = 1 \cdot 10^{-3}$ (N x s)/m²; $\rho_n = 10^3$ kg/m³; $\rho_m = 10^3$ kg/m³; and $v_1 = 1$ m/s. According to the calculations performed, a gap of 9.35×10^{-5} m at a speed of $v_1 = 0.5$ m/s increased to 13.2×10^{-5} at a speed of $v_1 = 1$ m/s, with the change occurring in the form of an attenuating oscillating process. The period of the oscillations was on the order of 0.5×10^{-3} s, and the attenuation time was on the order of 10^{-2} s. Figures 5; references 3 (Russian).

The Solution of Plane Problems of the Nonstationary Filtration of a Heavy Fluid Into Unsaturated Porous Soil Within the Framework of a Model of Instantaneous Saturation

927F0181L Moscow IZVESTIYA ROSSIYSKOY AKADEMII NAUK: MEKHANIKA ZHIDKOSTI I GAZA in Russian No 1, Jan-Feb 92 (manuscript received 5 Dec 90) pp 86-94

[Article by A.N. Krayko and Sh. Salomov, Moscow and Bukhara; UDC 532.546.013.3]

[Abstract] The authors of this study have solved plane problems of the nonstationary filtration of heavy fluid into homogeneous unsaturated porous soil from a single excavation and from an infinite periodic system of identical excavations. The level of fluid in the excavation was assumed to be a known function of time t , which simulates the propagation of fluid along a channel. The filtration into the soil occupying the space outside (i.e., primarily below) the excavation was assumed to occur under the effect of gravity and was assumed to begin at the moment $t = 0$ after it instantaneously filled with fluid. The height of the fluid in the excavation was assumed to be constant when $0 < t < t_1$ and to decrease instantaneously to some also-constant level (including 0) when $t = t_1$. The case where the level of fluid in the excavation increases was also considered. The plane problems formulated were solved within the framework of the "model of instantaneous saturation" that has been discussed in two other publications. The "model of instantaneous saturation" is based on the actual process of the gradual penetration of fluid into capillary pores. Within the model's framework, the solution of the problems under consideration is reduced to the solution of a

Laplace equation in zones of total saturation (for each t) and to the calculation of their evolution based on the fluid velocities at the moving fronts that are found as a result of the aforesaid distribution. In the numerical algorithm created (in Fortran), the Laplace equation is solved by what is termed the "boundary elements method." When the numerical algorithm is used on a YeS-1061, the plane problems formulated may be solved in 15 to 35 minutes. The specific cases of a single excavation, multiple excavations, and "repeated flooding" are all detailed separately. Figures 4; references 4 (Russian).

The Development of Instability in the Wake Behind a Plate Located Parallel to the Flow

927F0181D Moscow IZVESTIYA ROSSIYSKOY AKADEMII NAUK: MEKHANIKA ZHIDKOSTI I GAZA in Russian No 1, Jan-Feb 92 (manuscript received 25 Dec 90) pp 26-32

[Article by P.A. Kuybin and V.Ya. Rudyak, Novosibirsk; UDC 532.517.3]

[Abstract] The wake behind a plate circulated at a zero angle of attachment is said to be the least studied shear current. Wakes of this type have a symmetrical velocity profile and are characterized by two unstable modes, namely, symmetrical and asymmetrical. Calculations performed within the framework of a linear theory of stability have demonstrated that this flow is most susceptible to antisymmetric (sinusoidal) disturbances. The gain factors of the sinusoidal model are about twice those of the symmetrical (varicose) mode. The main mechanism of the development of instability in the nonlinear stage in the mixing layer (for example, the current resulting when the plate is circulated by a flow having different velocities over and under the plate) has been shown to be subharmonic. Although such currents have been studied in a number of publications, many questions regarding the nonlinear evolution of disturbances in the wake remain unanswered. In view of this fact, the authors of this study have performed systematic calculations of the development of instability in the wake behind a plate located parallel to the flow around it. Specifically, they examined the laminar wake behind a plate located parallel to a flow of incompressible fluid. The source of the disturbances was assumed to be located in the vicinity of the trailing edge of the plate. The problem was reduced to a series of nonlinear differential equations that were integrated by the Runge-Kutta method. The calculations demonstrated that when perturbations with the frequency f of any one mode are introduced into the current, the primary instability will develop at precisely that frequency. Excitation of an antisymmetric mode was observed to result in the formation of a sinusoidal wake. In the initial linear stage of the disturbance's development, the forms of the disturbance remained sinusoidal, increasing only in amplitude. Nonlinear effects then began to appear, and a Karman path-type vortex began to appear. Excitation of a varicose mode was found to result in the formation of a vortex path that was symmetrical relative to the wake's

axial line. The generation of combination frequencies with different degrees of definition was found to be a characteristic feature of the nonlinear stage of the development of instability. As predicted by the linear theory, the current was found to be less susceptible to the symmetrical mode. This explained the fact that the appearance of combination frequencies during excitation of a symmetrical mode was observed much farther down the flow than in the case when an antisymmetrical mode was excited. The decrease in the initial amplitude did not qualitatively alter the nature of the current's evolution. When both modes were simultaneously excited at a specified frequency, the amplitude of one was significantly higher and remained so rather far down the flow. The nonlinear stage in the development of instability was found to be extremely complex; combination frequencies of both modes were observed to form and to interact both with one another and with the fundamental harmonics. The calculations performed confirmed the qualitative pattern of the interaction of the fundamental harmonic with the subharmonic. Although the disturbances introduced interacted with one another actively, resonance amplification of the subharmonic was not observed regardless of the value of the phase shift. In fact, suppression of the subharmonic disturbances was found to occur. Reducing the amplitude of the disturbances introduced was not found to qualitatively alter the pattern of the current's development; rather, it only increased the duration of the linear stage. The effect of amplifying subharmonic disturbances during the excitation of symmetric and antisymmetric modes of a given frequency f was observed over a wide range of levels of initial disturbance amplitudes. The same effect was also found to occur in a plane-parallel approximation. Figures 5; references 12: 6 Russian, 6 Western.

A Three-Parameter Model of Turbulence: A Numerical Study of the Boundary Layer in a Nozzle With Blanket Cooling

927F0181G Moscow IZVESTIYA ROSSIYSKOY AKADEMII NAUK: MEKHANIKA ZHIDKOSTI I GAZA in Russian No 1, Jan-Feb 92 (manuscript received 4 Jun 91) pp 48-57

[Article by V.I. Kovalev, V.G. Lushchik, V.I. Sizov, and A.Ye. Yakubenko, Moscow; UDC 532.526.4:532.525]

[Abstract] One of the main problems in developing high-power liquid-propellant rocket engines is that of protecting the nozzle walls from heat fluxes reaching tens of megawatts per square meter in the vicinity of the nozzle's critical section. In view of this fact, the authors of this study used a three-parameter model of turbulence that was introduced and developed in previous publications to perform a numerical investigation of the boundary layer in a nozzle cooled by a blanket of gas. They began their investigation by using continuity, motion, and energy equations to calculate the current and heat transfer in a compressible turbulent boundary layer of homogeneous gas with a specified pressure

gradient. A series of test calculations were performed to verify the validity of the computation method and program developed. The results were compared with published calculations of the boundary layer in nozzles of liquid-propellant rocket engines with outer wall cooling that were performed by using the integral method. The maximum discrepancy between the two sets of results did not exceed 15%. The results obtained by using the proposed three-parameter model were also found to be in qualitative agreement with the results of experiments reported in yet another publication. Next, the three-parameter model was used as a basis for investigating the boundary layer in the nozzle of a liquid-propellant rocket engine with blanket cooling that was designed by the Energomash Scientific Production Association. The effectiveness of the proposed method was demonstrated once again. The authors concluded by cautioning that the results obtained by using their proposed method should be considered estimates because the method calls for using one and the same nozzle contour and the corresponding change in Mach number, as well as a wall temperature that remains unchanged along the nozzle's length for all of the design versions being compared. They emphasize that this same flaw is inherent to computation methods using the principle of dividing a flow into a nucleus and boundary layer, and they go on to suggest that eliminating the flaw will require making mutual corrections in the calculations of the flow in the nucleus and boundary layer or else developing a method for start-to-finish calculation of the current from the wall to the nozzle axis. They suggest that the latter strategy be attempted by using a so-called approximation of the narrow channel based on the boundary value equations used herein and on parabolized Navier-Stokes equations that give consideration to the two-dimensionality of the current in the nozzle. Figures 4; references 14: 13 Russian, 1 Western.

The Motion of a Disperse Impurity in a Laminar Boundary Layer on a Plane Plate

927F01811 Moscow IZVESTIYA ROSSIYSKOY
AKADEMII NAUK MEKHANIKI ZHIDKOSTI I
GAZA in Russian No 1, Jan-Feb 92 (manuscript
received 25 Dec 90) pp 66-73

[Article by Ye.S. Asmolov; UDC 532.529+532.526.2]

[Abstract] The author of this study examined the effect of the motion of a disperse impurity in a laminar boundary layer on a plane plate. Consideration is given to both Stokes' force and to the additional cross force resulting from the transverse nonuniformity of the circulation of the individual particles. Other authors writing on the same topic have used the limiting values of the cross forces (Saffman's force) to determine the velocity and density of the disperse impurity; in contrast, the author of this study also considers the dependence of Saffman's force on the ratio of the Reynolds numbers calculated on the basis of 1)

the circulation of an individual particle and 2) the magnitude of the transverse gradient of the velocity of the flow undisturbed by the impurity. Figures 5; references 9-7 Russian, 2 Western.

The Structure and Dynamics of Finite-Amplitude Pressure Disturbances in a Fluid-Saturated Porous Medium With Gas Bubbles

927F0181K Moscow IZVESTIYA ROSSIYSKOY
AKADEMII NAUK MEKHANIKI ZHIDKOSTI I
GAZA in Russian No 1, Jan-Feb 92 (manuscript
received 5 Sep 90) pp 80-85

[Article by V.Ye. Dontsov, Novosibirsk; UDC
532.546:532.529.5]

[Abstract] The author of this article has examined the structure and dynamics of finite-amplitude pressure disturbances in a fluid-saturated porous medium with gas bubbles. Previous studies have shown that two types of waves are created when longitudinal pressure disturbances are propagated in such media. The two types of waves in question may be termed "fast" and "slow" waves. They are caused by the fact that the fluid and solid framework each have different compressibility and density. The two types of waves have also been shown to have very different propagation speeds and attenuation coefficients caused by a longitudinal shift of the porous skeleton and the fluid in the wave. Introducing gas bubbles into a porous medium that has been saturated with fluid increases its compressibility significantly. This in turn results in a reduction in the waves' velocity and an increase in their attenuation. Yet elsewhere a system of linear equations has been derived for the three-phase mixture porous medium-fluid-gas bubble. The said equation system gives consideration to the vibrations of the bubbles in the wave. In a previous publication, the author of this article has himself derived a system of nonlinear equations that give consideration to the nonlinearity introduced by gas bubbles, as well as to the viscous attenuation resulting from the radial motion of the fluid in the porous medium around the oscillating bubbles. In a continuation of this line of research, the author worked to obtain a set of experimental data on the structure and dynamics of moderately intense pressure disturbances in a fluid-saturated porous medium with gas bubbles. The experiments were conducted in a shock tube with a working section in the form of a vertically configured thick-wall steel tube (inner diameter, 52 mm; length, 0.5 m) filled with a working medium. A chaotic packing of acrylic glass spheres about 2 mm in diameter that were saturated with a fluid with gas bubbles was used as the working medium. Water and a water-and-glycerin solution serve as the working fluids, and air and carbon dioxide served as the gases. The gas bubbles occupied the maximum pore sizes when the gas content was less than 0.1 and equaled about 0.7 of the size of the spheres. The evenness of the bubbles' distribution along the length of the porous medium was controlled by the propagation rate of the pressure disturbances. The propagation of two types of waves, i.e., step

and bell-shaped, were studied. Piezoelectric pressure transducers with a 2-mm-diameter sensitive element were used to record the pressure wave profiles. The experiments conducted demonstrated that in a porous medium saturated with a fluid with gas bubbles, nonlinear and dispersion effects have a significant impact on wave propagation. Viscous dissipation was also found to have a significant effect on wave attenuation. The structure and attenuation of a "fast" pressure wave in highly permeable porous media were determined to be dictated by the combined effect of heat losses and dissipation due to a longitudinal shift of the fluid and porous skeleton in the wave. Analysis of the experimental data indicated that the mathematical expressions presented describe the wave formation processes in a satisfactory manner. Increases in the coefficient R_s were discovered to result in an increase in the effects that dissipation and nonlinearity have on a "slow" soliton and may thus result in the formation of "slow" solitons and shock waves. Figures 3; references 8: 5 Russian, 3 Western.

A Model of the Precipitation of Particles From a Turbulent Gas-Dispersion Flow With Absorbing Walls

927F0181H Moscow IZVESTIYA ROSSIYSKOY AKADEMII NAUK MEKHANIKI ZHIKOSTI I GAZA in Russian No 1, Jan-Feb 92 (manuscript received 4 Feb 91) pp 58-65

[Article by I.N. Gusev, Ye.I. Guseva, L.I. Zaychik; UDC 532.529:532.517.3]

[Abstract] The authors of this study worked to develop a nonlocal model of the precipitation of particles from a gas-dispersion flow in channels with absorbing walls. Specifically, they worked to develop a model that does not involve empirical information regarding the structure of the pulsing motion of the particles. A system of differential equations for the moments of the disperse phase's velocity was used to determine the effects caused by the particles' inertia. The cases of a stationary stabilized flow of a gas dispersion in both plane-parallel and axisymmetric channels were considered. The validity of the model was confirmed by way of the example of currents in channels with smooth walls and with nappy roughness. The calculations performed established that the range of the change in τ_s may be divided into three regions, namely, the precipitation of fine particles (τ_s is about 1 or less), medium particles (τ_s is between about 1 and 100), and large particles (τ_s is about 100 or greater). Turbulent and Brownian diffusion were found to be the main mechanisms dictating the precipitation of fine particles. The intensity of precipitation was observed to diminish as τ_s increases; this effect was linked to a decrease in the coefficient of Brownian diffusion that occurs as particle size increases. Turbulent diffusion and turbulent migration caused by the unevenness of the distributions of the particles' concentration and the intensity of the turbulent velocity pulsations of the bearing flow, as well as Saffman's force, were determined to be the main mechanisms dictating the precipitation of

medium-sized particles. The contribution of Brownian motion was found to be insignificant. The increase in the precipitation rate as τ_s increases was explained in terms of the increase in the role of the migration mechanism of transfer. The decrease in the precipitation coefficient (after a maximum is reached at $\tau_s \approx 100$) as the inertia of the large particles increases was therefore linked to the decrease in the intensity of the turbulent pulsations of the lateral velocity. The results of the calculations performed were found to be in good agreement with experimental data presented by several other authors. The suggestion that the use of coatings providing nappy roughness be used to intensify precipitation onto channel walls was examined briefly. Calculations based on the proposed model confirmed that even a small amount of roughness results in a sharp increase in precipitation rate. Figures 4; references 22: 9 Russian, 13 Western.

The Susceptibility of Supersonic Boundary Layer to Acoustic Disturbances

927F0181F Moscow IZVESTIYA ROSSIYSKOY AKADEMII NAUK MEKHANIKI ZHIKOSTI I GAZA in Russian No 1, Jan-Feb 92 (manuscript received 21 Dec 90) pp 40-47

[Article by A.V. Fedorov and A.P. Khokhlov, Moscow; UDC 532.526.2:533.6.011.5]

[Abstract] In a previous publication the authors of this article studied the mechanism of the excitation of the first and second modes of a boundary layer in the vicinity of the sharp leading edge of a plate struck by an acoustic wave at a zero angle (i.e., the wave vector is parallel to the flow). For small frequency parameter values, they constructed an asymptotic theory and found the initial amplitudes of the unstable modes. Their analysis was based on the fact of the synchronization of the natural vibrations of the boundary layer with the acoustic waves as indicated yet elsewhere. The modes were excited by the diffraction of sound due to the displacing effect of the boundary layer. In the study reported herein, the authors have generalized their previous study to the case where the external wave strikes the plate at arbitrary angles. Two excitation channels are identified: The first is associated with the diffraction of the acoustic wave in the spatial inhomogeneity caused by the displacing effect of the boundary layer; the second is associated with the occurrence of concentrated acoustic field sources as the wave scatters on the leading edge. The latter factor is shown to be primarily responsible for the initial amplitude of the unstable modes, where the angles of the sound's incidence are far from being even close to 0. A characteristic feature occurs at small angles of incidence that is revealed by introducing narrow regions in the vicinity of the threshold wave number values where both excitation channels are approximately of equal strength. Composite formulas are derived for the initial amplitudes of the unstable modes. The formulas are equally suited for acoustic waves with all

angles of incidence. The calculations and analysis presented thus confirmed that a supersonic boundary layer is most susceptible to acoustic waves striking the plate at small angles of incidence. Figures 3; references 3: 2 Russian, 1 Western.

The Convective Stability of a Horizontal Rotating Layer of Fluid With Spiral Turbulence

927F0181E Moscow IZVESTIYA ROSSIYSKOY
AKADEMII NAUK MEKHANIKI ZHIDKOSTI I
GAZA in Russian No 1, Jan-Feb 92 (manuscript
received 3 Sep 90) pp 33-39

[Article by B.L. Smorodin; UDC 532.517.4:013.4]

[Abstract] The author of this study examined the problem of the convective stability of a horizontal rotating layer of fluid with spiral turbulence. The horizontal fluid layer is assumed to be rotating evenly around the vertical axis. It is further assumed that the heat flux at the layer's boundaries is fixed and that the intensity of the spiral background does not depend on the rotation speed or degree of heating. The cases of zero spiraling ($S_1 = 0$, $S_2 = 0$) and a stationary layer ($Re = 0$) are examined. The exact boundary value calculations performed and an examination of the behavior of critical disturbances as a function of the rotation parameter Re revealed that for a layer with heat-insulated boundaries, monotonic disturbances are critical for equilibrium. Two mechanisms were found to be at work in a layer of spiral fluid with heat-insulated boundaries: 1) the fact that increases in spiraling cause the critical wave number to shift to the region of longer wavelengths and 2) the fact that heat insulation of the boundaries makes vertical convective heat transfer disadvantageous and thus results in nearly horizontal critical motions. The case where S_1 and Re are both unequal to 0 is also examined. Unlike the spiral and thermal mechanisms, rotation of the layer was found to increase the critical wave number and thus increase the convection threshold in the process. The oscillation mode was found to depend on both the effect of the spiral mechanism and on rotation. Charts of quasi-equilibrium stability were plotted for the cases of Prandtl numbers of $P = 1$ and $P = 0.025$. Figures 5, tables 3; references 7; Russian, Western.

Selected Nonlinear Wave Effects in a Fluid-Saturated Porous Medium

927F0181J Moscow IZVESTIYA ROSSIYSKOY
AKADEMII NAUK MEKHANIKI ZHIDKOSTI I
GAZA in Russian No 1, Jan-Feb 92 (manuscript
received 19 Apr 91) pp 74-79

[Article by R.F. Ganiyev, S.A. Petrov, and L.Ye. Ukrain-
skiy, Moscow; UDC 532.546]

[Abstract] Most of the research that has been conducted on the propagation of waves in porous fluid-saturated

media has examined the problem in its linear formulation. A number of technologies have recently been developed that entail the propagation of waves with large amplitudes. As the amplitudes of the waves propagated increases, so too do the nonlinear effects associated with them. In view of these facts, the authors of the study reported herein examined selected one-dimensional nonlinear effects that are manifested when waves are propagated in weakly permeable fluid-saturated porous media. They begin their mathematical analysis by deriving the appropriate Burgers equation and then proceed to determine the dependence of the coefficients of the Burgers equation on the bulk compression modulus. The effect of nonlinearity on the attenuation of monoharmonic waves is estimated, and the characteristic features of the nonlinear parametric interaction of two waves excited in a medium by two monoharmonic sources with different frequencies are established. The calculations performed indicate that for a porous medium with the parameters selected, the effect of nonlinearity when waves are propagated from a multi-harmonic source are insignificant at source amplitudes of less than 1 atm. Failure to give consideration to nonlinearity in the case of large amplitudes is, however, shown to be a source of significant computation errors. Figures 3; references 7: 5 Russian, 2 Western.

The Circulation of a Cylinder by Rarefied Gas at a Gliding Angle

927F0182G Moscow IZVESTIYA ROSSIYSKOY
AKADEMII NAUK MEKHANIKI ZHIDKOSTI I
GAZA in Russian No 1, Jan-Feb 92 (manuscript
received 11 May 90) pp 146-154

[Article by K.V. Nikolayev; UDC 533.6.011.8]

[Abstract] The author of this study conducted a numerical study of the circulation of a cylindrically blunted wing edge by a flow of rarefied monoatomic gas. The Monte Carlo method of direct statistical modeling was used with the following parameters: Mach number of the undisturbed flow (M_∞), 20; ratio of body surface temperature to deceleration temperature ($T_w = T_\infty/T_0$), 0.03; glide angle (χ), $\leq 75^\circ$; and Reynolds number (Re_0), ≤ 30 . The calculations performed indicated that a steep shock wave front forms at the Reynolds numbers studied. The departure of the shock wave from the body was found to increase as the glide angle was increased. This phenomenon was determined to be caused by the decrease in the normal component of the velocity of the undisturbed flow to the shock wave and was found in accordance with the laws of gas dynamics. Behind the shock wave front was a zone of small gradients that occupied about a third of the thickness of the entire disturbed region in which the gas' temperature and density remained virtually unchanged. This zone was identified as the zone of nonviscous gas-dynamic current in which the flow turns and decelerates. Because the velocity slowly decreases at this point, the pressure increases slowly until it reaches the magnitude of the doubled velocity head. Large gas-dynamic gradients were also found to exist close to the

cold surface of the body. In the case of circulation without a glide angle, the temperature decreased monotonically as the wall was approached whereas the density increased monotonically. In the presence of a glide angle close to the wall, there was a deceleration of that component of the velocity that is parallel to the cylinder's generatrix. The calculations indicated that this velocity component remains unchanged in the shock wave, which is consistent with the laws of gas dynamics. A rapid change in the said velocity component close to the wall was found to cause strong energy dissipation, which results in a sharp increase in gas temperature. The maximum temperature was found to correspond to the minimum on the density profile. The results reported herein were consistent with results obtained by different mathematical methods and reported elsewhere. The study results indicated that when a cylinder is circulated with Reynolds numbers of about 30 or greater, the disturbed region may be divided into three zones: a shock wave, a "nonviscous" flow, and a boundary layer. This three-zone pattern was found to be the main difference between the circulation of a cylinder and that of a sphere (in which case the disturbed region is not as thick and the shock wave zone merges with the boundary layer zone at Reynolds numbers of about 30). Figures 5; references 13: 12 Russian, 1 Western.

A Theory of Stability of Periodic Flows of Viscous Gas

927F0181B Moscow IZVESTIYA ROSSIYSKOY AKADEMII NAUK. MEKHANIKA ZHIDKOSTI I GAZA in Russian No 1, Jan-Feb 92 (manuscript received 26 Mar 91) pp 10-16

[Article by M.A. Brutyan and P.L. Krapivskiy, Moscow; UDC 532.517.013.4]

[Abstract] The authors of this study have investigated the stability of a very simple unidirectional periodic flow of compressed viscous gas induced by a mass force that is periodic along one of its coordinates. They confine their examination to two-dimensional flows, and they focus their attention on one aspect of what have been termed Kolmogorov flows. Specifically, they examine the analogue of a Kolmogorov flow in a compressible gas. During the course of the mathematical analysis presented, the authors demonstrate that the critical Reynolds number of the loss of the said flow's stability may be calculated exactly and that the characteristics of the large-scale coherent vortex structure formed by the flow may be determined qualitatively. The authors propose that their results be looked upon as a possible approach to the problem of the formation of large-scale structures in viscous gas. They conclude by stating that because the approximation of a continuous medium works only in the case of small Knudsen numbers, the hydrodynamic description presented herein is valid only when $M \ll 1$, whereas unexpected behavior of the dependence $R_c = R_c(M)$ begins in the region $M = O(1)$ or, in other words,

the region in which Navier-Stokes equations in the given problem are no longer valid. Figure 1; references 17: 8 Russian, 9 Western.

Characteristic Features of a Circulating Flow of Rarefied Gas in a Short Rotating Cylinder With a Fixed Face

927F0182O Moscow IZVESTIYA ROSSIYSKOY AKADEMII NAUK. MEKHANIKA ZHIDKOSTI I GAZA in Russian No 1, Jan-Feb 92 (manuscript received 18 Feb 91) pp 188-190

[Article by V.D. Borisevich, S.Yu. Krylov, and S.V. Yupatov, Moscow; UDC 533.6.011.8:519.245]

[Abstract] In a previous study, two of the three authors of the study reported herein used the method of direct statistical modeling to study a circulating flow of rarefied gas in a rotating cylinder (with a height commensurate to its radius) caused by the decelerating effect of one of the cylinder's faces. The intensity of the flow was found to decrease as the rarefaction of the gas increased to a Knudsen number of $Kn = 1$ and to remain constant thereafter. The direction of circulation characteristic for a continuum was found to be maintained. In this publication, the authors have turned their attention to the occurrence of secondary flows as the height of the rotating cylinder with a fixed face is decreased. The studies performed established that in the case of a dimensionless height of $h = H/a \approx 0.25$ (where a is the radius of the cylinder), a two-eddy circulating flow structure forms in the volume of the cylinder. The direction of one of the eddies appears paradoxical at first glance. As in the previous study, the method of direct statistical modeling was used. Specifically, the calculations performed established that as h decreases, the height distribution of such flow characteristics as gas density, gas temperature, and azimuthal velocity component assume an increasingly symmetrical appearance relative to both faces of the cylinder. Only in a narrow region close to the lateral surface ($x \geq 1-h$, $x = r/a$) was an asymmetry analogous to the case of $h \geq 1$ observed. For $h = 0.06$, these flow characteristics were found to have a distribution close to the case of a plane Couette flow. As the radial coordinate increased, the gas temperature increased because of its proportionality to the local Mach number, which increases on account of the increase in the azimuthal component of the gas' velocity. The gas' density was found to change in a radial direction in accordance with an exponential law corresponding to the angular velocity of the rotation (which equaled $\omega/2$). In addition to the azimuthal gas flow in the cylinder, there was a secondary circulating flow caused by the decelerating effect of the top face. In the case of a continuum, the gas moves toward the cylinder axis at the fixed face and toward the side wall at the rotating face. This was explained in terms of the familiar disturbance of the balance between the centrifugal force and the radial pressure gradient in face boundary layers. Analogous flows have been observed in the case of rarefied gas in a cylinder with a height greater than or equal to its

radius. As the cylinder diameter was reduced to $h = 0.5$, two additional symmetrical eddies appeared. Beginning at a value of $h = 0.25$ they joined into a single eddy directed toward the circulation described above. As h decreased further, the latter was displaced into a narrow near-wall region ($x \geq 1 - h$), and most of the cylinder's volume was occupied by the flow with a circulation direction that cannot be explained from the standpoint of the dynamics of viscous gas. This seemingly paradoxical flow was explained by the fact that unlike in the case of a continuum, in the case of highly rarefied gas in a short ($h \leq 0.25$) cylinder, the characteristics of the flows of gas close to each of the cylinder's two faces are determined by the boundary conditions on the opposite face. Figure 1; references 7: 5 Russian, 2 Western.

Exact Solutions of a Model Bhatnagar-Gross-Kruk Boltzmann Equation in Problems of Temperature Jump and Weak Evaporation

927F01821 Moscow IZVESTIYA ROSSIYSKOY AKADEMII NAUK MEKHANIKA ZHIDKOSTI I GAZA in Russian No 1, Jan-Feb 92 (manuscript received 13 Mar 90) pp 163-171

[Article by Ye.B. Dolgosheina, A.V. Latyshev, and A.A. Yushkanov, Moscow; UDC 533.72]

[Abstract] Jumps in temperature and density over an evaporated surface have been shown to exert a significant effect on the course of various physical processes, including thermophoresis, the heat conduction of gases, and evaporation processes. Numerous researchers have attempted to find exact or numerical solutions to the said problems. In a continuation of this line of research, the authors of this article have obtained an exact solution to a model Boltzmann equation with a Bhatnagar-Gross-Kruk [BGK] collision operator in problems of weak evaporation and jumps in the temperature and density of rarefied gas in a half-space. The Keyes method was used to find generalized eigenvectors of the respective characteristic equation. The theorem of the existence and singularity of the solution to the formulated problems with boundary conditions both on and far from a plane surface is proved. To prove the said theorem, the authors developed an apparatus to diagonalize and factor a Riemann-Hilbert vector boundary value problem with a matrix coefficient whose diagonalizing matrix has branchpoints in a complex plane. Numerical solutions of two sample problems are also presented. References 23: 4 Russian, 19 Western.

Problems of the Circulation and Correction of Shape of Thin Profiles in an Incompressible Flow

927F0182E Moscow IZVESTIYA ROSSIYSKOY AKADEMII NAUK MEKHANIKA ZHIDKOSTI I GAZA in Russian No 1, Jan-Feb 92 (manuscript received 8 Apr 91) pp 130-137

[Article by V.E. Saren, Moscow; UDC 533.6.011.3]

[Abstract] The author of this article has formulated and solved the problems of the circulation and correction of the shape of a profile or airfoil cascade in a flow of ideal liquid within the framework of a first approximation of the theory of disturbances of the current around infinitely thin airfoil profiles. The approach followed is that of making sequential corrections in the boundary of a flow region based on small variations in the boundary values of the flow speed. An algorithm is presented for solving the linear boundary value problem in the case of thin profiles in an incompressible flow. A sample computation entailing three iterations is presented. A comparison of the results obtained by using the proposed method with the results of a check calculation confirmed that the proposed method yields results that have a precision adequate for practical purposes. Figures 3; references 6: 4 Russian, 2 Western.

The Buoyancy of Bodies in Disperse Media

927F0182J Moscow IZVESTIYA ROSSIYSKOY AKADEMII NAUK MEKHANIKA ZHIDKOSTI I GAZA in Russian No 1, Jan-Feb 92 (manuscript received 17 May 88) pp 172-174

[Article by A.V. Ostroumov, Moscow; UDC 532.3:532.29]

[Abstract] The author of this concise report examined the problem of the forces acting on bodies submerged in disperse media. Specifically, he demonstrated that the disperse phase has both dynamic and static effects on the body. The dynamic effect results from the particles being decelerated by the body and thus transferring their impulse to it; the static effect results from the weight of the particles that settle on the body. A series of expressions are derived for the static and dynamic effect of spherical disperse particles on the submerged body. The buoyancy force in a disperse medium is shown to not obey Archimedes' law; rather, the buoyancy force depends on the shape of the body, its orientation in space, and on time. The analysis presented further demonstrates that the hydrostatic component of the buoyancy force (which is always taken into account) is actually smaller than the component resulting from the contact effect of the disperse particles on the body (which is generally ignored). This is shown to be true even when the body does not accumulate particles. The following expression is derived to describe this effect: $V/S < H_* = B[\phi(t) + A]$, where V is the volume of the body, S is the body's area in a plane, A and B are coefficients representing time in seconds and rate in meters per second, and H_* is a parameter characterizing the threshold value of V/S (i.e., the ratio characterizing the body's elongation in a vertical direction). A table is presented that details the values of A and B of the following commonly encountered systems of bodies in disperse media: mineral particles in air, water drops in air, mineral particles in water, and air bubbles in water. Overall, the analysis presented demonstrates that the contact effect of disperse particles may play a significant role in the overall balance of forces acting on bodies

located in a disperse medium and that the terms describing this effect in an impulse equation must not be omitted without the necessary substantiation. Table 1.

The Aerodynamic Drag of a Cylinder in a Two-Phase Flow

927F0182D Moscow IZVESTIYA ROSSIYSKOY AKADEMII NAUK. MEKHANIKA ZHIDKOSTI I GAZA in Russian No 1, Jan-Feb 92 (manuscript received 4 Mar 91) pp 123-129

[Article by V.A. Lashkov; UDC 533.6.011:532.529.5]

[Abstract] An experimental study was conducted to investigate the aerodynamic drag of a round cylinder circulated by a cross-flow of a gas suspension. The studies were performed in a cylinder/ejector-type wind tunnel. The solid phase was metered into the tunnel through a nozzle at a rate of 0.01 to 2.7 kg/s in a manner that required the required concentration of solid phase in the flow as determined by the ratio of the mass flow rate of the disperse phase to the mass flow rate of the carrier medium. Standard electrocorundum micropowders and ground powders (conforming to All-Union State Standard GOST 3647-80) were used. The particles were in the form of sharp-grained elongated fragments with a material density of 4,000 kg/m³. A cylinder with a length:diameter ratio of $L/D = 2$ was used as a model. The force loads acting on it were measured by using an aerodynamic strain gauge. An electrical signal passing from the output of the strain gauge amplifier to a computer was used to control the model's entry and exit to and from the flow. The velocity and density of the solid phase were measured by laser optical methods at that point in the flow where the model was mounted. As the concentration of solid phase in the flow was increased, the drag coefficient began to decrease smoothly. Then, beginning at some critical value K , it began to increase sharply. The range of K in which a decrease in the drag coefficient is observed was found to depend on the size of the particles constituting the solid phase: The smaller the particles, the narrower the range of K . When powders with a particle size of less than 40 μ m were used, the minimum possible concentration that could be metered into the solid phase immediately caused a sharp drop in the drag coefficient. The experiments further revealed that the concentration dependence of the coefficient of aerodynamic drag may be represented as the superimposition of two processes occurring as K increases, namely, the decrease in the drag coefficient at values of K close to 0 and a linear increase proportional to the concentration of solid phase in the flow. The presence of air in the flow was found to shift the separation point of the boundary layer on the model. Adding air to the flow was discovered to reduce the critical Reynolds number at which a drag "crisis" was observed in the model. The measurements taken demonstrated that the unevenness along the midsection of the model of the velocity profile of the carrier phase (air) was no worse than 2 to 3% and that the unevenness of the velocity of the solid particles did not exceed 3 to

4%. The density of the discrete phase was found to be between 8 and 10%. Figures 3; references 12 (Russian).

Three-Wave Resonance and Averaged Equations of the Interaction of Two Waves in Media Described by a Cubic Schrodinger Equation

927F0182B Moscow IZVESTIYA ROSSIYSKOY AKADEMII NAUK. MEKHANIKA ZHIDKOSTI I GAZA in Russian No 1, Jan-Feb 92 (manuscript received 14 Jun 91) pp 107-116

[Article by I.B. Bakholdin, Moscow; UDC 532.59]

[Abstract] Others have established the phenomenon of Mach reflection of Stokes waves from a vertical wall by obtaining a numerical solution of a cubic Schrodinger equation. In a previous publication, the author of this article interpreted the aforesaid phenomenon as the resonance interaction of three waves. He derived averaged equations of the interaction of two waves and considered the zone of interaction of the incident and reflected waves to be the self-similar solution of these equations. In the study reported herein, the author turns his attention to substantiating the possibility of describing these solutions in terms of three-wave resonance relationships. The calculated results in cases of large values of K (i.e., low discontinuity intensities) are found to deviate somewhat from published experimental data. This discrepancy is explained by the fact that in the solutions under consideration the waves near the resonance point are close to being solitary. The length of the solitary wave, i.e., the length of the segment where its intensity is some specified fraction of its amplitude, is said to increase as the amplitude decreases. This leads to the conclusion that the method of averaging may be used to find a numerical solution to the Schrodinger equation in the case of large values of K and that the calculations must be performed for a large period of time beginning from the moment when the wave interacts with the wedge. It is thus demonstrated that the domain of the self-similar solution may be replaced by a discontinuity such as the resonance interaction of the three waves as has previously been shown to be the case for solitons. Several consequences of this finding are examined, and the physical parameters of the waves under consideration are detailed. The mathematical meaning of the term "resonance" is said to be splitting into two waves. The properties of an example averaged system are studied. Figures 5; references 8: 7 Russian, 1 Western.

Plane Capillary Friction of Viscous Fluid With a Multiply Connected Boundary in a Stokes Approximation

927F0182C Moscow IZVESTIYA ROSSIYSKOY AKADEMII NAUK. MEKHANIKA ZHIDKOSTI I GAZA in Russian No 1, Jan-Feb 92 (manuscript received 11 Dec 89) pp 117-122

[Article by S.A. Chivilikhin, Saint Petersburg; UDC 532.68:532.516]

[Abstract] The author of this article has performed a mathematical analysis of the process of the relaxation of an isolated volume of viscous incompressible Newtonian fluid to an equilibrium configuration under the effect of capillary forces. The fluid is assumed to have the shape of an infinite cylinder of arbitrary shape with a smooth and compact multiply connected boundary. It is also assumed that during the course of the relaxation process, the inner cavity implodes, and the cylinder asymptotically acquires a round configuration. The approach used has evolved on the basis of a number of publications that use a quasi-stationary Stokes approximation to describe the current and to calculate the boundary angle, the implosion of a round capillary tube, and a hollow cylinder. Another concept that is central to the approach used is the analogy between hydrodynamics equations in a Stokes approximation and elasticity theory equations. The computations performed demonstrate that the true pressure distribution is provided by the minimum integral of the pressure squared throughout the region given a fixed integral of the pressure along the boundary. An explicit expression is derived for the pressure in the form of the projection of a generalized function having a carrier at the boundary with the subspace of the harmonic functions. The velocity field at the boundary of the region is also calculated. A top estimate is found for the law governing the decrease of the region's perimeter and for the time period during which the number of the boundary's connectivity components remains unchanged. References 16: 15 Russian, 1 Western.

Radiation and Radiation Cooling of Xenon Plasma Behind a Strong Shock Wave Front

927F0182H Moscow IZVESTIYA ROSSIYSKOY
AKADEMII NAUK: MEKHANIKA ZHIDKOSTI I
GAZA in Russian No 1, Jan-Feb 92 (manuscript
received 25 Feb 91) pp 155-162

[Article by S.V. Makarychev, G.D. Smekhov, and M.S. Yalovik, Moscow; UDC 533.6.07.8:533.9.07]

[Abstract] The authors of this study examined the emissivity and radiation cooling of highly ionized xenon plasma behind the front of a strong shock wave. The plasma was assumed to be homogeneous, and the flow in the shock wave was assumed to be one-dimensional. It was further assumed that transfer phenomena (except for the energy losses during radiation transfer) were insignificant and that heat conduction, viscosity, and diffusion in the flow could thus be ignored. The xenon plasma examined in the calculations performed during the study was assumed to consist of 32 components, including free electrons, neutral XeI atoms, single ions, double ions, and triple ions in a ground state. The iteration method was used to solve the equations formulated. The component composition and equilibrium parameters found were then used as a basis for calculating the intensity of radiation in line and continuous spectra and for determining the total radiation energy losses. The studies performed revealed that the equilibrium gas-dynamic temperature of xenon plasma behind a shock wave front

decreases as the illumination time increases. In the cases of both radiating and nonradiating plasma, increasing the initial xenon pressure was found to result in a temperature increase and an increase in the optical thickness of the plasma. Overall, the studies performed confirmed that devices based on the principle of gas-dynamic heating of xenon plasma in shock waves may be viewed as viable alternative high-power radiation sources using nonelectrical power sources. The use of the method presented is illustrated by way of the example of a calculation based on the conditions of actual experiments performed in a diaphragm-type shock tube with an inner diameter of 16 cm. A comparison of the results obtained by the proposed computation method and by experimentation confirmed that the proposed method yields satisfactory results. Figures 5, table 1; references 5: 4 Russian, 1 Western.

A Nonstationary Viscous Shock Layer During Supersonic Motion Through an Inhomogeneity

927F0182 Moscow IZVESTIYA ROSSIYSKOY
AKADEMII NAUK: MEKHANIKA ZHIDKOSTI I
GAZA in Russian No 1, Jan-Feb 92 (manuscript
received 26 Oct 90) pp 138-145

[Article by A.A. Markov, Moscow; UDC 533.6.011:533.686.4]

[Abstract] The author of this article has worked to develop a numerical model of the nonstationary effects occurring in a viscous shock layer around the critical current line close to the head portion of a rotating blunted body in an inhomogeneous external field with a pressure differential, temperature differential, and vorticity. The problem model is based on the concept of a perfect gas. The evolution of the nonlinear disturbances resulting from the passage through the heated zone and from a change in the blasting regimen is traced. A divergent finite difference second-order approximation scheme is used. The method is implemented by means of vector sweeps with consideration for the boundary conditions existing on the body's surface and behind the isolated bow shock wave. An analysis of the six graphs plotted on the basis of the computation results revealed that the model of a thin viscous shock layer is not suitable when a fairly exact description of the nonstationary processes considered herein is required. Figures 6; references 6: 5 Russian, 1 Western.

Motion Equation of Ball Lightning in the Air Stream Formed by a Flying Rocket

927F0182K Moscow IZVESTIYA ROSSIYSKOY
AKADEMII NAUK: MEKHANIKA ZHIDKOSTI I
GAZA in Russian No 1, Jan-Feb 92 (manuscript
received 21 Nov 90) pp 174-177

[Article by N.I. Gaydukov, Moscow; UDC 532.5.031]

[Abstract] The author of this concise report has examined the hydrodynamic interaction of ball lightning with

a rocket that is flying along a specified trajectory under the power of its own working engines. This interaction is, in a first approximation, modeled in terms of a moving point source of variable intensity. Because the lightning takes part in a hydrodynamic interaction with a source moving in relation to a stationary air medium, it is assumed that both the stationary source and lightning moving in relation to it are in a translational air flow that is variable in both magnitude and direction and that the components of the air flow's velocity are determined by the kinematic equation of the rocket's motion. Expressions are derived for finding those components of the force acting on the ball lightning that are the result of the air flow. The said expressions include the following: the inertial forces acting on the lightning during its potential circulation, the force exerted on the lightning by the external variable translational air flow, the force resulting from the interaction of the flow of the point source and the external translational flow, and the force of the radial effect exerted on the lightning by the variable-intensity point source. The expressions are used to derive an equation of the motion of ball lightning in the air field of a flying rocket under the assumption that the density of the lightning's plasma equals the density of the air. The resultant system of three ordinary differential equations cannot be solved by analytical methods in the general case. It may, however, be solved numerically given specified initial conditions if it is represented as six first-order equations with specified time functions. References 12 (Russian).

Jet Flow on Ribbed Curvilinear Surfaces

927F0182L Moscow IZVESTIYA ROSSIYSKOY AKADEMII NAUK: MEKHANIKA ZHIDKOSTI I GAZA in Russian No 1, Jan-Feb 92 (manuscript received 21 Feb 91) pp 177-179

[Article by Yu.A. Lashkov, I.N. Sokolova, and Ye.A. Shumilkina, Moscow; UDC 432.525.2]

[Abstract] The authors of this study investigated the possibility of using the technique of microribbing curvilinear surfaces to reduce turbulent friction in Coanda flows. The study flow was a plane stream originating from a constricting nozzle along the tangent to a ribbed cylinder. By significantly elongating the nozzle ($L/\delta = 20$ to 100) and placing plates at the ends of the cylinder, the researchers were able to create a two-dimensional flow. During the tests, the initial thickness of the flow ($\delta' = \delta/r$, with r being the radius of the cylinder) was varied from 0.06 to 0.32. To date, most studies of the Coanda effect (adhesion of the stream to the surface) have been conducted with smooth curvilinear surfaces. In contrast, the researchers conducting the present study used ribbed surfaces with a triangular rib cross section of varying height ($h = 0.04$ to 0.22 mm) and rib spacing ($s = 0.06$ to 0.53 mm). They also studied a surface with rounded rib tips ($h = 0.06$ mm, $s = 0.20$ mm). The experiments performed demonstrated that the Coanda effect occurs on surfaces with both lengthwise and crosswise ribs regardless of whether the ribs have sharp or rounded

tips. The only exception to this finding occurred in the case of a flow thickness of $\delta' = 0.32$ circulating across a ribbed cylinder with large ribbing ($h = 0.22$ mm). In the case of lengthwise microribbing ($h = 0.04$ mm), a Coanda flow with $\delta' = 0.12$ to 0.24 may be achieved with lower losses of total pressure in the flow than is possible on smooth surfaces. The separation angle corresponding to the position of the point of the flow's departure from the cylinder and the pressure at which destruction of the Coanda flow occurs are virtually identical for smooth and lengthwise-ribbed surfaces. For a flow with an initial thickness of $\delta' = 0.12$, the separation angle will be about 160° , and the separation pressure will equal 4.2 to both smooth and lengthwise-ribbed surfaces. The studies performed indicated that the optimal parameters of ribbing in Coanda flows on ribbed surfaces are not identical in different engineering problems. The friction on a curvilinear surface may, for example, be reduced in the case of comparatively thin streams by using fairly low-height lengthwise ribbing. The optimal ribbing parameters are approximately the same in the case of a plane plate. The most effective way of reducing the effects of a flow on an enclosure is to use crosswise ribbing of fairly low height, and the best way of preventing a Coanda flow is to use thick streams with fairly high crosswise ribbing. Figures 4; references 4: 3 Russian, 1 Western.

Thermocapillary Evacuation of Fluid Coming Through a Porous Wall

927F0182M Moscow IZVESTIYA ROSSIYSKOY AKADEMII NAUK: MEKHANIKA ZHIDKOSTI I GAZA in Russian No 1, Jan-Feb 92 (manuscript received 26 Sep 90) pp 179-182

[Article by Yu.V. Sanochnik, Moscow; UDC 532.526:536.24]

[Abstract] The author of this concise report has performed a mathematical analysis of the thermocapillary evacuation of fluid coming through a horizontal porous wall. It is assumed that the fluid is arriving through a permeable base and that the temperature distribution on the free boundary is symmetrical. The said situation is similar to that arising when a liquid working medium is fed through a porous electrode unevenly heated by an electric arc and is also similar to "wick" cooling of the surface of a solid body. Under specified conditions, the problem under consideration may also serve as a model of the even motion of a melting front during nonuniform heating of a body's surface. The cases of a free boundary and a curved free boundary are examined. The possible convection modes and corresponding boundary profiles are classified. The analysis performed indicated that if the fluid feed rate exceeds the amount of fluid that may be evacuated by a capillary force, a "hump" will form in the heating center, in which case the pressure gradient will act on the same side as the surface force does. On the other hand, if the capillary force is capable of evacuating more fluid than is entering through the lower boundary layer, a depression will form in the heating center in a stationary state, and the pressure gradient will impede

the effect of the surface force. The signs of the curvature of the layer's boundary and the velocity profile $u(y)$ (u and y being the horizontal and vertical components of the velocity, respectively) coincide. If $\alpha'\Delta Th^2 < 2vpv_0l^2$, then throughout the layer there will be a flow in the direction of the effect of the surface force, and the velocity profile will be monotonic with its convexity turned to the side of the motion. If, on the other hand, $\alpha'\Delta Th^2 > 2vpv_0l^2$, the pattern will be more complicated. If $1/3 < 2vpv_0l^2/\alpha'\Delta Th^2 < 1$, the horizontal component of the fluid's velocity will not change size, and the concavity of its profile will be turned to the side of the motion. When $2vpv_0l^2 < \alpha'\Delta Th^2/3$, the discrepancy between the feed rate and heating will be so great that the flow will stratify. In the lower part of the layer, the fluid will move to the heating center; in the upper part, it will move in the direction of the capillary force. A backflow will form near the bottom owing to deformation of the boundary. References 4: 3 Russian, 1 Western.

Generalized Model of a Plane Geofiltration Flow

927F0182N Moscow IZVESTIYA ROSSIYSKOY
AKADEMII NAUK: MEKHANIKA ZHIDKOSTI I
GAZA in Russian No 1, Jan-Feb 92 (manuscript
received 20 Nov 1990) pp 182-184

[Article by V.M. Shestakov, Moscow; UDC 532.546]

[Abstract] The scheme of a plane geofiltration flow first proposed by Dupuit in 1857 and later used by Boussinesq and Forchheimer was based on averaging the flow's pressures along the vertical. Model experiments conducted in the 1950's demonstrated that the Dupuit-Boussinesq-Forchheimer scheme for a homogeneous flow may have extensive applications if the equality of its horizontal pressure gradients (as averaged by depth and on the free surface) could be assumed. In view of these findings, the author of this concise report has examined a generalized model of a plane geofiltration flow. The author begins his further generalization of the model of a plane flow based on the assumption of the constancy of the horizontal pressure gradients (l_1) in each section where the horizontal (lateral) filtration speeds (v_1) rates are determined by the expression $v_1 = k_1 l_1 = k_1(q/T)$, where k_1 represents the horizontal filtration coefficients and q and T are the flow's specific flow rate and conductivity. He proceeds to develop expressions for a homogeneous flow structure and for a two-layer flow structure consisting of upper and lower layers. He also considers a generalized model of a plane flow that allows for the dynamics of the gravitation capacity of the flow based on a "capillary bleeding" scheme in which the zone of incomplete saturation above the free surface is replaced by a hydraulically equivalent "capillary bleeding" zone with some leakage coefficient $\chi_{\text{capillary}}$. He concludes by stating that the generalized model of a plane flow is most significant in solving flow trajectory design problems such as those arising in the study of the pollution of underground waters. Test calculations demonstrated that the generalized model results in trajectories with an entirely satisfactory precision at least in the

case of infiltration areas exceeding the doubled flow depth. References 6: 4 Russian, 2 Western.

A Body of Minimum Resistance Moving in Media Under the Assumption of the Law of Locality

927F0182A Moscow IZVESTIYA ROSSIYSKOY
AKADEMII NAUK: MEKHANIKA ZHIDKOSTI I
GAZA in Russian No 1, Jan-Feb 92 (manuscript
received 15 Apr 91) pp 95-106

[Article by N.A. Ostapenko and G.Ye. Yakunina, Moscow; UDC 532.58:517.97]

[Abstract] The authors of this study formulated and solved a variational problem of a body of minimum resistance moving at a constant speed in media assumed to be subordinate to the law of locality. In accordance with the law of locality, it was assumed that the force of the medium's effect on the body's elementary surface area depended solely on the orientation of the force relative to the direction of the motion. The normal (pressure) and tangential (friction) components of the force were represented so as to encompass a broad set of conditions realized when a body moves in gases or dense media. The problem of finding the optimal shape of the body in question was divided into two parts, which is to say that the lengthwise and crosswise contours were determined independently of one another. The optimal crosswise contour given a specified minimum radius is also found. A sample problem is solved numerically, and the resultant solution is plotted on a graph. Figures 4; references 7 (Russian).

Designing an Airfoil With a Flap Simulated by a Point Vortex

927F0181A Moscow IZVESTIYA ROSSIYSKOY
AKADEMII NAUK: MEKHANIKA ZHIDKOSTI I
GAZA in Russian No 1, Jan-Feb 92 (manuscript
received 15 Feb 90) pp 3-9

[Article by N.B. Ilinskiy and A.V. Potashev, Kazan; UDC 532.5.031]

[Abstract] In an effort to improve the aerodynamic properties of airfoils (specifically, in an effort to improve their lift), the authors of this study worked to design an airfoil with a flap simulated by a point vortex. They used the method of quasi-solutions of inverse boundary value problems to design and construct the airfoil based on a specified velocity distribution along the contour of the profile of the main part of the airfoil. An analytical solution of the problem is found. Next, calculations are performed with a set of numerical values in order to illustrate the effects of change in the vortex's intensity. Graphs plotted for different vortex intensities show that as the shape of the vortex comes to approximate that of the airfoil's profile (i.e., when Γ_0' is increased), the velocity at the trailing edge of the profiles plotted by using the quasi-solutions method increases and may

even exceed v_{∞} . In other words, the calculations performed demonstrate that using a flap makes it impossible to increase the lift coefficient not only thanks to the forces acting on the flap but also by increasing the level of the velocities at the upper surface of the main profile while the attached nature of the flow is preserved. The theoretical and numerical calculations presented have thus made it possible to design those airfoil shapes that are guaranteed remain closed when they have a flap (foreflap) simulating a vortex. The solution presented is said to be a first approximation of the more general problem of finding the shape of an airfoil and flap based on specified velocity distributions. The authors conclude by stating that the proposed method will yield satisfactory results in the case of small flap dimensions and that more complicated methods of modeling the flap are required to give fuller consideration to its dimensions. They suggest that formulations in which the flap is replaced by a curvilinear section or closed curve with distributed characteristic features are promising in that such approaches will preserve the simple connectedness of the flow region and, hence, the operability of the quasi-solutions method. Figures 4, table 1; references 4 (Russian).

Formation of a Large Radiation-Induced Fire

927F0181C Moscow IZVESTIYA ROSSIYSKOY AKADEMII NAUK: MEKHANIKA ZHIDKOSTI I GAZA in Russian No 1, Jan-Feb 92 (manuscript received 28 Mar 91) pp 17-25

[Article by Yu.A. Gostintsev, G.M. Makhviladze, V.B. Novozhilov, Moscow; UDC 532.517.3:536.46]

[Abstract] A model described in two previous publications by one of this article's authors is used as the basis for an investigation of the initial stage of the development of a fire induced by luminous radiation accompanying a strong explosion in the atmosphere. The various aspects of the situation existing over the center of the combustion are examined: the aerodynamics of the ground air layer and the configuration and characteristics of the resultant soot cloud. The calculations and analysis of a large-scale fire that are performed are based on published estimates indicating that two-thirds of all flammable materials in cities are made of wood and wood products, 5 to 10% are made of polymers and

rubber, and the rest are made of various organic chemical compound (including oil, asphalt, and gasoline). The analysis performed indicated that in the initial stage of a radiation-induced fire, the flow over the center of the fire is virtually one-dimensional and is directed vertically upward. The compression wave caused by sharp heating of the surface is propagated in the same direction. At a moment somewhere around 0.3 to $0.5 \times t_1$, the gas' motion becomes stronger, and the lateral motion of the combustion products becomes noticeable. A zone with a reverse flow is formed at the fire's edge. A vortex structure is later formed from this zone. A soot cloud results that has a mass fraction of soot particles exceeding 0.01 of its maximum value β_{max} . Calculations have demonstrated that by the end of the fire's initial stage (i.e., when $t = t_1$), the time dependences of the cloud's characteristics are such that the average and maximum temperature and the average, maximum, and minimum concentrations of oxidizing agent and impurities assume a quasi-stationary nature. The average concentration of oxidizing agent in the cloud was nearly identical (about 0.14) for all versions of the calculations performed. A shortage of oxygen ("oxygen starvation") begins to be felt at the surface; it is especially strong at the fire's center where the mass fraction of oxidizing agent drops to about 10^{-4} . As the power of the explosion increases, the area occupied by the fire expands significantly. This in turn results in a drop in the cloud's average temperature. The total amount of finely dispersed aerosol released from the cloud into the atmosphere increases as the fuel combustion rate and power of the explosion increase. Analysis of both existing literature calculations of soot clouds and their own work led the authors to conclude that the amount of soot released in the initial stage of a large-scale radiation-induced fire (S) will be about $0.15S_1$ (S_1 is the amount of soot released by the time the fire has been completely put out and is calculated from three quantities: the area of the fire, the amount of flammable materials present per unit surface, and the ratio of the amount of soot to the total mass of the burned fuel). The figure of $0.15S_1$ is recommended for use in calculations of the primary atmospheric pollution occurring in the initial stage of a radiation-induced fire when the movement of the aerosol beyond the tropopause is especially intense in view of the aerosol's transfer not only in the convective column but also by the powerful buoyant thermal wind. Figures 4; references 15: 10 Russian, 5 Western.

END OF

FICHE

DATE FILMED

19 June 1992